UNIVERSITA' DEGLI STUDI ROMA TRE
Department of Physics "Edoardo Amaldi"

Doctoral School in Mathematical and Physical Sciences
XXI Cycle A.Y. 2008

Doctorate Thesis
Università ROMA TRE - Université de la Méditerranée
***Co-tutorship* Agreement**

Low energy limit in Loop Quantum Gravity

Dr. Elena Magliaro

Director of the Ph.D. School:

prof. Guido Altarelli
Roma Tre University, Department of Physics, Rome

Supervisors:

prof. Orlando Ragnisco
Roma Tre University, Department of Physics, Rome

prof. Carlo Rovelli
Université de la Méditerranée, Centre de Physique Théorique de Luminy, Marseille

Dedicated to my husband Claudio, to my family and to all my friends at CPT.

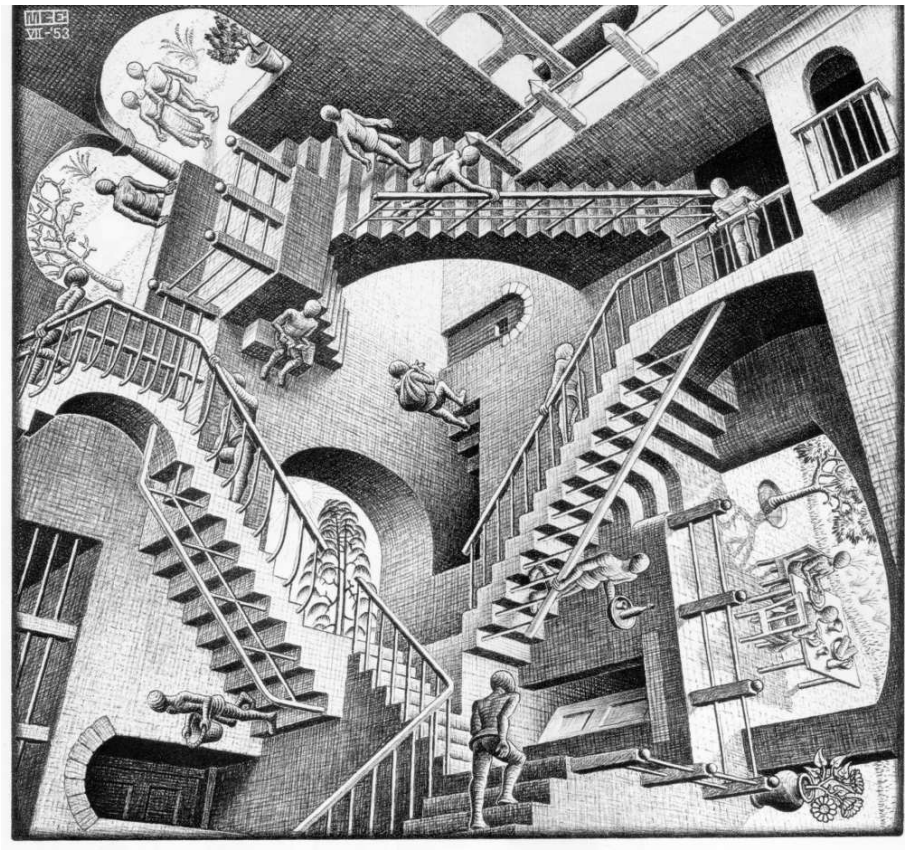

on the back: Maurits Cornelius Escher, *Relativity*

Contents

1 Introduction **6**

2 Hamiltonian General Relativity **10**
2.1 *Canonical formulation of General Relativity in ADM variables* 10
2.2 *Lagrangian analysis* 12
2.3 *Triad formalism* 13
2.4 *Ashtekar-Barbero variables* 14
2.5 *Constraint algebra* 14
2.6 *The holonomy* 16

3 The structure of Loop Quantum Gravity **17**
3.1 *Kinematical state space $\mathcal{K}$* 17
3.2 *Invariant states under gauge transformations and diffeomorphisms* 19
3.3 *Electric flux operator* 24
3.4 *Area and volume operators* 26
3.5 *Physical interpretation of quantum geometry* 27
3.6 *Dynamics* 27

4 Covariant formulation: spinfoam **30**
4.1 *Path integral representation* 30
4.2 *Regge discretization* 32
4.3 *Quantum Regge calculus and spinfoam models* 34
4.4 *BF theory* 36
4.5 *Barret-Crane model* 37

5 Graviton propagator in Loop Quantum Gravity **41**
5.1 *n-point functions in general covariant field theories* 42
5.2 *Graviton propagator in Loop Quantum Gravity* 44
5.3 *Compatibility between of radial, Lorenz and harmonic gauges* 48

6 Non diagonal components **55**
6.1 *Action of field operators* 55
6.2 *The boundary state* 55
6.3 *Symmetrization of the state* 57
6.4 *Calculation of complete propagator* 57

7 A new model: EPRL vertex **60**
7.1 *The goal of the model: imposing weakly the simplicity constraints* 60
7.2 *Description of the model* 61
7.3 *Outlook and summary* 65

8 Asymptotics of LQG fusion coefficients **67**
8.1 *Analytical expression for the fusion coefficients* 67
8.2 *Asymptotic analysis* 70
8.3 *Semiclassical behavior* 74
8.4 *The case* $\gamma = 1$ 76

9 Numerical investigations on the semiclassical limit **77**
9.1 *Wave packets propagation* 78
9.2 *Summary of semiclassical properties of fusion coefficients* 80
9.3 *The semi-analytic approach* 82
9.4 *Physical expectation values* 84
9.5 *Improved numerical analysis* 84
9.6 *Correlation function* 85

10 Outlooks and conclusions **89**

Acknowledgments **90**

A Properties of $9j$-symbols **91**

B Regge asymptotic formula for $3j$-symbols **91**

1 Introduction

General Relativity and Quantum Mechanics are the two revolutionary theories that have changed physics in the last century; they had enlarged our knowledge and had permitted to explain most of the phenomena that we observe. In particular the microscopic observations of nuclear and subnuclear physics have been explained with Quantum Mechanics (QM) evolved in Quantum Fields Theory (QFT) and, on the other side, the large scale phenomena of the Universe have been explained with General Relativity (GR). QM and GR are the two conceptual pillars on which modern physics is built. However they have destroyed the coherent picture of the world provided by prerelativistic classical physics: GR has modified the notion of space and time; QM the notion of causality , matter and measurements, but these modified notions do not fit together easily. On the one hand QM requires a static spatial background and an external time variable, while GR describes spacetime as a single dynamical entity; moreover GR is a classical deterministic theory while Quantum Mechanics is probabilistic and teaches us that any dynamical field is quantized. Both theories work extremely well at opposite scales but this picture is clearly incomplete (1) unless we want to accept that Nature has opposite foundations in the quantum and in the cosmological realm.
The search for a theory which merges GR and QM in a whole coherent picture is the search for a theory of Quantum Gravity (QG). At the present stage we have not such a theory. The essential difficulty is that the theoretical framework is not at all helped by experimental measurement, because the regimes where we expect the prediction of quantum gravity to become relevant (Planck scale) is outside our experimental or observational ranch, at least so far. Recently, one possibility to test some features of quantum spacetime came from the study of ultra high energy cosmic rays (2; 3; 4) and Gamma Ray Bursts (5; 6; 6): since these cosmic rays propagate along cosmological distance, also an effect of the order of Planck scale could be detectable.
The problem for theoretical physicists is: how to describe quantum spacetime? There were various attempts to construct a theory: the conventional methods of quantization, leading to perturbative Quantum Gravity (i.e. the quantum theory of gravitons propagating over Minkowski spacetime) fails, because they bring to a non-renormalizable theory. Nowadays there are essentially two research programs that can be considered a candidate theory of QG: String Theory and Loop Quantum Gravity (LQG). The first is an attempt to unify all interactions, based on the physical assumption that elementary object are extended, rather then point-like, but still it is not clear if it is background independent. LQG has the main objective to combine General Relativity and Quantum Mechanics (but it is possible to include also matter) and it is a "canonical" quantization of Hamiltonian General Relativity. In brief, the Loop Quantum Gravity main features are:

- It implements the teaching of General Relativity. First, the world is relational; only events independent from coordinates are meaningful; physics must be described by generally covariant theories. Second, the gravitational field is the geometry of spacetime. The spacetime geometry is fully dynamical: the gravitational field defines the geometry on top of which its own degrees of freedom and those of matter fields propagate. GR is not a theory of fields moving on a curved background geometry; GR is a theory of fields moving on top of each other (7), namely it is background independent.

- It assumes QM, suitably formulated to be compatible with general covariance, to be correct; also the Einstein equations, though they can be modified at high energy, are assumed correct.
- It is non perturbative: the metric is not split in a Minkowskian background plus a perturbation.
- There are not extra-dimensions: it is formulated in four spacetime dimensions.
- It predicts a discrete combinatorial structure for quantum spacetime: the spectrum of quantum geometrical observables, such as the length, the area and the volume operator, is discrete (8) and the quantum states of geometry are defined in relationals terms. Moreover it is UV finite.
- Its application in cosmology gave rise to Loop Quantum Cosmology (9). Some of the main results achieved by this theory are the explanation of the Bekenstein-Hawking formula for black-hole entropy (10; 11; 12; 13) and the absence of the initial big bang singularity (14).

At the moment, while the kinematics of the theory it is pretty clear, there are ambiguities in the definition of the dynamics. The Spinfoam formalism is an attempt to define the Lagrangian covariant version of LQG. In this context it is easier to implement the dynamics; in fact there are many spinfoam models and the hope is to find some of them equivalent to Loop Quantum Gravity (the kinematical equivalence has been already proven ((15)), and the full equivalence is proven in 3-dimensions (16)), in analogy with ordinary Quantum Mechanics which admits both the Hamiltonian canonical formulation and the path integral representation.
As we said above, we do not have the support of experiments, but one strong indication of the viability of the theory would be the recovering of the semiclassical limit, together with the internal consistency. The two main directions in studying the semiclassical limit are the comparison of n-point functions computed in LQG with the ones of perturbative quantum gravity , and the propagation of semiclassical wave packets, introduced by myself in a joint work with C. Perini and C. Rovelli (17).
The main problem in the first approach is to define n-point functions which are background independent; the dependence on the n points seems indeed to disappear if we implement diffeomorphism invariance. We can get over this difficulty in the context of general boundary formulation of Quantum Field Theory (18). In (19) is presented a surprising result: the calculation of some components of graviton propagator gives the Newton law $1/L^2$.
One technical point in the calculation of graviton propagator is the gauge choice; in fact Loop Quantum Gravity calculations involve gauge choices that can be interpreted as putting the linearized gravitational field in radial gauge (i.e. the graviton field has vanishing radial components); but perturbative quantum gravity Feynman rules are mostly known in harmonic gauge, so a direct comparison seems to be not viable. The first original result presented in this thesis is the proof of compatibility between radial and harmonic gauge in linearized General Relativity and of radial and Lorenz gauge in electromagnetism (20). Thanks to this result, it is possible in principle to compare the full tensorial structure of the LQG propagator with the one of the standard propagator. Moreover it is an interesting result in classical field theory by itself.

The full propagator is calculated in (21) using the Barrett-Crane spinfoam model, and the calculation shows that some components are constant; from this analysis follows that the spinfoam model used to implement dynamics is inadequate, because it freezes some degrees of freedom. The result in (21) was followed by a big effort to find spinfoam models able to correct this problem, and some new spinfoam models were born (15; 22; 23; 24). At this point, to verify the viability of these models, it is necessary to calculate the corrected graviton propagator, but to do that we must know the large distance asymptotic of the vertex of these new spinfoam models. Essentially, spinfoam vertices correspond to combinatorial symbols: for example, in three dimensions the vertex is proportional to the Wigner $6j$-symbol.
The second original result presented in this thesis is the analytical asymptotic formula for the fusion coefficients (25), which are a building block of the EPRL vertex (22) (that is the generalization of EPR for arbitrary values of the Immirzi parameter). A consequence of our asymptotic analysis is the following remarkable semiclassical property of the fusion coefficient: they map semiclassical $SO(3)$ tetrahedra into semiclassical $SO(4)$ tetrahedra; this is an highly non trivial property which sheds light on the classical limit of the EPRL model. The missing piece is the asymptotic formula for the $15j$-symbol, and we are still working on it.
Now we come to the second technique, complementary to the calculation of n-point functions, in the study of the semiclassical limit: the semiclassical wave packet propagation. The introduction of this approach (17) and its improvement (26) are one of the most important original contribute.
The idea is as old as quantum physics: in ordinary Quantum Mechanics, a theory has the correct semiclassical limit, if semiclassical wavepackets follow the trajectory predicted by classical equations of motion. The equations of motion of any dynamical system can be expressed as constraints on the set formed by the initial, final and (if it is the case) boundary variables. For instance, in the case of the evolution of a free particle in the time interval t, the equations of motion can be expressed as constraints on the set $(x_i, p_i; x_f, p_f)$. These constraints are of course $m(x_f - x_i)/t = p_i = p_f$ (for the general logic of this approach to dynamics, see (7)). In General Relativity, Einstein equations can be seen as constraints on boundary variables; we can construct in Loop Quantum Gravity semiclassical wave packets centered on the classical value of geometrical conjugate quantities (intrinsic and extrinsic curvature, analogous to x and p). It follows immediately from these considerations that a boundary wave packet centered on these values must be correctly propagated by the propagation kernel, if the vertex amplitude is to give the Einstein equations in the classical limit.
We studied numerically the propagation of some degrees of freedom of LQG, finding a surprisingly good semiclassical behavior. The propagation of semiclassical equilateral tetrahedra in the boundary of a 4-simplex is perfectly "rigid", i.e. four Gaussian wavepackets evolve into one Gaussian wavepacket with the same parameters, except for a flip in the phase. This is in agreement with the classical flat solution of Einstein equations. We showed this result in two independent ways: the first is semi-analytical and is based on a numerical result on the $15j$-symbol viewed as a propagation kernel, and on the the asymptotic properties of the fusion coefficients studied in (25); the second is purely numerical. We regard our results as a strong indication that the EPR model has the good semiclassical limit; in (26) we present also the numerical calculation of other physical interesting observables. We believe that this new approach

is very promising and there are still unexplored possibilities.

2 Hamiltonian General Relativity

In this section we briefly summarize the Hamiltonian formulation of General Relativity. The Hamiltonian is a linear combination of constraints; these constraints define the dynamics of General Relativity. In order to quantize the theory, we perform a suitable change of variables: we introduce the Ashtekar-Barbero variables. We express the constraints in these new variables and write their algebra. We conclude introducing the concept of holonomy which will play a major role in the quantum theory.

2.1 *Canonical formulation of General Relativity in ADM variables*

Hamiltonian formulation of a field theory requires the splitting of the spacetime in space and time (27; 28; 29; 30; 31). The first step consists in choosing a time function t and a vector field t^μ on the spacetime such that the hypersurfaces Σ_t at constant t are Cauchy spacelike surfaces and $t^\mu \nabla_\mu t = 1$.
The second step consists in defining a configuration space of fields q on Σ_t and conjugate momenta Π.
The last step consists in defining a Hamiltonian: a functional $H[q, \Pi]$ of the form

$$H = \int_{\Sigma_t} \mathcal{H}(q, \Pi)\,, \tag{1}$$

where $\mathcal{H}$ is the Hamiltonian density; the Hamilton equations $\dot{q} = \frac{\delta \mathcal{H}}{\delta \Pi}$ and $\dot{\Pi} = -\frac{\delta \mathcal{H}}{\delta q}$ are equivalent to the field equations of Lagrangian theory.
Given the Lagrangian formulation there is a standard prescription to obtain the Hamiltonian one defining

$$\mathcal{H}(q, \Pi) = \Pi\, \dot{q} - \mathscr{L}\,, \tag{2}$$

where $\dot{q} = \dot{q}(q, \Pi)$ and $\Pi = \frac{\partial \mathcal{L}}{\partial \dot{q}}$.
Now come to General Relativity (32). Consider a globally hyperbolic spacetime $(M, g_{\mu\nu})$; this can be foliated in Cauchy surfaces, Σ_t, parametrized by a global time function $t(x^0, x^1, x^2, x^3)$. Take n^μ the unitary vector field normal to Σ_t. The spacetime metric induces a spatial metric $h_{\mu\nu}$ on every Σ_t given by the formula

$$h_{\mu\nu} = g_{\mu\nu} + n_\mu n_\nu\,. \tag{3}$$

The metric $h_{\mu\nu}$ is spatial in the sense that $h_{\mu\nu} n^\mu = 0$. Take t^μ a vector field on M satisfying $t^\mu \nabla_\mu t = 1$; we decompose it in its tangent and normal components to Σ_t

$$t^\mu = N^\mu + N n^\mu\,, \tag{4}$$

where

$$N = -t^\mu n_\mu = (n^\mu \nabla_\mu t)^{-1}\,, \tag{5}$$

$$N_\mu = h_{\mu\nu} t^\nu\,. \tag{6}$$

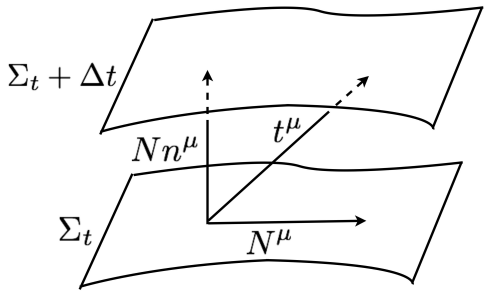

Figure 1: ADM foliation

We can interpret the vector field t^μ as the "flux of time" across spacetime, in fact we "move forward in time" with the parameter t starting from the surface Σ_0 and reaching the surface Σ_t. If we identify the hypersurfaces Σ_0 and Σ_t through diffeomorphism obtained following the integral curves of t^μ, we can reinterpret the effect of moving through the time as the changing of the spatial metric on a *fixed* 3-dimensional manifold Σ from $h_{ab}(0)$ to $h_{ab}(t)$. Hence we can view a globally hyperbolic spacetime as the representation of a time evolution of a Riemannian metric on a fixed 3-dimensional manifold.
The quantity N is called lapse function and measures the flow of proper time with respect to the time coordinate t when we move in a direction normal to Σ_t. N^μ is called shift vector and it measures the shift of t^μ in direction tangent to Σ_t. N and N^μ are not considered as dynamical because they describe only the way of moving through time. Suitable initial data of the Cauchy problem for General Relativity are the spatial metric $h_{\mu\nu}$ on Σ_0 and its "time derivative". The notion of time derivative of a spatial metric on Σ_t is provided by the extrinsic curvature

$$K_{\mu\nu} \equiv \nabla_\mu \xi_\nu \,, \tag{7}$$

where ξ_ν is the unitary timelike vector field tangent to the timelike geodesics normal to Σ_t (ξ^μ is equal to n^μ on Σ_t). $K_{\mu\nu}$ is purely spatial; it can be expressed as a Lie derivative

$$K_{\mu\nu} = \frac{1}{2}\mathcal{L}_\xi g_{\mu\nu} = \frac{1}{2}\mathcal{L}_\xi h_{\mu\nu} \,; \tag{8}$$

If we choose $N^\mu = 0$,

$$K_{\mu\nu} = \frac{1}{2}\frac{\partial h_{\mu\nu}}{\partial t} \,. \tag{9}$$

In terms of N, N^μ and t^μ, the metric is

$$g^{\mu\nu} = h^{\mu\nu} - n^\mu n^\nu = h^{\mu\nu} - N^{-2}(t^\mu - N^\mu)(t^\nu - N^\nu) \,, \tag{10}$$

where we have used that $n^\mu = N^{-1}(t^\mu - N^\mu)$.

2.2 *Lagrangian analysis*

The Lagrangian density for General Relativity in empty space is $\mathscr{L}_{\rm GR} = (2\kappa)^{-1}\sqrt{-g}R$ where R is the Ricci scalar and $\kappa = 8\pi G/c^3$. The action of General Relativity is then

$$S_{\rm GR} = \frac{1}{2\kappa}\int \mathrm{d}^4x\sqrt{-g}R\,. \tag{11}$$

It is convenient to use the variables N, N^μ and $h_{\mu\nu}$ instead of $g_{\mu\nu}$; in terms of these variables we obtain

$$\mathscr{L}_{\rm GR} = \frac{1}{2\kappa}\sqrt{h}\,N[{}^{(3)}R + K_{\mu\nu}K^{\mu\nu} - K^2]\,, \tag{12}$$

where $K_{\mu\nu}$ can be written as

$$K_{\mu\nu} = \frac{1}{2N}[\dot{h}_{\mu\nu} - D_\mu N_\nu - D_\nu N_\mu]\,, \tag{13}$$

D_μ is the covariant derivative with respect to $h_{\mu\nu}$, ${}^{(3)}R$ is the Ricci scalar calculated with respect to $h_{\mu\nu}$, and $\dot{h}_{\mu\nu} = h_\mu{}^\rho h_\nu{}^\sigma \mathcal{L}_t h_{\rho\sigma}$.
The momentum conjugate to $h_{\mu\nu}$ is

$$\Pi^{\mu\nu} = \frac{\delta L}{\delta\dot{h}_{\mu\nu}} = \frac{1}{2\kappa}\sqrt{h}(K^{\mu\nu} - Kh^{\mu\nu})\,. \tag{14}$$

The Lagrangian does not contain any temporal derivative of N and N^a, so their conjugate momenta are zero. N and N^a are not dynamical variables as noticed before, so they must be considered as Lagrange multipliers in the Lagrangian.
Variation of the action (11) w.r.t. shift and lapse produces the following constraints:

$$V^\nu[h,\Pi] \equiv -2D_\mu(h^{-1/2}\Pi^{\mu\nu}) = 0\,, \tag{15}$$

$$S[h,\Pi] \equiv -(h^{1/2}[{}^{(3)}R - h^{-1}\Pi_{\rho\sigma}\Pi^{\rho\sigma} + \frac{1}{2}h^{-1}\Pi^2]) = 0\,. \tag{16}$$

The first is called vector constraint, and the second scalar constraint. These constraints, together with the Hamilton equations

$$\dot{h}_{\mu\nu} = \frac{\delta H}{\delta\Pi^{\mu\nu}}\,, \tag{17}$$

$$\dot{\Pi}^{\mu\nu} = -\frac{\delta H}{\delta h_{\mu\nu}}\,, \tag{18}$$

define the dynamics of General Relativity; i.e. they are equivalent to vacuum Einstein's equations. Finally, the Hamiltonian density is

$$\mathcal{H}_{\rm GR} = \frac{1}{2\kappa}h^{1/2}\{N[-{}^{(3)}R + h^{-1}\Pi_{\mu\nu}\Pi^{\mu\nu} - \frac{1}{2}h^{-1}\Pi^2] - 2N_\nu[D_\mu(h^{-1/2}\Pi^{\mu\nu})]\}\,. \tag{19}$$

We deduce that the Hamiltonian is a linear combination of (first class) constraints, i.e. it vanishes identically on the solutions of equations of motion. This is a general property of generally covariant systems.
The variables chosen in this formulation are called ADM (Arnowitt, Deser and Misner) (33) variables. We note that ADM variables are tangent to the surface Σ_t, so we can use equivalently the genuine 3-dimensional quantities h_{ab}, Π^{ab}, N^a, N $(a, b = 1, 2, 3)$; these are the pull back on Σ_t of the 4-dimensional ones. Since the 4-dimensional variables that we have used are equivalent to 3-dimensional variables, the 20 equations (17) and (18) reduces to 12.

2.3 *Triad formalism*

The spatial metric h_{ab} can be written as (34)

$$h_{ab} = e^i_a e^j_b \delta_{ij} \qquad i, j = 1, 2, 3\,; \tag{20}$$

$e^i_a(x)$ is one possible transformation which permits to write the metric in the point x in flat diagonal form. The index i of e^i_a is called internal and e^i_a is called a triad, because it defines a set of three 1-forms. We can introduce the densitized inverse triad

$$E^i_a \equiv \frac{1}{2}\epsilon_{abc}\epsilon^{ijk} e^j_b e^k_c\,; \tag{21}$$

using this definition, the inverse metric h^{ab} can be related to the densitized triad as follows:

$$h\, h^{ab} = E^a_i E^b_j\, \delta^{ij}\,. \tag{22}$$

We also define

$$K^i_a \equiv \frac{1}{\sqrt{\det(E)}} K_{ab} E^b_j \delta^{ij}\,. \tag{23}$$

It is not difficult to see that E^a_i and K^i_a are conjugate variables, so the symplectic structure is

$$\{E^a_j(x), K^i_b(y)\} = \kappa\, \delta^a_b \delta^i_j \delta(x, y)\,, \tag{24}$$

$$\{E^a_j(x), E^b_i(y)\} = \{K^j_a(x), K^i_b(y)\} = 0\,. \tag{25}$$

We can write the vector and the scalar constraint (15-16) in terms of the new conjugate variables E^a_i and K^i_a. However these variables are redundant; in fact we are using the nine E^a_i to describe the six independent components of h^{ab}. This is clear also from a geometrical point of view: we can choose different triads e^i_a by local $SO(3)$ rotations acting on the internal index i without changing the metric:

$$R^i{}_m(x) R^j{}_n(x) e^m_a(x) e^n_b(x) \delta_{ij} = e^i_a e^j_b \delta_{ij}. \tag{26}$$

Hence if we want to formulate General Relativity in terms of these redundant variables we have to impose an additional constraint that makes the redundancy manifest. The missing constraint is:

$$G_i(E^a_j, K^j_a) \equiv \epsilon_{ijk} E^{aj} K^k_a = 0. \tag{27}$$

2.4 *Ashtekar-Barbero variables*

In the LQG approach the action that is quantized is the Holst action (35), obtained adding to the action of General Relativity a term that does not change the equations of motion

$$S_{\text{Holst}} = -\frac{1}{2\kappa}\int_{\mathcal{M}}\left[{}^*(e\wedge e)\wedge R + \frac{1}{\gamma}(e\wedge e)\wedge R\right] - \frac{1}{2\kappa}\int_{\partial\mathcal{M}}\left[{}^*(e\wedge e)\wedge R + \frac{1}{\gamma}(e\wedge e)\wedge R\right], \quad (28)$$

where γ is any non vanishing real number, called Immirzi parameter; e is a tetrad, the four dimensional extension to the triad; R is the curvature of the connection defined as $R = \mathrm{d}A + A\wedge A$. The introduction of the Holst term is *required* for the canonical formailsm in order to have a dynamical theory of connections: without it, as shown by Ashtekar, the connection variable does not survive the Legendre transform (36). If we consider this action, the variable conjugate to E^a_i is, instead of K^i_a, the Ashtekar-Barbero connection (37; 38; 39; 40)

$$A^a_i = \Gamma^i_a + \gamma K^i_a\,, \quad (29)$$

where Γ^a_i is the spin connection, giving the rule of triad parallel transport

$$\Gamma^i_a = -\frac{1}{2}\epsilon^{ij}{}_k e^b_j(\partial_{[a}e^k_{b]} + \delta^{kl}\delta_{ms}e^c_l e^m_a\partial_b e^s_c)\,, \quad (30)$$

A^i_a is a connection that transforms in the standard inhomogeneous way under local $SO(3)$ transformations. The Poisson bracket of the new variables are

$$\{E^a_j(x), A^i_b(y)\} = \kappa\gamma\,\delta^a_b\delta^i_j\delta(x,y)\,, \quad (31)$$

$$\{E^a_j(x), E^b_i(y)\} = \{A^j_a(x), A^i_b(y)\} = 0\,. \quad (32)$$

2.5 *Constraint algebra*

As we have seen in the previous section, General Relativity can be formulated in terms of a real $SO(3)$ (or $SU(2)$) connection $A^i_a(x)$[1] and a 3d real momentum field $E^a_i(x)$, defined on a three-dimensional space Σ. On physical solutions the connection A^i_a is given by (29) The theory is defined by the Hamiltonian system constituted by three constraints (27), (15), (16). In terms of the variables (E^a_i, A^i_a) they read

$$\begin{array}{ll} G_i \equiv & D_a E^a_i = 0\,, \qquad \text{Gauss law} \\ V_b \equiv & E^a_i F^i_{ab} - (1+\gamma^2)K^i_b G_i = 0\,, \\ S \equiv & \frac{E^a_i E^b_j}{\sqrt{\det(E)}}(\epsilon^{ij}{}_k F^k_{ab} - 2(1+\gamma^2)K^i_{[a}K^j_{b]}) = 0\,, \end{array} \quad (33)$$

where D_a and F^i_{ab} are respectively the covariant derivative and the curvature of A^i_a defined by

$$D_a v_i = \partial_a v_i - \epsilon_{ijk}A^j_a v^k\,, \quad (34)$$

$$F^i_{ab} = \partial_a A^i_b - \partial_b A^i_a + \epsilon^i{}_{jk}A^j_a A^k_b\,. \quad (35)$$

[1] $SO(3)$ and $SU(2)$ have the same algebra, so we can choose both a connection with values in $\mathfrak{su}(2)$ and $\mathfrak{so}(3)$. In the literature is more common the second choice but recent results seems to indicate that the first one is more natural.

We can rewrite the constraints using the following equation

$$E_i^a(x) = \frac{\delta \mathcal{S}[A]}{\delta A_a^i(x)}, \tag{36}$$

where $\mathcal{S}[A]$ is the Hamilton functional, a solution of Hamilton-Jacobi equation. It is defined as the value of the action concerning a region $\mathcal{R}$ with boundary $\partial\mathcal{R} = \Sigma$, calculated on the solution of field equations determined by the configuration of A on the boundary (actually, the argument of $\mathcal{S}$ is the value of A on the boundary). Indeed one configuration of A on the boundary Σ determines a solution (e_μ^I, A_μ^I) of Einstein equations in the region $\mathcal{R}$; this solution induces on Σ a 3-dimensional field $E_a^i[A]$.
Substituting the equation (36) into the system (33) it can be shown that the first two equations require the invariance of $\mathcal{S}[A]$ under both local $SO(3)$ transformations and 3-dimensional diffeomorphism, and the last is the Hamilton-Jacobi equation for General Relativity defining dynamics. To verify this invariance it suffices to write the constraints in a regularized form integrating them against suitable "test" functions:

$$G(\alpha) \equiv \int_\Sigma \mathrm{d}^3x\, \alpha^i G_i(E_j^a, A_a^j) = \int_\Sigma \mathrm{d}^3x\, \alpha^i D_a E_i^a = 0, \tag{37}$$

where α is a vector field in the internal space (a section of the vector bundle). A direct calculation implies

$$\delta_\alpha A_a^i = \big\{A_a^i, G(\alpha)\big\} = -D_a\alpha^i \qquad \text{and} \qquad \delta_\alpha E_i^a = \{E_i^a, G(\alpha)\} = [E^a, \alpha]_i\,.$$

If we write $A_a = A_a^i\tau_i \in \mathfrak{so}(3)$ and $E^a = E_i^a\tau^i \in \mathfrak{so}(3)$ where τ^i are $SO(3)$ generators, we can write the finite version of the previous transformations

$$A'_a = gA_ag^{-1} + g\partial_a g^{-1} \qquad \text{and} \qquad E'^a = gE^ag^{-1}\,,$$

that is the standard transformation of the connection and of the electric field under gauge transformations in Yang-Mills theory. Recall that the gauge group of General Relativity written in triad formalism is $SO(3)$. The vector constraint V_b generates 3-dimensional diffeomorphisms on Σ; this is clear from the action of the smeard constraint

$$V(f) \equiv \int_\sigma \mathrm{d}^3x\, f^a V_a = \int_\sigma \mathrm{d}^3x\, f^a E_i^b F_{ba}^i = 0 \tag{38}$$

on canonical variables, where f is a vector field on Σ:

$$\delta_f A_a^i = \big\{A_a^i, V(f)\big\} = \mathcal{L}_f A_a^i = f^b F_{ab}^i \qquad \text{and} \qquad \delta_f E_i^a = \{E_i^a, V(f)\} = \mathcal{L}_f E_i^a\,,$$

the exponentiation of these infinitesimal transformations brings to the action of finite diffeomorphisms of Σ on the fundamental variables. So $V(f)$ acts as the infinitesimal diffeomorphism

associated to the vector field f. Finally, one can show that the scalar constraint S generates the time evolution of the surface Σ_t, up to spatial diffeomorphisms and local $SO(3)$ gauge transformations. In fact the Hamiltonian of General Relativity $H[\alpha, N^a, N]$ can be written as

$$H[\alpha, N^a, N] = G(\alpha) + V(N^a) + S(N)\,, \tag{39}$$

where

$$S(N) = \int_\Sigma \mathrm{d}^3x\, NS(E^a_i A^i_a)\,. \tag{40}$$

The Hamilton equations of motion are therefore

$$\dot{A}^i_a = \{A^i_a, H[\alpha, N^a, N]\} = \{A^i_a, G(\alpha)\} + \{A^i_a, V(N^a)\} + \{A^i_a, S(N)\}\,, \tag{41}$$
$$\dot{E}^a_i = \{E^a_i, H[\alpha, N^a, N]\} = \{E^a_i, G(\alpha)\} + \{E^a_i, V(N^a)\} + \{E^a_i, S(N)\}\,. \tag{42}$$

These equations define the action of $S(N)$ on observables (functions on the phase space), that is their time evolution up to diffeomorphism and gauge transformations. In General Relativity coordinate time evolution has no physical meaning; it is analogous to a $U(1)$ gauge transformation in QED.

The constraint algebra is:

$$\{G(\alpha), G(\beta)\} = G([\alpha, \beta])\,, \tag{43}$$
$$\{G(\alpha), V(f)\} = G(\mathcal{L}_f \alpha)\,, \tag{44}$$
$$\{G(\alpha), S(N)\} = 0\,, \tag{45}$$
$$\{V(f), V(g)\} = V([f, g])\,, \tag{46}$$
$$\{S(N), V(f)\} = -S(\mathcal{L}_f N)\,, \tag{47}$$
$$\{S(N), S(M)\} = V(\overline{f}) + \text{terms proportional to Gauss law}\,, \tag{48}$$

where $\overline{f}^a = h^{ab}(N\partial_b M - \partial_b N)$.
Now we introduce a the concept of holonomy which has a major role in the quantization of General Relativity.

2.6 *The holonomy*

The holonomy is the matrix of parallel transport along a curve, i.e. the matrix that applied to a vector has the same effect of parallel transport the vector along the curve. Consider a connection A on a vector bundle with base M and structure group G, and a curve γ on the base manifold M parametrized as

$$\gamma : [0, 1] \to M \tag{49}$$
$$s \mapsto x^\mu(s). \tag{50}$$

The holonomy $H[A,\gamma]$ of the connection A along the curve γ is the element of G defined as follows: consider the differential equation

$$\frac{\mathrm{d}}{\mathrm{d}s}h[A,\gamma](s) + \dot{x}^\mu(s)A_\mu(\gamma(s))h[A,\gamma](s) = 0, \tag{51}$$

with initial data

$$h[A,\gamma](0) = \mathbb{1}\,, \tag{52}$$

where $h[A,\gamma](s)$ is a G-valued function of the parameter s. The solution to this Cauchy problem is

$$h[A,\gamma](s) = \mathcal{P}\exp\int_0^s \mathrm{d}\tilde{s}\,\dot{\gamma}^\mu(\tilde{s})A^i_\mu(\gamma(\tilde{s}))\tau_i\,, \tag{53}$$

where τ_i is a basis of the Lie algebra of the group G and the path order exponential $\mathcal{P}$ is defined by the series

$$\mathcal{P}\exp\int_0^s \mathrm{d}\tilde{s}\,A(\gamma(\tilde{s})) \equiv \sum_{n=0}^{\infty}\int_0^s \mathrm{d}s_1\int_0^{s_1}\mathrm{d}s_2 ... \int_0^{s_n-1}\mathrm{d}s_n\,A(\gamma(s_n))...A(\gamma(s_1))\,. \tag{54}$$

The holonomy is

$$H[A,\gamma] \equiv \mathcal{P}\exp\int_0^1 \mathrm{d}s\,A^i(s)\tau_i = \mathcal{P}\exp\int_\gamma A\,. \tag{55}$$

The connection A is the rule that defines the meaning of parallel transport of an internal vector from a point of M to another near point: the vector v in x is defined parallel to the vector $v + A_\mu \mathrm{d}x^\mu v$ in $x + \mathrm{d}x$. The holonomy gives the parallel transport for points at finite distance. A vector is parallel transported along γ into the vector $H[A,\gamma]v$. Even if there is a finite set of points where γ is not smooth and A is not defined, the holonomy of a curve γ is well defined. The reason is that we can break γ in pieces, where everything is smooth, and we can define the holonomy of γ as the product of the holonomies of the single pieces.

3 The structure of Loop Quantum Gravity

In this section we perform the quantization and get into Loop Quantum Gravity; we search for states that satisfy the constraints, and construct some geometrical operators. We discover that area and volume operators have discrete spectrum: this discreteness is one on the most important results of Loop Quantum Gravity.

3.1 *Kinematical state space* $\mathcal{K}$

We can quantize Hamiltonian General Relativity in the Ashtekar-Barbero variables defining the theory in terms of Schrödinger wave functionals $\Psi[A]$ on $\mathcal{G}$ (the space of smooth connections A defined on a 3-dimensional surface Σ) and interpreting the action $S[A]$ as $\hbar$ times the phase of $\Psi[A]$, i.e. interpreting the classical Hamilton-Jacobi theory as the iconal approximation of the quantum wave equation; this can be obtained substituting the derivative of Hamilton functional (the electric field) with derivative operators. The first two constraints require the invariance of

$\Psi[A]$ both under $SO(3)$ gauge transformations, and 3-dimensional diffeomorphism. Imposing the Hamiltonian constraint leads to the Wheeler-DeWitt equation that governs the quantum dynamics of space-time.

Cylindrical functions Let $\mathcal{G}$ be the set of smooth 3-dimensional real connections A defined everywhere (except, possibly isolated points) on a 3-dimensional surface Σ with the 3-sphere topology. Consider an ordered collection Γ (graph) of smooth oriented paths γ_l where $l = 1, ...L$ and a smooth complex valued function $f(U_1, ...U_L)$ of L group elements. A couple (Γ, f) defines the complex functional of A

$$\Psi_{\Gamma,f}[A] \equiv f(H[A, \gamma_1], ..., H[A, \gamma_L])\,; \tag{56}$$

we call these functionals "cylindrical functions"; their linear span is denoted with $\mathcal{S}$. In an suitable topology $\mathcal{S}$ is dense in the space of continuous functionals of A.

Scalar product on $\mathcal{S}$ If two functionals $\Psi_{\Gamma,f}[A]$ and $\Psi_{\Gamma,g}[A]$ are supported on the same oriented graph Γ, define

$$< \Psi_{\Gamma,f}, \Psi_{\Gamma,g} > \equiv \int \mathrm{d}U_1, ...\mathrm{d}U_L \overline{f(U_1, ...U_L)} g(U_1, ...U_L), \tag{57}$$

where $\mathrm{d}U$ is the Haar measure over $SO(3)$ (invariant measure over the group with respect to the group itself). It is possible to extend this definition also to functionals defined on different graphs. If Γ and Γ' are two disjointed graphs constituted respectively by n and n' curves, define $\Gamma'' = \Gamma \bigcap \Gamma'$ constituted by $n + n'$ curves,

$$\tilde{f}(U_1, \ldots, U_n, U_{n+1}, \ldots U_{n+n'}) \equiv f(U_1 \ldots, U_n)\,, \tag{58}$$
$$\tilde{g}(U_1, \ldots, U_n, U_{n+1}, \ldots U_{n+n'}) \equiv g(U_{n+1} \ldots, U_{n+n'})\,; \tag{59}$$

then define the scalar product as

$$< \Psi_{\Gamma,f}, \Psi_{\Gamma',g'} > \equiv < \Psi_{\tilde{\Gamma},\tilde{f}}, \Psi_{\tilde{\Gamma},\tilde{g}} > \ . \tag{60}$$

If Γ and Γ' are not disjoint, we can break $\Gamma \bigcap \Gamma'$ into the two disjoint pieces Γ and $\Gamma' - (\Gamma \bigcap \Gamma')$, so we are in the previous case.
Notice that here the states do not live on a single lattice Γ, but rather on all possible lattices in Σ, so that there is not a cut-off on short scale degrees of freedom.

Loop states and loop transform An interesting example of states with finite norm is when $(\Gamma, f) = (\alpha, \mathrm{Tr})$, i.e. when Γ is constituted by a single closed curve α (a loop) and f is the trace on the group[2]:

$$\Psi_{\alpha,\mathrm{Tr}}[A] \equiv \Psi_\alpha[A] = \mathrm{Tr}\, H[A, \alpha] = \mathrm{Tr}\, \mathcal{P} e^{\oint_\alpha A}\,. \tag{61}$$

[2]Here the trace is taken in the fundamental representation.

The norm of this state, induced by the scalar product (57), is given by

$$|| \Psi_\alpha ||^2 = \int \mathrm{d}U \mid \mathrm{Tr}\, U \mid^2 = 1. \tag{62}$$

A "multiloop" is a collection $[\alpha] = (\alpha_1, ...\alpha_n)$ of a finite number of loops, and a multiloop state is defined as

$$\Psi_{[\alpha]}[A] = \Psi_{\alpha_1}[A]...\Psi_{\alpha_n}[A] = \mathrm{Tr}\, H[A, \alpha_1] \dots \mathrm{Tr}\, H[A, \alpha_n]\,. \tag{63}$$

The functional on the loop space

$$\Omega_\Psi[\alpha] = < \Psi_\alpha, \Psi > = \Omega_\Psi[\alpha] = \int \mathrm{d}\mu_0[A]\, \mathrm{Tr}\, \mathcal{P} e^{\oint_\alpha A} \Psi[A]\,, \tag{64}$$

is called loop transform of the state $\Psi[A]$. Intuitively it is a sort of infinite dimensional Fourier transform from the A space to the α space. The measure μ_0 is the Ashtekar-Lewandowski measure (41).

Kinematical Hilbert space Define the kinematical Hilbert space $\mathcal{K}$ of quantum gravity as the completion of $\mathcal{S}$ in the norm defined by the scalar product (57), and $\mathcal{S}'$ the topological dual of $\mathcal{S}$; the Gelfand triple $\mathcal{S} \subset \mathcal{K} \subset \mathcal{S}'$ constitutes the kinematical rigged Hilbert space.

The key to construct a basis in $\mathcal{K}$ is the Peter-Weyl theorem: a basis on the Hilbert space of square integrable functions over $SO(3)$ w.r.t. the Haar measure is given by the matrix elements of irreducible representations. The $SO(3)$ irreducible representations are labeled by integer spins j (if we use $SU(2)$ as gauge group we have to consider also semi-integer spins). Call $\mathcal{H}_j \simeq \mathbb{C}^{2j+1}$ the Hilbert space on which is defined the representation j. $\{\overset{j}{R}{}^\alpha{}_\beta\}_{j,\alpha,\beta}$ is a basis for $L^2(SO(3))$, where $\overset{j}{R}{}^\alpha{}_\beta$ are the matrix elements of the j-th irreducible representation. For every graph Γ choose an ordering and an orientation; then a basis in the subspace $\mathcal{K}_\Gamma = L^2[SO(3)^L]$ of cylindrical functions with support on a fixed graph Γ with L paths, is

$$\Psi_{\Gamma, j_l, \alpha_l, \beta_l}[A] \equiv \sqrt{\dim(j_1) \dots \dim(j_L)}\; \overset{j}{R}{}^{\alpha_1}{}_{\beta_1}\left(H[A, \gamma_1]\right) \dots \overset{j_L}{R}{}^{\alpha_L}{}_{\beta_L}\left(H[A, \gamma_L]\right), \tag{65}$$

where $\dim(j) \equiv (2j+1)$ is the dimension of the representation j. The states $\Psi_{\Gamma, j_l, \alpha_l, \beta_l}[A]$ are an orthonormal basis in $\mathcal{K}$. We mention that the Hilbert space $\mathcal{K}$ can be viewed as (i.e. is isomorphic to) an L^2 Hilbert space; it is the space of square integrable functions of the connection w.r.t. the measure μ_0, where the connection is allowed to be distributional.

3.2 *Invariant states under gauge transformations and diffeomorphisms*

The classical Gauss and vector constraint can be implemented in the quantum theory. Functions of connection are quantized as multiplicative operators while the electric field is quantized as a

functional derivative:

$$\widehat{A}^i_a(x)\Psi[A] = A^i_a(x)\Psi[A]\,, \tag{66}$$

$$\widehat{E}^a_i(x)\Psi[A] = -i\hbar\kappa\gamma\frac{\delta}{\delta A^i_a(x)}\Psi[A]\,. \tag{67}$$

The quantum Gauss and vector constraints impose the invariance of Ψ under local $SO(3)$ transformations and diffeomorphisms. Call $\mathcal{K}_{SO(3)}$ the space of $SO(3)$ invariant states, $\mathcal{K}_{Diff}$ the space of states invariant both under $SO(3)$ and diffeomorphisms; call $\mathcal{H}$ the space of solutions of the scalar constraint in $\mathcal{K}_{\rm Diff}$; we have the sequence of Hilbert spaces:

$$\mathcal{K} \stackrel{SO(3)}{\longrightarrow} \mathcal{K}_{SO(3)} \stackrel{\rm Diff}{\longrightarrow} \mathcal{K}_{\rm Diff} \stackrel{H}{\longrightarrow} \mathcal{H}\,. \tag{68}$$

Action of quantum constraints on $\mathcal{K}$ Under local gauge $SO(3)$ transformations

$$g : \Sigma \to SO(3)$$

the connection transforms as

$$A \to A_g = gAg^{-1} + g{\rm d}g^{-1}\,, \tag{69}$$

while the holonomy transforms as

$$U[A,\gamma] \to U[A_g,\gamma] = g(x_f)U[A,\gamma]g(x_i)^{-1}\,, \tag{70}$$

where x_i,$x_f \in \Sigma$ are the initial and final points of the path γ.
Now we can read the action of Gauss constraint on a cylindrical function $\Psi_{\Gamma,f}$. For a given couple (Γ, f) define

$$f_g(U_1...,U_L) \equiv f(g(x^{\gamma_1}_f)U_1 g(x^{\gamma_1}_i)^{-1}, ...g(x^{\gamma_L}_f)U_L g(x^{\gamma_L}_i)^{-1})\,; \tag{71}$$

it is easy to see that quantum states transforms in the following way:

$$\Psi_{\Gamma,f}[A] \mapsto U_g\Psi_{\Gamma,f}[A] \equiv \Psi_{\Gamma,f}[A_{g^{-1}}] = \Psi_{\Gamma,f_{g^{-1}}}[A]\,. \tag{72}$$

Since the Haar measure is invariant under the left and right group action, it follows that the scalar product (57) is invariant under gauge transformations.
Consider now an invertible function $\phi : \Sigma \to \Sigma$ such that the function and its inverse are smooth everywhere, except, possibly, for a finite number of isolated points where they are continuous. Call these functions (indicated with Diff*) extended diffeomorphisms. Under an extended diffeomorphism the connection transforms as a 1-form

$$A \to \phi^* A, \tag{73}$$

and the holonomy transforms as

$$U[A,\gamma] \to U[\phi^* A,\gamma] = U[A,\phi^{-1}\gamma]\,; \tag{74}$$

i.e. applying a diffeomorphism ϕ to A is equivalent to applying the diffeomorphism to the curve γ. So a cylindrical function $\Psi_{\Gamma,f}$ transforms under Diff* as:

$$\Psi_{\Gamma,f}[A] \mapsto \Psi_{\Gamma,f}[\phi^* A] = \Psi_{\phi^{-1}\Gamma,f}[A]\,. \tag{75}$$

It is immediate to verify the invariance under diffeomorphisms of the scalar product: the right hand side of (57) does not depend explicitly on the graph.

Intertwiners Before exhibiting the states which are solutions to the Gauss constraint, it is useful to introduce the *intertwiners*. Consider N irreducible representations $j_1, \dots, j_N$ and their tensor product

$$\mathcal{H}_{j_1 \dots j_N} = \mathcal{H}_{j_1} \otimes \dots \otimes \mathcal{H}_{j_N}\,. \tag{76}$$

The tensor product can be decomposed into a sum of irreducible representations. In particular $\mathcal{H}^0_{j_1 \dots j_N} \subset \mathcal{H}_{j_1 \dots j_N}$ is the subspace formed by invariant vectors, called *intertwiners* between the irreducible representations $j_1, \dots, j_N$; this k-dimensional space decomposes in k trivial irreducible representations. The basis elements of $\mathcal{H}^0_{j_1 \dots j_N}$ are the basis intertwiners.

More explicitly, the elements of $\mathcal{H}_{j_1 \dots j_N}$ are tensors $v^{\alpha_1 \dots \alpha_N}$ with an index in every representation; the elements of $\mathcal{H}^0_{j_1, \dots j_N}$ are invariant tensors $v^{\alpha_1 \dots \alpha_N}$ under the joint action of $SO(3)$ on all their index, i.e. they satisfy

$$\overset{j_1}{R}{}^{\alpha_1}{}_{\beta_1}(U) \dots \overset{j_N}{R}{}^{\alpha_N}{}_{\beta_N}(U)\, v^{\beta_1 \dots \beta_N} = v^{\alpha_1 \dots \alpha_N} \quad \forall\, U \in SO(3)\,. \tag{77}$$

The *intertwiners* $v_i^{\alpha_1 \dots \alpha_N}$ with $i = 1, \dots, k$ are a collection of k such invariant tensors, orthonormal w.r.t. the scalar product of $\mathcal{H}_{j_1 \dots j_N}$, i.e. they satisfy

$$\overline{v_i^{\alpha_1 \dots \alpha_N}} v_{i' \alpha_1 \dots \alpha_N} = \delta_{ii'}\,. \tag{78}$$

Solution to the Gauss constraint: spin-network states Spin-network (42; 43) states are particular cylindrical functions. Given an oriented graph Γ embedded in Σ, be j_l with $l = 1, \dots, L$ irreducible representations associated to the L links of the graph and i_n intertwiners associated to each node. The triple $S = (\Gamma, j_l, i_n)$ is called embedded spin-network; now we can construct the following state associated to a spin-network:

$$\begin{aligned} &\Psi_{\Gamma,\, j_l\, i_n}[A] \equiv \\ &\equiv \sum_{\alpha_l \beta_l} v_{i_1}^{\beta_1 \dots \beta_{n_1}}{}_{\alpha_1 \dots \alpha_{n_1}} v_{i_2}^{\beta_{n_1+1} \dots \beta_{n_2}}{}_{\alpha_{n_1+1} \dots \alpha_{n_2}} \dots v_{i_N}^{\beta_{n_{N-1}+1} \dots \beta_L}{}_{\alpha_{n_{N-1}+1} \dots \alpha_L} \Psi_{\Gamma,\, j_l\, \alpha_l,\, \beta_l}[A]\,. \end{aligned} \tag{79}$$

The pattern of contraction of the indices is dictated by the topology of the graph itself: the index α_l (β_l) of the link l is contracted with the corresponding index of the intertwiner v_{i_n} of the node n where the link l begins (ends).

Spin-network states and their (possibly infinite) linear combinations are invariant under $SO(3)$. Most importantly, they are *all* the invariant states in $\mathcal{K}$. The gauge invariance follows immediately from the invariance of the intertwiners and from the transformation properties (72). Spin-network states are an orthonormal basis for $\mathcal{K}_{SO(3)}$; this basis is not unique as it depends on the choice of an intertwiner basis at each node.

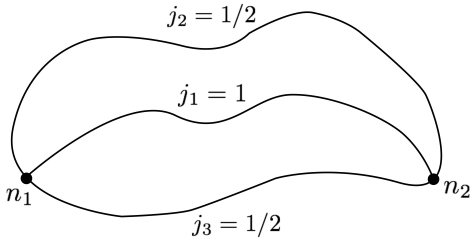

Figure 2: A spin-network with two trivalent nodes

An example Consider for simplicity the $SU(2)$ (instead of $SO(3)$) spin-network in figure (2); we have to associate to each of the two nodes the tensor product of two fundamental and one adjoint $SU(2)$ irreducible representations. Since the tensor product of these representations contains a single trivial representation

$$\frac{1}{2} \otimes \frac{1}{2} \otimes 1 = (0 \oplus 1) \otimes 1 = 1 \oplus 0 \oplus 1 \oplus 2,$$

there is only one possible normalized intertwiner, given by the triple of Pauli matrices: $v^{i,AB} = \frac{1}{\sqrt{3}}\sigma^{i,AB}$. Hence the associated spin-network state is

$$\Psi_S[A] = \overset{1/2}{R}\,(H[A,\gamma_2])^A{}_B\sigma_i{}^B{}_A\,\overset{1}{R}\,(H[A,\gamma_1])^i{}_j\sigma^{j,D}{}_C\,\overset{1/2}{R}\,(H[A,\gamma_3])^C{}_D\,. \tag{80}$$

Four-valent intertwiners: virtual links In the case of 3-valent nodes there is only one possible (normalized) intertwiner; if the node is instead 4-valent, the intertwiner is not unique. A possible basis is obtained by decomposition in virtual links, namely writing the intertwiner as two 3-valent intertwiners with a couple of indices contracted.
Concretely, a basis $\{v_i^{abcd}\}$ for the vector space $\mathrm{Inv}[H_{j_1} \otimes H_{j_2} \otimes H_{j_3} \otimes H_{j_4}]$ is

$$v_i^{abcd} = v^{dae}v_e{}^{bc} = \sqrt{2i+1}$$

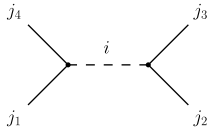

(81)

where a dashed line has been used to denote the virtual link associated to the coupling channel; the index e is in the representation i and the two nodes in the graph represent Wigner $3j$-symbols. The link labeled by i is called virtual link, and the open links labeled by j_1, j_4 are said to be paired. Two other choices of pairing are possible, giving two other bases:

$$\tilde{v}_i^{abcd} = \sqrt{2i+1}$$

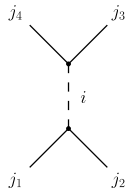

$$, \qquad \tilde{\tilde{v}}_i^{abcd} = \sqrt{2i+1}$$

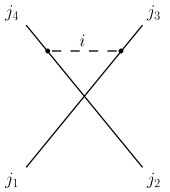

. (82)

The formula for the change of pairing, called recoupling theorem, is

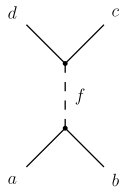

$$= \sum_m \dim(m)(-1)^{b+c+f+m} \left\{ \begin{array}{ccc} a & c & m \\ d & b & f \end{array} \right\}$$

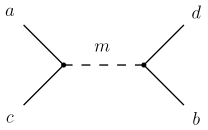

, (83)

where

$$\left\{ \begin{array}{ccc} j_1 & j_2 & j_3 \\ j_4 & j_5 & j_6 \end{array} \right\} \tag{84}$$

is the Wigner $6j$-symbol. The $6j$-symbol is defined as the contraction of four $3j$-symbols, according to the tetrahedral pattern in figure (3).

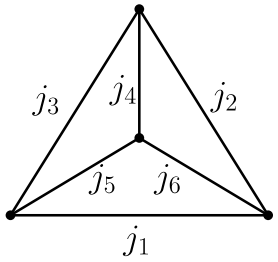

Figure 3: $6j$-symbol

Diffeomorphism invariance Spin-network states $\Psi_S[A]$ are not invariant under diffeomorphisms, because a diffeomorphism can change the graph, hence the state; moreover it can modify the ordering and the orientation of the links. In fact the diffeomorphism invariant states live in $\mathcal{S}'_{SO(3)}$, not in $\mathcal{K}_{SO(3)}$. [3] The action of the diffeomorphism group is defined in $\mathcal{S}'_{SO(3)}$ by the duality

$$(U_\phi \Phi)(\Psi) \equiv \Phi(U_{\phi^{-1}} \Psi) \ , \tag{85}$$

so a diffeomorphism invariant element Φ of $\mathcal{S}'_{SO(3)}$ is a linear functional such that

$$\Phi(U_\phi \Psi) \equiv \Phi(\Psi) \ . \tag{86}$$

We can define a map $P_{\rm Diff} : \mathcal{S}_{SO(3)} \to \mathcal{S}'_{SO(3)}$ as (44; 45):

$$(P_{\rm Diff}\Psi)(\Psi') \equiv \sum_{\Psi''=U_\phi \Psi} < \Psi'', \Psi' >_{SO(3)} \tag{87}$$

[3] $\mathcal{S}'_{SO(3)}$ is formed by the functionals Φ such that $(U_g \Phi)(\Psi) \equiv \Phi(U_{g^{-1}} \Psi) = \Phi(\Psi)$.

The sum is over all the states Ψ'' in $\mathcal{S}_{SO(3)}$ for which there exist a diffeomorphism $\phi \in \text{Diff}^*$ such that $\Psi'' = U_\phi \Psi$; the main point is that this sum is finite, since a diffeomorphism that acts on a spin-network state can either transform it in an orthogonal state, or leave it unchanged, or change the link ordering and orientation, but these latter operations are discrete and contribute only with a multiplicity factor. Clearly $P_{\text{Diff}}\Psi$ is invariant under diffeomorphisms and functionals of the form (87) cover all the diffeomorphism invariant state space, i.e. the image of P_{Diff} is $\mathcal{K}_{\text{Diff}}$. States linked by a diffeomorphism are projected by P_{Diff} in the same element of $\mathcal{K}_{\text{Diff}}$. The scalar product on $\mathcal{K}_{\text{Diff}}$ is naturally defined as

$$< \Phi, \Phi' >_{\text{Diff}} = < P_{\text{Diff}}\Psi, P_{\text{Diff}}\Psi' >_{\text{Diff}} \equiv (P_{\text{Diff}}\Psi)(\Psi') \,. \tag{88}$$

***Knots* and *s-knot* states** Denote $g_k \Psi_S$ the state obtained from a spin-network Ψ_S by a diffeomorphism g_k, where the maps g_k form the discrete subgroup of diffeomorphisms which change only ordering and orientation of the links of the spin-network. It is clear that

$$< P_{\text{Diff}}\Psi_S, P_{\text{Diff}}\Psi'_S >= \begin{cases} 0 & \Gamma \neq \phi\Gamma' \\ \sum_k < \Psi_S, g_k \Psi'_S > & \Gamma = \phi\Gamma' \quad \text{for some } \Phi \in \text{Diff}^* \,. \end{cases} \tag{89}$$

An equivalence class under diffeomorphisms of non oriented graphs is called a *knot*; two spin-networks Ψ_S and $\Psi_{S'}$ define orthogonal states in $\mathcal{K}_{\text{Diff}}$ unless they are in the same equivalence class. So states in $\mathcal{K}_{\text{Diff}}$ are labeled by a knot and they are distinguished only by the coloring of links and nodes. The orthonormal states obtained coloring links and nodes are called spin-knot states, or s-knots (or abstract spin-networks, and, very often, simply spin-networks).

(90)

3.3 *Electric flux operator*

The operators (66) and (67) are not well defined in $\mathcal{K}$. The holonomy operator $\widehat{H}[A, \gamma]$ is a function of A, so it is a multiplicative operator well defined on $\mathcal{S}$:

$$\widehat{H}^A{}_B[A, \gamma]\Psi[A] = H^A{}_B[A, \gamma]\Psi[A] \,. \tag{91}$$

In order to know the action of the electric field operator $\widehat{E}$ on spin-networks, we calculate its action on the holonomy:

$$\frac{\delta}{\delta A^i_a(y)} H[A, \gamma] = \int \mathrm{d}s \, \dot{x}^a(s) \delta^3(x(s), y)(H[A, \gamma_1]\tau_i H[A, \gamma_2]), \tag{92}$$

where s is an arbitrary parametrization of the curve γ, $x^a(s)$ are the coordinates along the curve, γ_1 and γ_2 are the two parts in which γ is divided by the point $x(s)$. Note that the right

side of (92) is a two-dimensional distribution (δ^3 is integrated on ds), hence it is natural to look for an operator well defined in $\mathcal{K}$ regularizing $\hat{E}$ in two dimensions. In fact this operator is the quantization of the electric flux. Consider a two-dimensional surface $\mathbf{S}$ embedded in the three-dimensional manifold Σ; be $\sigma = (\sigma^1, \sigma^2)$ coordinates on $\mathbf{S}$. The surface is defined by $\mathbf{S} : (\sigma^1, \sigma^2) \mapsto x^a(\sigma^1, \sigma^2)$. The quantum electric flux is

$$\widehat{E}_i(\mathbf{S}) \equiv -i\hbar\kappa\gamma \int_{\mathbf{S}} \mathrm{d}\sigma^1 \mathrm{d}\sigma^2 \, n_a(\sigma) \frac{\delta}{\delta A_a^i(\sigma)} \ , \tag{93}$$

where

$$n_a(\sigma) = \epsilon_{abc} \frac{\partial x^b(\sigma)}{\partial \sigma^1} \frac{\partial x^c(\sigma)}{\partial \sigma^2} \tag{94}$$

is the 1-form normal to $\mathbf{S}$. If we now calculate the action of $\widehat{E}_i(\mathbf{S})$ on the holonomy, we obtain

$$\begin{aligned} &\widehat{E}_i(\mathbf{S}) H[A, \gamma] = \\ &- i\hbar\kappa\gamma \int_{\mathbf{S}} \int_{\gamma} \mathrm{d}\sigma^1 \mathrm{d}\sigma^2 \mathrm{d}s \, \epsilon_{abc} \frac{\partial x^a}{\partial \sigma^1} \frac{\partial x^b}{\partial \sigma^2} \frac{\partial x^c}{\partial s} \delta^3(x(\sigma), x(s)) \, H(A, \gamma_1) \tau_i H(A, \gamma_2) \ . \end{aligned} \tag{95}$$

This integral vanishes unless the curve γ and the surface $\mathbf{S}$ intersect. Suppose they have a single intersection; then the result is

$$\widehat{E}_i(\mathbf{S}) H(A, \gamma) = \pm i\hbar H(A, \gamma_1) \tau_i H(A, \gamma_2) \ , \tag{96}$$

where the sign is dictated by the relative orientation of γ w.r.t. $\mathbf{S}$; the action of the operator $\widehat{E}_i(\mathbf{S})$ consists in inserting the matrix $(\pm i\hbar\tau_i)$ at the intersection point; an operation called "grasping". When many intersections p are present (figure 4) the result is

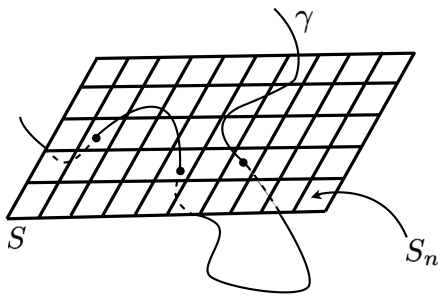

Figure 4: A partition of $\mathbf{S}$

$$\hat{E}_i(\mathbf{S}) H(A, \gamma) = \sum_p \pm i\hbar H(A, \gamma_1^p) \tau_i H(A, \gamma_2^p) \ . \tag{97}$$

The action on an arbitrary representation of the holonomy is

$$\hat{E}_i(\mathbf{S}) \overset{j}{R}(H[A,\gamma]) = \sum_p \pm\hbar\kappa\gamma \overset{j}{R}(H[A,\gamma_1^p]) \overset{j}{\tau}_i \overset{j}{R}(H[A,\gamma_2^p]) \,. \tag{98}$$

3.4 *Area and volume operators*

Area operator The electric field flux $E^i(\mathbf{S})$ is not gauge invariant because it has one $SO(3)$ index; but its modulus is gauge invariant. Now consider the operator $\hat{E}^2$ and suppose that the graph of a spin-network Ψ_S has a single intersection with $\mathbf{S}$. Let j be the spin of the link intersecting $\mathbf{S}$. Each $\hat{E}^i$ inserts a matrix $\overset{j}{\tau}_i$; since $-\overset{j}{\tau}_i\overset{j}{\tau}_i = j(j+1)\mathbb{1}$ is the Casimir of $SO(3)$ in the j representation, the action of the operator $\hat{E}^2$ on the spin-network Ψ_S when there is an intersection between the graph and the surface $\mathbf{S}$ is

$$\widehat{E}^2(\mathbf{S})\Psi_S = (\hbar\kappa\gamma)^2 j(j+1)\Psi_S \,. \tag{99}$$

Now we are ready to quantize the area (8; 46; 47; 48): in General Relativity the physical area of a surface $\mathbf{S}$ is

$$\mathbf{A}(\mathbf{S}) = \int_{\mathbf{S}} \mathrm{d}^2\sigma \sqrt{n_a E_i^a n_b E_i^b} = \lim_{n\to\infty} \sum_n \sqrt{E^2(\mathbf{S}_n)} \,, \tag{100}$$

where $\mathbf{S}_n$ are N smaller surfaces in which $\mathbf{S}$ is partitioned. For N enough large the operator associated to $\mathbf{A}(\mathbf{S})$, acting on a spin-network , is such that every $\mathbf{S}_n$ is intersected at most once by the links of the spin-network. So we have immediately

$$\widehat{\mathbf{A}}(\mathbf{S})\Psi_S = \hbar\kappa\gamma \sum_p \sqrt{j_p(j_p+1)}\, \Psi_S \,. \tag{101}$$

This beautiful result tells us that $\widehat{\mathbf{A}}$ is well defined on $\mathcal{K}$ and spin-networks are eigenfunctions of this operator. Here we have supposed that the spin-network has no nodes on $\mathbf{S}$. We show the result of the complete calculation in the general case:

$$\widehat{\mathbf{A}}(\mathbf{S})\Psi_S = \hbar\kappa\gamma \sum_{u,d,t} \sqrt{\frac{1}{2}j_u(j_u+1) + \frac{1}{2}j_d(j_d+1) + \frac{1}{2}j_t(j_t+1)}\, \Psi_S \,, \tag{102}$$

where u labels the outcoming parts of the links, d the incoming and t the tangent links with respect to the surface. We must stress that the classical quantity $\mathbf{A}(\mathbf{S})$ is precisely the physical area of the surface $\mathbf{S}$, hence we have also a precise physical prediction: every area measure can give only a result in the spectrum of the operator $\hat{\mathbf{A}}(\mathbf{S})$: the area is quantized. The quantum of area carried by a link in the fundamental representation $j = 1$ ($j = 1/2$ for $SU(2)$) is the smaller eigenvalue; its value is of order of the Plank area:

$$\mathbf{A}_0 \approx 10^{-66} cm^2 \qquad (\gamma = 1) \,. \tag{103}$$

Volume operator We now construct an operator $\hat{\mathbf{V}}(\mathcal{R})$ corresponding to the volume of a region $\mathcal{R}$. The volume of a 3-dimensional region $\mathcal{R}$ is given by the expression (8; 49; 50; 51; 52; 53)

$$\mathbf{V}(\mathcal{R}) = \int_{\mathcal{R}} d^3x \sqrt{\frac{1}{3!} \mid \epsilon_{abc} E^a_i E^b_j E^c_k \epsilon^{ijk} \mid} = \lim_{n\to\infty} \sum_n \sqrt{\epsilon_{abc} E_i(S^a) E_j(S^b) E_k(S^c) \epsilon^{ijk}}\,, \qquad (104)$$

where the sum is over the N cubes in which the region $\mathcal{R}$ is partitioned, and S are three sections of the n-th coordinate cube. Now consider the quantization of the right hand side of (104) and consider its action on a spin-network; when N is enough large, then each coordinate cube will contain at most one node. It turns out that spin-networks are eigenstates and the eigenvalues receive one contribution from each node, but the node must be at least 4-valent to give a non zero contribution. The spectrum of the volume is discrete.

3.5 *Physical interpretation of quantum geometry*

Since only the nodes of the spin-network Ψ_S contribute to the volume operator action, the volume of the region $\mathcal{R}$ is a sum of terms, one for every node contained in $\mathcal{R}$, hence every node represents a quantum of volume; these quanta are separated by surfaces whose area is measured by the operator $\mathbf{A}(\mathbf{S})$. All links of Ψ_S that intersect the surface $\mathbf{S}$ contribute to the area spectrum. Two space elements are contiguous if the corresponding nodes are connected by a link l; in this case they are separated by a surface of area $A_l = \hbar\kappa\gamma G\sqrt{j_l(j_l+1)}$ where j_l is the spin associated to the link l. The intertwiners associated to the nodes are the quantum numbers of volume and the spins associated to the links are quantum numbers of area. The graph Γ determines the contiguity relations between the chunks of space, and can be interpreted as the dual graph of a decomposition of the physical space; hence a spin-network state represents the discrete quantized metric.

Also s-knot states have a precise physical interpretation; indeed passing from a spin-network state to an s-knot state we preserve all the information, except for its localization in the 3-dimensional manifold; this is precisely the implementation of the diffeomorphism invariance also in the classical theory, where the physical geometry is an equivalence class of metrics under diffeomorphisms. An s-knot state represents a discrete quantized geometry, it is formed by abstract quanta of space not living on a three-dimensional manifold, they are only localized one respect to another.
One of the most impressive results of LQG is that the theory predicts Plank scale discreteness, on the basis of a standard quantization procedure, in the same manner in which the quantization of the energy levels of an atom is predicted by nonrelativistic Quantum Mechanics.

3.6 *Dynamics*

The quantization of the scalar constraint S is a difficult task mainly for two reason: first of all it is highly non linear, not even polynomial in the fundamental fields A and E. This gives origin to ambiguities and possible ultraviolet divergences; moreover there is no clear geometrical

interpretation of the transformation generated by S. Nevertheless the quantization is possible, and we review the procedure found by Thiemann (54; 55).
The scalar constraint is the sum of two terms:

$$S(N) = S^E(N) - 2(1+\gamma^2)T(N)\,, \tag{105}$$

where E stands for Euclidean. The procedure consists in rewriting S in such a way that the complicated non polynomial structure gets hidden in the volume observable. For example the first term can be rewritten as

$$S^E(N) = \frac{\kappa\gamma}{4}\int_\Sigma \mathrm{d}^3x\, N\epsilon^{abc}\delta_{ij}\, F^j_{ab}\{A^i_c, \mathbf{V}\}\,. \tag{106}$$

In the last expression we know how to quantize the volume and regularize the connection. Given an infinitesimal loop α_{ab} in the ab-plane in the coordinate space, with coordinate area ϵ^2, the curvature tensor F_{ab} can be regularized observing that

$$h_{\alpha_{ab}}[A] - h^{-1}_{\alpha_{ab}}[A] = \epsilon^2 F^i_{ab}\tau_i + \mathcal{O}(\epsilon^4)\,. \tag{107}$$

Similarly the Poisson bracket $\{A^i_a, \mathbf{V}\}$ is regularized as

$$h^{-1}_{e_a}[A]\{h_{e_a}[A], \mathbf{V}\} = \epsilon\{A_a, \mathbf{V}\} + \mathcal{O}(\epsilon^2)\,, \tag{108}$$

where e_a is a path along the $a-$coordinate of coordinate length ϵ. Using this we can write

$$\begin{aligned} S^E(N) &= \lim_{\epsilon\to 0}\sum_I N_I\epsilon^3\epsilon^{abc}\,\mathrm{Tr}[F_{ab}[A]\{A_c, \mathbf{V}\}] = \\ &= \lim_{\epsilon\to 0}\sum_I N_I\epsilon^{abc}\,\mathrm{Tr}[(h_{\alpha^I_{ab}}[A] - h_{\alpha^I_{ab}}[A]^{-1})h^{-1}_{e^I_c}[A]\{h_{e^I_c}, \mathbf{V}\}]\,. \end{aligned} \tag{109}$$

where in the first equality we have replaced the integral in (106) by a sum over cells, labeled with the index I, of coordinate volume ϵ^3. The loop α^I_{ab} is an infinitesimal closed loop of coordinate area ϵ^2 in the $ab-$plane associated to the I-th cell, while the edge e^I_a is the corresponding edge of coordinate length ϵ, dual to the $ab-$plane. If we quantize the last expression in (109) we obtain the quantum scalar constraint

$$\widehat{S}^E(N) = \sum_I N_I\epsilon^{abc}\,\mathrm{Tr}[(\widehat{h}_{\alpha^I_{ab}}[A] - \widehat{h}_{\alpha^I_{ab}}[A]^{-1})\widehat{h}^{-1}_{e^I_c}[A][\widehat{h}_{e^I_c}, \widehat{\mathbf{V}}]]\,. \tag{110}$$

The regulated quantum scalar constraint acts only at spin-network nodes; this is a consequence of the very same property of the volume operator. In fact it acts only at nodes of valence $n > 3$. Due to the action of infinitesimal loop operators representing the regularized curvature, the scalar constraint modify spin-networks by creating new links around nodes, so creating a

triangle in which one vertex is the node:

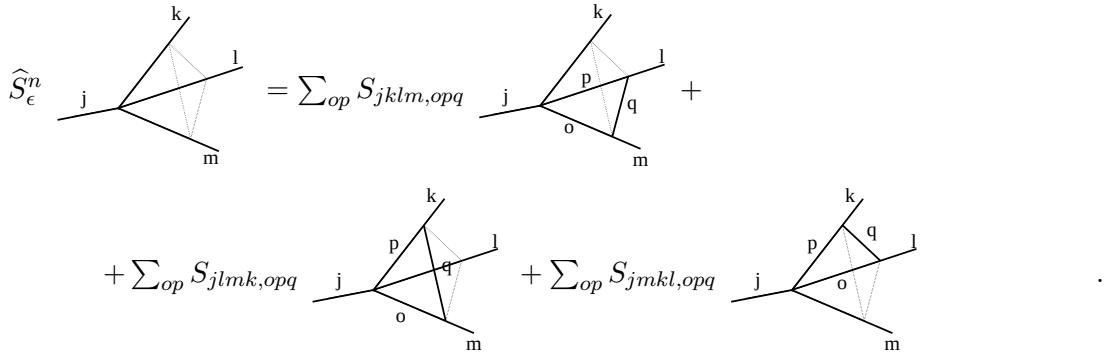

(111)

A similar procedure can be done for the second term in the scalar constraint (105). Now to remove the regulator ϵ we note that the only dependence on ϵ is in the position of the extra link in the resulting spin-network, but in the diffeomorphism invariant context, i.e. when acting on $\mathcal{K}_{\text{Diff}}$, the position of the new link is irrelevant. Hence the limit

$$\langle \Phi, \widehat{S}(N)\Psi\rangle = \lim_{\epsilon\to 0}\langle \Phi, \widehat{S}_\epsilon(N)\Psi\rangle$$

exists trivially for any $\Psi, \Phi \in \mathcal{K}_{\text{Diff}}$.
An important property of the quantum scalar constraint is that the new nodes carry zero volume and they are invisible to a second action of the quantum scalar constraint. There is a non trivial consistency condition on the quantum scalar constraint: it must satisfy the identity (48). The correct commutator algebra is recovered, in the sense that

$$\langle \Phi \mid [\widehat{S}(N), \widehat{S}(M)] \mid \Psi\rangle = 0 \tag{112}$$

for any Φ, Ψ in $\mathcal{K}_{\text{Diff}}$. We say that the quantization of GR does not give rise to anomalies.
Two open issues are the quantization ambiguities (in regularizing the connection we chose the fundamental representation for holonomies but we could choose any; moreover there are operator ordering ambiguities) and L. Smolin's objection of ultra-locality (56). This objection consist in the fact that in the classical theory, given the value of the gravitational field on a closed three dimensional boundary, the scalar constraint induces a constraint on the metric inside, namely it is equivalent to Einstein equations; now, because the quantum scalar constraint acts only in the immediate vicinity of nodes and does not change the value of the spins of the links that connect different nodes, it is not clear how, in the semi-classical context, quantizations of scalar constraint that are ultra-local can impose conditions restricting unphysical degrees of freedom in the interior of a region, once boundary conditions are given.
We should point out that exact solutions of the scalar constraint are known for specific quantizations (57; 58; 59). In the following we deal with the dynamics through another approach: the Spinfoam covariant formulation.

4 Covariant formulation: spinfoam

Spinfoams are a covariant Lagrangian formulation of quantum gravity, which is expected to be equivalent to the Hamiltonian one, that is Loop Quantum Gravity. The equivalence between Lagrangian and Hamiltonian formulation has been proven in three dimensions by Perez and Noui (16); in the four dimensional case the new models (15; 22; 23; 24) show the equivalence at kinematical level. The spinfoam formulation is based on a path integral "à la Feynmann" that implements the sum over geometries; actually the sum is over 2-complexes (spin foams, fig 4.1), i.e. collections of faces, edges and vertices combined together and labeled with the representations of the gauge group. We can think to this formalism as a way to represent the time evolution of spin-networks: we can interpret a spinfoam as an history of spin-networks.
The two formulations have different properties: Lagrangian formalism is simpler, more transparent and keeps symmetries and covariance manifest. The Hamiltonian formalism is more general and rigorous. The Spinfoam formalism allows to calculate explicitly transition amplitudes in quantum gravity between two states with fixed geometry (spin-networks). Recently the spinfoam formalism has been largely developed, mostly because of the difficulties in understanding the LQG dynamics.
In this section we give the definition of spinfoam models and motivate intuitively the reason and the sense in which they are the path integral representation of the action of the scalar constraint. It is easier to start in three dimensions, introducing the Ponzano Regge spinfoam model; this is based on the Regge-triangulation of a 3-dimensional manifold. Then we extend this model to four dimensions obtaining the BF theory. BF theory is not still General Relativity; it becomes General Relativity under the imposition of some constraints. In the quantum theory, imposing strongly these constraints leads to the Barrett-Crane model.

4.1 *Path integral representation*

A spin foam σ is a 2-complex Γ with a representation j_f associated to each face and an intertwiner i_e associated to each edge (60). A spinfoam model (61) is defined by the partition function

$$Z = \sum_{\Gamma} w(\Gamma) Z[\Gamma] \tag{113}$$

where

$$Z[\Gamma] = \sum_{j_f, i_e} \prod_f A_f(j_f) \prod_e A_e(j_f, i_e) \prod_v A_v(j_f, i_e)\,; \tag{114}$$

$w(\Gamma)$ is a weight associated to the 2-complex, A_f, A_e and A_v are the amplitudes associated to faces, edges and vertices. For most models $A_f(j_f)$ is simply the dimension of the representation $\dim(j_f) = 2j_f + 1$. So a spinfoam model is defined by:
1) a set of 2-complexes, and associated weights;
2) a set of representations and intertwiners;
3) a vertex and an edge amplitude.
Let us motivate intuitively the close relation between LQG dynamics and spin foams (62; 63; 64).

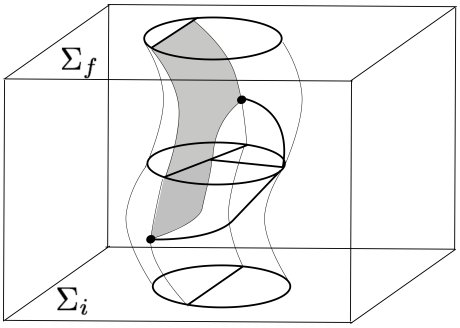

Figure 5: A spin foam seen as evolution of spin-networks

The solutions to the scalar constraint can be characterized by the definition of a generalized projection operator P from the kinematical Hilbert space $\mathcal{H}$ onto the kernel $\mathcal{H}_{\rm phys}$ of the scalar constraint. Formally we can write P as

$$P = \int D[N] \exp i \int_\Sigma N(x) \widehat{S}(x) \,. \tag{115}$$

For any state $\Psi \in \mathcal{K}$, $P\Psi$ is a formal solution of the scalar constraint S. Moreover P naturally defines the physical scalar product

$$< \Psi, \Psi' >_{\rm phys} \equiv < P\Psi, \Psi' >_{\mathcal{K}} \ . \tag{116}$$

The matrix elements between spin-networks states can be expressed as a sum over spin-network histories (65; 66), or spin foams (figure 5):

$$< \Psi_S, \Psi_{S'} >_{\rm Phys} \equiv Z = \sum_\Gamma w(\Gamma) Z[\Gamma] \,. \tag{117}$$

Imagine that the graph moves upward along a "time coordinate" of spacetime, sweeping a worldsheet, changing at each step under the action of S; this worldsheet defines a possible history. An history $\Psi_S \to \Psi_{S'}$ is a 2-complex with boundary given by the graphs of the spin-networks Ψ_S and $\Psi_{S'}$ respectively, whose *faces* (the worldsurfaces of the links of the graphs), are denoted with f, and whose *edges* (the worldlines of the nodes) are denoted as e. Since the scalar constraint acts on nodes, the individual steps in the history can be represented as the branching off of the edges. We call *vertices* the points where edges branch, and denote them as v. We obtain in this manner a collection of faces, meeting at edges, in turn meeting at vertices; the set of those elements and their adjacency relations defines a 2-complex Γ.
The underlying discreteness discovered in LQG is crucial: in the spinfoam representation, the functional integral for gravity is replaced by a sum over amplitudes of combinatorial objects given by foam-like configurations. A spin foam represents a possible history of the gravitational field and can be interpreted as a set of transitions trough different quantum states of space. Boundary data in the path integral are given by quantum states of 3-geometry.

We present also another important feature of the spinfoam models: most of spinfoam amplitudes can be obtained, for a given triangulation, by a particular field theory called group field theory

$$Z[\Gamma] = Z_{\rm GFT}[\Gamma]\,. \tag{118}$$

A group field theory is defined in terms of a Feynman expansion

$$Z_{\rm GFT} = \sum_{\Gamma} \frac{\lambda^{v[\Gamma]}}{{\rm sym}[\Gamma]} Z_{\rm GFT}[\Gamma]\,, \tag{119}$$

where the sum is over the triangulations and $v[\Gamma]$ is the number of vertices in the triangulation. Very roughly, the physical meaning of group field theory is the following (67; 68; 69; 70): in a realistic quantum gravity model, the sum over 2-complexes must be present in order to capture the infinite number of degrees of freedom. But the difference with lattice QFT is that the lattice spacing cannot be sent to zero because there is not a cut off scale. In the covariant approach to quantization one usually considers the discretized classical theory defined over a fixed triangulation; then some prescription is needed to recover the sum over all quantum geometries. This sum is usually done by means of group field theory. The parameter λ is equivalent to the number of cells in Regge calculus, and the discussion in (4.2) clarifies also the physical meaning of the group field theory λ expansion.

4.2 *Regge discretization*

The starting point of spin foams is the triangulation of space time, introduced by Regge in the early 1960's, called Regge calculus (71); it is a natural way to approximate General Relativity by means of a discrete lattice theory. We now illustrate the basic principles of Regge calculus, in the Euclidean General Relativity. A Riemannian manifold (M, g), where M is a smooth manifold and g its metric, can be approximated by means of a *piecewise flat* manifold (Δ, g_Δ), formed by flat simplices (triangles in 2d, tetrahedra in 3d, 4-simplices in 4d...) glued together in such a way that the geometry of their shared boundaries matches. Here Δ is the abstract triangulation, and the discretized metric g_Δ assumes a constant value on the edges of simplices and is determined by the size of simplices. For instance, a curved 2d surface can be approximated by a surface obtained by gluing together flat triangles along their sides: curvature is then concentrated on the points where triangles meet, possibly forming "the top of a hill". With a sufficient number N of simplices, we can (fixing the abstract triangulation and varying the size of the individual n-simplices) approximate sufficiently well any given (compact) Riemannian manifold with a Regge triangulation. Thus, over a fixed Δ we can define an approximation of GR, in a manner analogous to the way a given Wilson lattice defines an approximation to Yang-Mills field theory, or the approximation of a partial differential equation with finite–differences defines a discretization of the equation. Therefore the Regge theory over a fixed Δ defines a cut-off version of GR.

The meaning of Regge cut-off There is a main difference between this kind of discretization and lattice QCD: the Regge cut-off is neither ultraviolet nor infrared. In lattice QCD, the number N of elementary cells of the lattice defines an infrared cut-off: long wavelength degrees of freedom are recovered by increasing N. On the other hand, the physical size a of the individual cells enters the action of the theory, and short wavelength degrees of freedom are recovered in lattice QCD by decreasing a. Hence a is an ultraviolet cut-off. In Regge GR, on the contrary, there is no fixed background size of the cells that enters the action. A fixed Δ can carry both a very large or a very small geometry. The cut-off implemented by Δ is therefore of a different nature than the one of lattice QFT. It is not difficult to see that it is a cut-off in the *ratio* between the smallest allowed wavelength and the overall size of the spacetime region considered. Thus, fixing Δ is equivalent to cutting-off the degrees of freedom of GR that have much smaller wavelength than the arbitrary size L of the region one considers. Since the quantum theory has no degrees of freedom below the Planck scale, it follows that a Regge approximation is good for L small, and it is a low-energy approximation for L large.

Geometrical construction Consider a 4d triangulation. This is formed by oriented 4-simplices (v), tetrahedra (e), triangles (f), segments and points. The notation refers to the pictures dual to the triangulation (v for vertices, e for edges and f for faces) that will be useful in the spinfoam context. The metric is flat within each 4-simplex v. All the tetrahedra, triangles and segments are flat and, respectively, straight. The geometry induced on a given tetrahedron from the geometry of the two adjacent 4-simplices is the same. In d dimensions, a $(d-2)-$simplex is surrounded by a cyclic sequence of d-simplices, separated by the $(d-1)$-simplices that meet at the $(d-2)$-simplex. This cyclic sequence is called the *link* of the $(d-2)$-simplex. For instance, in dimension 2, a point is surrounded by a link of triangles, separated by the segments that meet at the point; in dimension 3, it is a segment which is surrounded by a link of tetrahedra, separated by the triangles that meet at the segment; in dimension 4, which is the case that concerns our world, a triangle f is surrounded by a link of 4-simplices $v_1, \dots, v_n$, separated by the tetrahedra that meet at the triangle f. In Regge calculus, curvature is concentrated on the $(d-2)$-simplices. In dimension 4, curvature is therefore concentrated on the triangles f. It is generated by the fact that the sum of the dihedral angles of the 4-simplices in the link around the triangle may be different from 2π. We can always choose Cartesian coordinates covering one 4-simplex, or two adjacent 4-simplices; but in general there are no continuous Cartesian coordinates covering the region formed by all the 4-simplices in the link around a triangle. The variables used by Regge to describe the geometry g_Δ of the triangulation Δ are given by the set of the lengths of all the segments of the triangulation.
Regge has also written the Einstein action in this discretized context: in three dimensions the discretized Einstein-Hilbert action for a tetrahedron v is

$$S_v = \sum_f l_f \theta_f(l_f)\,, \tag{120}$$

where θ_f is the dihedral angle associated to the segment f, that is the angle between the outward normals of the triangles incident to the segment. One can show that the action

$$S_{\text{Regge}} = \sum_v S_v \,, \tag{121}$$

called the Regge action, is an approximation to the integral of the Ricci scalar curvature, namely to the Einstein-Hilbert action.

4.3 *Quantum Regge calculus and spinfoam models*

Quantum Regge calculus is a quantization of discretized General Relativity (72). Consider the 3d case, which is easier and is the one studied by Ponzano and Regge. The idea is to define a partition function as a sum over Regge geometries:

$$Z = \int \mathrm{d}l_1 \dots \mathrm{d}l_N \, e^{iS_{\text{Regge}}} \,; \tag{122}$$

this is a sum over the N segment lengths of a fixed triangulation. Regge discovered a surprising property of the Wigner $6j$-symbol: in the large j limit the following asymptotic formula holds, linking the $\{6j\}$ to the Regge action (120):

$$\{6j\} \sim \frac{1}{\sqrt{12\pi V}} \cos\left(S_v(j_n) + \frac{\pi}{4}\right). \tag{123}$$

The two exponential terms coming from the cosine correspond to forward and backward propagation in coordinate time, and $\pi/4$ does not affect classical dynamics. Under the assumption that the lengths are quantized, Ponzano and Regge proposed the following formula for 3d quantum gravity:

$$Z_{\text{PR}} = \sum_{j_1 \dots j_N} \prod_f \dim(j_f) \prod_v \{6j\}_v \,. \tag{124}$$

This formula has the general form (114) where the set of two complexes summed over is formed by a single 2-complex; the representations summed over are the unitary irreducible of $SU(2)$, the intertwiners are trivial and the vertex amplitude is $A_v = \{6j\}$. It defines a spinfoam model called the Ponzano Regge model. The formula (124) can be obtained by direct evaluation of a path integral when we introduce appropriate variables. To this aim, consider the 2-skeleton Δ^* dual of a fixed triangulation Δ of the spacetime 3-manifold. Δ^* is defined as follows: place a vertex v inside each tetrahedron of Δ; if two tetrahedra share a triangle e, we connect the two corresponding vertices by an edge e, dual to the triangle e; for each segment f of the triangulation we have a face f of Δ^*. Finally for each point of Δ we have a 3d region of Δ^*, bounded by the faces dual to the segments sharing the point (Table 1).

Let $h_e = \mathcal{P} \exp\left(\int_e \omega^i \tau_i\right)$ be the holonomy of the $SU(2)$ spin connection along each edge of Δ^*; let l^i_f be the line integral of the triad (gravitational field) e^i along the segment f of Δ. h_e and l^i_f are the basic variables. The discretized Einstein-Hilbert action in these variables reads

$$S[l_f, h_e] = \sum_f l^i_f \mathrm{Tr}[h_f \tau_i] = \sum_f \mathrm{Tr}[h_f l_f] \,, \tag{125}$$

Δ_3	Δ_3^*
tetrahedron	*vertex* (4 edge, 6 faces)
triangle	*edge* (3 faces)
segment	*face*
point	*3d region*

Δ_4	Δ_4^*
4-simplex	*vertex* (5 edge,10 faces)
tetrahedron	*edge* (4 faces)
triangle	*face*
segment	*3d region*
point	*4d region*

Table 1: Relation between a triangulation and its dual, in three and four dimensions. In parenthesis: adjacent elements.

where $h_f = h_{e_1^f} \dots h_{e_n^f}$ is the product of group elements associated to the edges $e_1^f, \dots, e_n^f$ bounding the face f. In the last expression l_f are elements in the lie algebra $\mathfrak{su}(2)$ ($l_f \equiv l_f^i \tau_i$). If we vary this action w.r.t. the lengths l_f^i we obtain the equations of motion $h_f = 1$namely the lattice connection is flat. Using this fact, and varying w.r.t. h_e, we obtain the equations of motion $l_{f_1}^i + l_{f_2}^i + l_{f_3}^i = 0$ for the three sides f_1, f_2, f_3 of each triangle. This is the discretized version of the Cartan equation $De = 0$.
Now we can define the path integral as

$$Z = \int \mathrm{d}l_f^i \mathrm{d}h_e \exp iS[l_f, h_e]\,, \tag{126}$$

where $\mathrm{d}h_e$ is the Haar measure over $SU(2)$. Up to an overall normalization factor,

$$Z = \int \mathrm{d}h_e \prod_f \delta(h_{e_1^f} \dots h_{e_n^f}) = \sum_{j_1 \dots j_N} \prod_f \dim(j_f) \int \mathrm{d}h_e \prod_f \mathrm{Tr}\ \overset{j_f}{R}\ (h_{e_1^f} \dots h_{e_n^f})\,, \tag{127}$$

where we have expanded the δ over the group using the formula

$$\delta(h) = \sum_j \dim(j) \mathrm{Tr}\ \overset{j}{R}\ (h) \tag{128}$$

in which the sum is over all unitary irreducible representations of $SU(2)$. Since every edge is shared by three faces, the integrals over a single holonomy h_e are of the form

$$\int_{SU(2)} \mathrm{d}U\ \overset{j_1}{R}\ (U)^a{}_{a'}\ \overset{j_2}{R}\ (U)^b{}_{b'}\ \overset{j_3}{R}\ (U)^c{}_{c'} = v^{abc} v_{a'b'c'}\,, \tag{129}$$

where v^{abc} is the normalized intertwiner ($v^{abc} v_{abc} = 1$) between the representations of spin j_1, j_2, j_3. Each of the two invariant tensors in the r.h.s. is associated to one of the two vertices that bounds the edge. In all we have four intertwiners for each vertex; these intertwiners get fully contracted among each other following a tetrahedral pattern.
This contraction is precisely the Wigner $6j$-symbol. Bringing all together we obtain the Ponzano-Regge partition function (124).

4.4 *BF theory*

Here we extend the above construction to four dimensions. As a first step we do not consider GR, but a much simpler 4d theory, called BF theory, which is topological and is a simple extension to 4d of the topological 3d GR. BF theory for the group $SO(4)$ is defined by two fields: a 2-form B^{IJ} with values in the Lie algebra of $SO(4)$, and an $SO(4)$ spin connection Γ^{IJ} . The action is a direct generalization of the 3d one:

$$S[B,\Gamma] = \int B_{IJ} \wedge R^{IJ}[\Gamma]\,. \tag{130}$$

We can obtain the action of General Relativity from the one of BF theory substituting the field B^{IJ} with $\epsilon^{IJ}{}_{KL} e^K \wedge e^L$, and this is the reason for which we describe BF theory as an intermediate step.
We discretize BF theory on a fixed triangulation; the discrete configuration variables are B^{IJ}_f, which are the integrals of the continuous 2-form over the triangles f (f stands for face which is dual to triangles). The construction of the dual 2-skeleton in 4d is in Table 1. Following the same procedure of the 3d case, we obtain an equation analog to (127) where the sum is over $SO(4)$ irreducible representations. Now we are in four dimensions, and every edge bounds four faces; so we have to compute integrals of the form

$$\int_{SO(4)} \mathrm{d}U \ \overset{j_1}{R}(U)^a{}_{a'} \ \overset{j_2}{R}(U)^b{}_{b'} \ \overset{j_3}{R}(U)^c{}_{c'} \ \overset{j_4}{R}(U)^d{}_{d'} = \sum_i v_i^{abcd} v^i_{a'b'c'd'}\,. \tag{131}$$

Here i labels an orthonormal basis v_i^{abcd} ($v_i^{abcd} v_{j\,abcd} = \delta_{ij}$) in the space of the intertwiners between the representations of spin j_1, j_2, j_3, j_4. Now each vertex bounds ten faces and so for each vertex we have ten representations. Analogously to the three dimensional case, where the vertex amplitude was given by a $\{6j\}$, we find that here the vertex amplitude is the $15j$-symbol (the Wigner $15j$ up to dimensionals factors):

$$\begin{aligned} &A(j_1,\dots j_{10}, i_1,\dots,i_5) \\ &\equiv \sum_{a_1\dots a_{10}} v^{a_1 a_6 a_9 a_5}_{i_1} v^{a_2 a_7 a_{10} a_1}_{i_2} v^{a_3 a_7 a_8 a_2}_{i_3} v^{a_4 a_9 a_7 a_3}_{i_4} v^{a_5 a_{10} a_8 a_4}_{i_5} = \{15j\}_{SO(4)}\,, \end{aligned} \tag{132}$$

where the indices a_n are in the $SO(4)$ representation j_n. The pattern of the contraction of the indices reproduces the structure of a four simplex (figure 6). We can then write the partition function

$$Z = \sum_{j_f, i_e} \prod_f \dim(j_f) \prod_v \{15j\}_v\,. \tag{133}$$

In conclusion, the spinfoam model of BF theory is defined by the following choices:
1) the set of two complexes summed over is formed by a single 2-complex (2-skeleton dual to a 4-dimensional triangulation);
2) the representations summed over are the unitary irreducibles of $SO(4)$;
4) the vertex amplitude is $A_v = \{15j\}$.

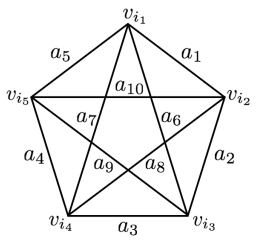

Figure 6: A $15j$-symbol

4.5 *Barret-Crane model*

Now we are ready to look for a spinfoam model for GR. As we have anticipated, to obtain GR from BF we must replace B^{IJ} with

$$B^{IJ} = \epsilon^{IJ}{}_{KL} e^K \wedge e^L \,. \tag{134}$$

How to implement this constraint in the quantum theory? First, we replace it with the equivalent constraint Equation (134) can be substituted by

$$B^{IJ} \wedge B^{KL} = V \epsilon^{IJKL} \,, \tag{135}$$

where V is proportional to the volume element. To discretize the theory we integrate the B field over triangles f, obtaining the bivector B^{IJ}_f (its modulus is the area of the triangle), and for each tetrahedron t the equation (135) can be split in

$$B^*_f \cdot B_f = 0 \,, \tag{136}$$

$$B^*_f \cdot B_{f'} = 0 \,, \qquad f \text{ and } f' \text{ share an edge}, \tag{137}$$

$$B^*_f \cdot B_{f'} = \pm 2V(v) \qquad f \text{ and } f' \text{ are opposite faces of } t, \tag{138}$$

where $V(v)$ is the volume of the 4-simplex v. In the quantum theory B^{IJ}_f can be identified with the generators of an $SO(4)$ representation (in analogy with the 3d case in which the continuous variables l^i_f could be identified with the generators of the representation j_f). Moreover it is immediate to see that the four bivectors $B^{IJ}_{f_1}(t), \ldots, B^{IJ}_{f_4}(t)$, associated to the four triangles of a single tetrahedron satisfy the closure relation

$$B^{IJ}_{f_1}(t) + B^{IJ}_{f_2}(t) + B^{IJ}_{f_3}(t) + B^{IJ}_{f_4}(t) = 0 \,; \tag{139}$$

this is the discrete analog of Gauss constraint. Equation (136) is called diagonal simplicity constraint, and it becomes, in the quantum theory, a restriction on the representations summed over. Recall indeed that, since the Lie algebra of $SO(4)$ is $\mathfrak{su}(2) \oplus \mathfrak{su}(2)$, the irreducible representations of Spin(4), the universal covering of $SO(4)$, are labeled by couples of spins (j_+, j_-) . So the diagonal simplicity constraint in the generic (j_+, j_-) irrep reads

$$\epsilon_{IJKL} \hat{B}^{IJ}_f \hat{B}^{KL}_f = \hat{B}^i_+ \hat{B}_{+i} - \hat{B}^i_- \hat{B}_{-i} = [j_+(j_+ + 1) - j_-(j_- + 1)]\mathbb{1} = 0 \,; \tag{140}$$

from which $j_+ = j_-$, namely the irreps are constrained to be simple (or balanced). B^i_+ and B^i_- are the self-dual and antiself-dual part of B^{IJ} w.r.t. the "timelike" unit vector $n = (1, 0, 0, 0)$: $B^i_\pm = -\frac{1}{4}\epsilon^i{}_{jk}B^{jk} \pm \frac{1}{2}B^{i0}$ This suggests that quantum GR can be obtained by restricting the sum over representations in (133) to the sole simple representations.
The other two constraints (137) and (138) are called off-diagonal and dynamical simplicity constraints respectively; the off-diagonal restricts the intertwiners between four (simple) $SO(4)$ irreps to have components only in the simple irreps in the Clabsh-Gordan decomposition. In particular the intertwiners are constrained to be the Barret-Crane ones:

$$i_{\rm BC}^{(aa')(bb')(cc')(dd')} = \sum_i (2i+1)\, v^{abg} v^{gcd} v^{a'b'g'} v^{g'c'd'}\,, \tag{141}$$

where the $SO(4)$ indices are couple of $SU(2)$ indices, and the indices g and g' are in the representation i. The BC intertwiner has the property of being formed by a simple virtual link in any decomposition

$i_{\rm BC} = \sum_{i^x}(2i^x{+}1)$ 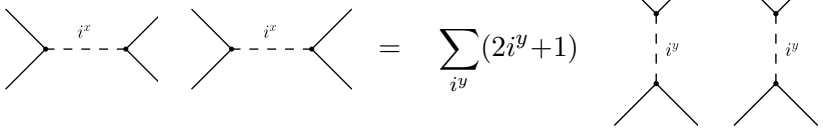 $= \sum_{i^y}(2i^y{+}1)$. (142)

Note that the scalar Casimir $\hat{B}_f \cdot \hat{B}_f$ is the quantization of the area of the triangle f and its eigenvalues $j_f(j_f+1)$ are the area quantum numbers. The BC vertex amplitude is then the $SO(4)$ $15j$-symbol where the spins are simple and the intertwiners are the BC ones:

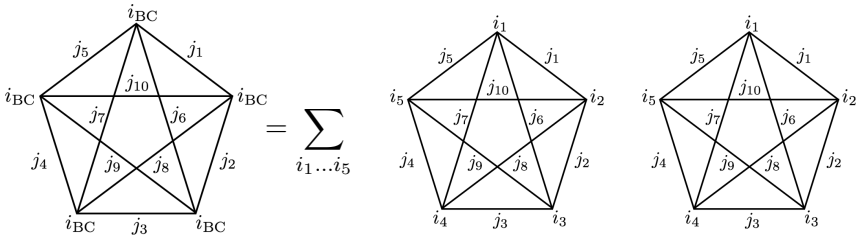

(143)

This symbol is called $10j$-symbol in quantum gravity literature. The Barret-Crane spinfoam model (73; 74) is defined by the partition function

$$Z_{\rm BC} = \sum_{\text{simple } j_f} \prod_f \dim(j_f) \prod_v A_v(j_1, \dots, j_{10})\,. \tag{144}$$

Asymptotics of $10j$-symbol At this point, a natural question arise: whether also the $10j$-symbol has the same property of $6j$-symbol of reproducing the Regge action in large spin limit; the answer is remarkably positive. A computation of the asymptotic expression of the Barrett-Crane vertex amplitude for non-degenerate configurations was obtained by Barrett and Williams

in (75). The large spin behavior of the vertex amplitude given by Crane and Yetter in (76) is

$$\{10j\} \sim \sum_{\sigma} P(\sigma) \cos S_{\text{Regge}}(\sigma) + k\frac{\pi}{4} + D\,, \tag{145}$$

where the sum is over 4-simplices σ, whose faces have area determined by the spins; $P(\sigma)$ is a non oscillating factor, D is the contribution of the so-called degenerate configurations and k is an integer depending on σ . In (77) Baez, Christensen and Egan showed that the term D is in fact dominant in the asymptotics of the $10j$, i.e. the leading order terms are contained in the set of degenered configurations! This has later been confirmed by the results of Freidel and Louapre (78) and Barrett and Steele (79). However, we anticipate that such degenerete terms do not seem to contribute to physical quantities such as the n-point functions.

Relation with LQG Consider the case in which the triangulated manifold has a boundary, and the triangle f belongs to the boundary. The face f cuts the boundary along a link, labeled with j_f. This is assumed to be one of the links of the boundary spin-network. This link intersects once and only once the triangle f, hence j_f is the quantum number determining the area of the triangle f; this is precisely the result that we found in Loop Quantum Gravity.
The interpretation of the intertwiners at the boundary is more delicate. Consider an edge e of the spin foam σ that cuts the boundary at a node n of the boundary spin-network. The node n, or the edge e, is dual to a tetrahedron sitting on the a boundary. Let f and f' be two adjacent triangles of this tetrahedron. Consider the action of the $SO(4)$ generators on the tensor product of the representation spaces associated to the two (faces dual to the two) triangles. This is given by the operators $\hat{B}^{IJ}_{ff'} = \hat{B}^{IJ}_{f} + \hat{B}^{IJ}_{f'}$ (we omit the tensor with the identity operator in the notation); be $\widehat{B}_{ff'} \cdot \widehat{B}_{ff'}$ the scalar Casimir on the tensor product of the representation spaces of the two triangles. Straightforward algebra shows that

$$B_{ff'} \cdot B_{ff'} = |B_f| + |B_{f'}| + 2\ \hat{n}_f \cdot \hat{n}_{f'}\,, \tag{146}$$

where $\hat{n}^I_f = \epsilon^I{}_{JKL} B^{JK}_f t^L$ and t^L is the normalized vector normal to f and f'. Finally, $\hat{n}_f \cdot \hat{n}_{f'} = A_f A_{f'} \cos\alpha_{ff'}$, where $\alpha_{ff'}$ is the dihedral angle between f and f'. This provides the interpretation of the color of a virtual link in the intertwiner associated to the node: if the virtual link that couples f and f' is simple, with spin $j_{ff'}$, we have

$$j_{ff'}(j_{ff'}+1) = A_f^2 + A_{f'}^2 + 2A_f A_{f'} \cos\alpha_{ff'}\,. \tag{147}$$

That is, the color of the virtual link is a quantum number determining the dihedral angle $\alpha_{ff'}$ between the triangles f and f'; or, in the dual picture, the angle between the two corresponding links that join at the node. Once more, this result is exactly the same in LQG.
Nevertheless there is a serious problem in matching Loop Quantum Gravity states with the boundary states of Barret-Crane model. From equation (142), we have

$$\langle i_{\text{BC}} | i, i\rangle = (2i+1)\,, \tag{148}$$

whatever is the pairing of the virtual link i. Since the simple $SO(4)$ intertwiner $|i,i\rangle$ diagonalizes the same geometrical quantity as the $SO(3)$ intertwiner $|i\rangle$, it is tempting to physically identify

the two and write

$$\langle i_{\rm BC}|i\rangle = (2i+1)\,. \tag{149}$$

But there is not any state $|\ i_{\rm BC}\rangle$ in the the $SO(3)$ intertwiner space having this property. This is now considered a major problem of the BC model, which, together with the bad behavior of some components of n-point functions, started the search for new models.

5 Graviton propagator in Loop Quantum Gravity

One important line of research in Loop Quantum Gravity is the study of its semiclassical limit. Though nowadays there are not experiments that permit to test directly a candidate theory of quantum gravity, one possibility is to compute the n-point functions from Loop Quantum Gravity and compare them with the corresponding expressions obtained in the conventional perturbative expansion of quantum General Relativity. Agreement at large distance could then be taken as evidence that the nonperturbative quantum theory has the correct low energy limit; while the differences at short distance reflect the improved ultraviolet behavior of the nonperturbative theory. The difficulty is that general covariance makes conventional n-point functions ill–defined in the absence of a background. A strategy for addressing this problem has been suggested in (80); the idea is to study the boundary amplitude, namely the functional integral over a finite spacetime region, seen as a function of the boundary value of the gravitational field (18). In conventional quantum field theory, this boundary amplitude is well–defined (see (81; 82)) and codes the physical information of the theory; so does in quantum gravity, but in a fully background–independent manner (83).
A generally covariant definition of n-point functions can be based on the idea that the distance between physical points –arguments of the n-point function– is determined by the state of the gravitational field on the boundary of the spacetime region considered. This strategy was first implemented in the letter (84), where some components of the graviton propagator were computed to the first order in the expansion parameter λ, then the full calculation is performed in (84) to second order in λ (for an implementation of these ideas in 3d, see (85; 86)). Only a few components of the boundary state contribute to low order in λ. This reduces the calculation to a 4d generalization of the "nutshell" 3d model studied in (87). The boundary amplitude defining n-point functions can be read as the creation, interaction and annihilation of "atoms of space", in the sense in which Feynman diagrams in conventional quantum field theory can be viewed as creation, interaction and annihilation of particles. Using a natural gaussian form of the background boundary state, peaked on the intrinsic *as well as* the extrinsic geometry of a Euclidean 3-sphere, an expression for the graviton propagator can be derived, and at large distance this agrees with the conventional graviton propagator.
In the first part of this section we show how to define n-point functions for general covariant field theories in the context of general boundary formulation. In order to explain the concept of boundary amplitude, we first illustrate a very simple example of a single degree of freedom system: the harmonic oscillator; then we introduce the general boundary formulation for field theories, in particular for quantum gravity. We conclude showing a formal expression for quantum gravity n-point functions.
In the second part we present the main ingredients for the graviton propagator definition and the results skipping the calculations. In the last part we stress the problem of the gauge choice for the comparison with the linearized theory and how it is solved by the compatibility between radial and harmonic gauge. In fact perturbative quantum gravity Feynman rules are mostly known in harmonic gauge, but Loop Quantum Gravity calculations involve gauge choices that can be interpreted as putting the linearized gravitational field in radial gauge (i.e. with vanishing radial components): a direct comparison seems to be not viable. However we demonstrate

(20) that radial and harmonic gauges are compatible. Thanks to this result, it is possible to compare the full tensorial structure of the LQG propagator with the one of the standard propagator.

5.1 *n-point functions in general covariant field theories*

In perturbative quantum gravity the metric is split in a flat background metric η plus a perturbation[4]: $g_{\mu\nu}(x) = \eta_{\mu\nu} + h_{\mu\nu}(x)$; the background is treated classically, and only the perturbation is quantized. The 2-point function is defined as in a conventional QFT as the vacuum expectation value

$$G^{\mu\nu\rho\sigma}(x,y) = \langle 0|h^{\mu\nu}(x)h^{\rho\sigma}(x)|0\rangle \ . \tag{150}$$

If we consider the full non-perturbative theory, diffeomorphism invariance seems to imply that the propagator G does not depend on the two arguments x and y, so it is a constant. This problem is only apparent, and it is beautifully solved by a change of perspective, namely defining n-point functions for general finite 3d boundaries; to understand how the general boundary formulation works we first illustrate a simple example in ordinary Quantum Mechanics, i.e. the 2-point function of harmonic oscillator. The harmonic oscillator propagator is defined as the vacuum expectation value of two position operators:

$$G_0(t_1,t_2) = \langle 0|\hat{x}(t_1)\hat{x}(t_2)|0\rangle = \langle 0|\hat{x}e^{-iH(t_1-t_2)}\hat{x}|0\rangle \, . \tag{151}$$

Passing to the Schrödinger representation we can write the 2-point function as an integral in position space

$$G_0(t_1,t_2) = \int \mathrm{d}x_1\mathrm{d}x_2\, \overline{\psi}_0(x_1)\, x_1 W(x_1,x_2;t_1,t_2)x_2\psi_0(x_2)\, , \tag{152}$$

where $\psi_0 = \langle x|0\rangle$ is the wave function of ground state.
$W(x_1,x_2;t_1,t_2) = \langle x_1|\hat{x}(t_1)\hat{x}(t_2)|x_2\rangle$ is called propagation kernel and it codes the dynamics of the system.
In the functional representation, instead, the 2-point function reads

$$G_0(t_1,t_2) = \int Dx\, x(t_1)x(t_2)e^{i\int L dt} \, . \tag{153}$$

The Schrödinger representation is recovered by breaking the functional integral into five regions: the two regions external to the initial and final time, the two regions at initial and final time and the region in between. The external integration gives the ground state, the internal integration gives the propagation kernel W and the integration at t_1 and t_2 is just the integration appearing in the Schrödinger representation.
Now we introduce the relativistic form of the propagator; by relativistic here we mean "general relativistic" in the sense illustrated in (7). So we put together the initial and final background configuration $\overline{\psi}_0$ and ψ_0 and we call them "boundary state" Ψ_0, where Ψ_0 lives in $H^* \otimes H$, H being the Hilbert space of square integrable functions on 3d space; H^* and H are viewed as the

[4]From now on we change notation for h; it is no more the induced metric.

spaces of initial data and final data, respectively, so we use the notation $H^*_{t_1}$ and H_{t_2} .
Then we can define the relativistic position operators $\hat{x}_1$ and $\hat{x}_2$, as acting separately on the two Hilbert spaces as the ordinary position operators. W can be interpreted as a bra on the tensor product $H^*_{t_1} \otimes H_{t_2}$. The 2-point function assumes the compact form

$$G_0(t_1, t_2) = \langle W_{t_1 t_2} | \hat{x}_1 \hat{x}_2 \Psi_0 \rangle \,. \tag{154}$$

The physical interpretation is the following: Ψ_0 represents the joint configuration at initial and final time with no excitations present; W codes the dynamics and $\hat{x}_1$, $\hat{x}_2$ create two excitations at initial and final time. The state $|\hat{x}_1 \hat{x}_2 \Psi_0\rangle$ is the excited boundary configuration detected in the experiment (7).
It is worth to note that the following normalization condition holds:

$$\langle 0 | e^{iH(t_1 - t_2)} | 0 \rangle = \langle W_{t_1 t_2} | \Psi_0 \rangle = 1 \,. \tag{155}$$

Its physical meaning is that the final background state is the time evolution of the initial background state; in other words, the boundary state satisfies the dynamics. In our case the condition holds because the ground state does not evolve in time. In quantum gravity jargon, the normalization (155) is called Wheeler-deWitt condition.
Instead of the ground state, we can consider a more general coherent boundary state with arbitrary positions q_1 and q_2, and momenta p_1 and p_2

$$\Psi_{q_1,p_1,q_2,p_2}(x_1, x_2) \equiv \overline{\psi}_{q_1,p_1}(x_1) \psi_{q_2,p_2}(x_2) \,. \tag{156}$$

The 2-point function constructed this way reads

$$G_{q_1,p_1,q_2,p_2}(t_1, t_2) = \langle W_{t_1,t_2} | \Psi_{q_1,p_1,q_2,p_2} \rangle \ , \tag{157}$$

and the Weeler-deWitt condition is

$$\langle W_{t_1 t_2} | \Psi_{q_1,p_1,q_2,p_2} \rangle = 1 \,. \tag{158}$$

We choose q_1 and p_1 to be the classical evolution of the initial condition (q_2, p_2); in that case the Wheeler-deWitt condition holds, because of the well-known properties of the harmonic oscillator dynamics. We call the quadruplet (q_1, q_2, p_1, p_2) a physical boundary configuration, denoted with $\mathbf{q}$. The 2-point function for a physical boundary configuration is the quantum amplitude for a quantum excitation to propagate over a classical trajectory starting with the classical initial condition (q_2, p_2).
Now we turn our attention to quantum field theory. As before we can define a 2-point function for the scalar field ϕ:

$$G_{\mathbf{q}}(\vec{x}, \vec{y}) = \int D\phi_1 D\phi_2 \, \overline{\psi}_{q_1,p_1}(\phi_1) \phi_1(\vec{x}) W(\phi_1, \phi_2; t_1, t_2) \psi_{q_2,p_2}(\phi_2) \phi_2(\vec{y}) \,. \tag{159}$$

In a free theory the boundary vacuum state can be written as a physical semiclassical state peaked on some configuration fields and momenta. W is the functional integral restricted to the region between two time slices

$$W(\phi_1, \phi_2; t_1, t_2) = \int_{\varphi|_{t_1} = \phi_1}^{\varphi|_{t_2} = \phi_2} D\varphi \; e^{i \int_{t_1}^{t_2} \mathrm{d}t \int \mathrm{d}^3 \vec{x} \mathscr{L}[\varphi]} \,. \tag{160}$$

Now it is the time for the crucial step: instead of time slices, we define the 2-point function for a general 3d boundary in the following way:

$$G_{\mathbf{q}} = \int D\phi\ \phi(x)\phi(y)\, W(\phi, \Sigma)\Psi(\phi)\,. \tag{161}$$

Here x and y live on the 3d hypersurface Σ, which is the 3d boundary of a finite 4d region R; W is the result of the integration over the interior of the boundary:

$$W(\phi; \Sigma) = \int_{\partial\varphi=\phi} D\varphi\ e^{i\int_R \mathrm{d}^4x\, \mathscr{L}[\varphi]}\,. \tag{162}$$

This definition is sensible also for quantum gravity. Perturbative quantum gravity is an ordinary QFT, so we can use the previous expression for the 2-point function, where instead of ϕ there is the perturbation h:

$$G^{abcd}_{\mathbf{q}}(\mathbf{x}, \mathbf{y}) = \int D\gamma\ h^{ab}(\mathbf{x})h^{cd}(\mathbf{y})W(\gamma)\Psi_{\mathbf{q}}(\gamma)\,; \tag{163}$$

here γ is the 3-metric of the boundary. Measure and action are Poincaré invariant; $\mathbf{x}$ and $\mathbf{y}$ are points on the 3d boundary. We demand the vanishing of the fields at infinity, or some other condition at infinity (this condition determines the boundary state since the latter results from the functional integration outside the boundary). Now, if we want to construct 2-point functions in nonperturbative quantum gravity we may assume measure and action to be invariant under diffeomorphisms, and W does not depend on Σ; now what is the meaning of the points x and y? Furthermore, we do not have a background to put conditions on the fields at infinity, so the boundary state Ψ is ill defined. The solution is simple: we cannot define the boundary state by the external functional integration, but this is not a problem, since we can use the expression (163) as the very definition of 2-point function. The boundary state can be chosen arbitrarily (it is a semiclassical state peaked on a physical boundary configuration) and the dependence on the boundary state determines the non-trivial behavior of the 2-point function under diffeomorphisms: $G_{\mathbf{q}}(\mathbf{x}, \mathbf{y}) = G_{\mathbf{q}'}(\mathbf{x}', \mathbf{y}')$. Now G is a well defined quantity in Riemannian geometry. The physical meaning of this formalism is the following: G defines an amplitude associated to a joint set of measurements performed on the 3d boundary: we detect the mean geometry $\mathbf{q}$ with two excitations (gravitons) in x and y. In nonrelativistic physics we have to know the spacetime location of detectors and then we measure fields (except for the gravitational field). On the other hand, in relativistic physics we measure the gravitational field and it is sufficient to determine also the geometry of the apparatus (or conversely, the measurement of the apparatus geometry is a measurement of the gravitational field on the boundary). We stress that the geometry in the interior is free to quantum-mechanically fluctuate; in fact W can be interpreted as a sum over geometries.

5.2 *Graviton propagator in Loop Quantum Gravity*

The general boundary framework can be concretely implemented in LQG (88; 59; 8; 61). Quantum geometries of the boundary correspond to spin-networks; the linearized gravitational field

operator corresponds to the well known LQG operator $\widehat{E}^i_a$; the boundary state is a functional of spin-networks peaked on the geometry $\mathbf{q}$; the boundary amplitude is provided by a spinfoam model. So the concrete formula for the 2-point function is

$$G^{abcd}_{\mathbf{q}}(\mathbf{x},\mathbf{y}) = \sum_s W[s]\widehat{h}^{ab}(\mathbf{x})\widehat{h}^{cd}(\mathbf{y})\Psi_{\mathbf{q}}[s]\,. \tag{164}$$

In the following we examine the ingredients of the graviton propagator (164).

The boundary state We choose a boundary state peaked on the intrinsic and the extrinsic geometry $\mathbf{q}$ of a Euclidean 3-sphere with radius much larger than Planck length. Below we shall only need the value of $\Psi_{\mathbf{q}}[s]$ for the spin-networks $s = (\Gamma, j_l, i_n)$ defined on graphs Γ which are dual to 3d triangulations Δ. We identify each such Δ with a fixed triangulation of $\Sigma_{\mathbf{q}}$. The area A_l of the triangle t_l of Δ, dual to the link l, determines the background values $j_l{}^{(0)}$ of the spins j_l, via

$$A_l = \kappa\hbar\sqrt{j_l{}^{(0)}(j_l{}^{(0)}+1)}\,. \tag{165}$$

Since s represents a 3d triangulation, we choose the spins (areas) centered around the spins (areas) of a regular triangulation; we take these background values large with respect to the Planck length, and we will later consider only the dominant terms in $1/j_l{}^{(0)}$.
We want a state $\Psi_{\mathbf{q}}[s] = \Psi_{\mathbf{q}}(\Gamma,\mathbf{j})$, where $\mathbf{j} = \{j_l\}$, to be peaked on these background values with vanishing relative uncertaties. The simplest possibility is to choose a Gaussian peaked on these values, for every graph Γ

$$\Psi_{\mathbf{q}}[s] = C_\Gamma\ \exp\left\{-\frac{1}{2}\sum_{ll'}\alpha_{ll'}\ \frac{j_l - j_l{}^{(0)}}{\sqrt{j_l{}^{(0)}}}\ \frac{j_{l'} - j_{l'}{}^{(0)}}{\sqrt{j_{l'}{}^{(0)}}} + \mathsf{i}\sum_l \Phi^{(0)}_l\, j_l\right\}\,. \tag{166}$$

where l runs on links of s, $\alpha_{ll'}$ is a given numerical matrix and C_Γ is a graph–dependent normalization factor for the Gaussian.

The phase factors in (166) play an important role (84). As we know from elementary Quantum Mechanics, the phase of a semiclassical state determines where the state is peaked in the conjugate variables, here the variables conjugate to the spins j_l.
In the large j_0 limit, only the graph corresponding to the boundary of a 4-simplex enters the calculation, so the 4-dimensional Regge action reduces to, $S_{\text{Regge}} = \sum_l \Phi_l(j_l)j_l$, where $\Phi_l(j_l)$ are the dihedral angles at the triangles[5], which are function of the areas themselves and recall that $\partial S_{\text{Regge}}/\partial j_l = \Phi_l$. It is then easy to see that these dihedral angles are precisely the variables conjugate to the spins and they code the extrinsic geometry of the boundary, while the spins code the intrinsic curvature, and in GR the extrinsic curvature is indeed the variable conjugate to the 3-metric. Thus $\Phi^{(0)}_l$ in (166) are the dihedral angles of the background regular triangulation.

[5]These are angles between the normals to the tetrahedra, and should not be confused with the angles between the normals to the triangles.

Field operator Now we want to define the graviton field operator, so let us define the metric deviation from flatness as $h^{ab} = g^{ab} - \delta^{ab}$; in order to rewrite the metric deviation in terms of triads, notice that, up to higher order corrections, $\det g \simeq 1 + \mathrm{tr}\, h$, so in traceless gauge we have finally $h^{ab} = E^{ai}E^b_i - \delta^{ab}$. We know the action of the area operator on a spin-network (99), so identifying $\mathbf{x}$ with a spin-network node (or equivalently with the center of a tetrahedron), the projection of $E^{ab}(\mathbf{x})$ along the normals[6] to the triangles surrounding the node acts diagonally on the spin-network, giving as eigenvalues the areas of triangles

$$\hat{E}^i_t(\mathbf{x})\hat{E}_{ti}(\mathbf{x})|s\rangle = (\hbar\kappa)^2 j_t(j_t+1)|s\rangle\,. \tag{167}$$

Here we put $\gamma = 1$ and the subscript t means that we have projected the triad along the normal to the triangle t (here the normals are defined as the vector product of the two sides of the triangles, so they live in the three dimensional space defined by the tetrahedron). This is the action of the so-called "diagonal components" where for diagonals we mean $t - t$ components.

Boundary amplitude The Barret-Crane spinfoam model provides an amplitude (144) for general boundary spin-networks; if we sum over all 4-geometries bounded by the given spin-network s we obtain

$$W[s] = \sum_{\partial\sigma = s} \prod_{f\in\sigma} \dim(j_f) \prod_{v\in\sigma} \lambda\{10j\}_v\,. \tag{168}$$

The next step is considering a large scale limit of the theory; we have seen that the boundary amplitude W is a sum over spin foams, but at order λ and large j's (selected by the boundary state) only one geometry survives, namely the spin foam corresponding to a 4-simplex; its dual boundary is a pentagonal spin-network, representing five tetrahedra glued together to form a triangulated 3-sphere. The resulting boundary amplitude is

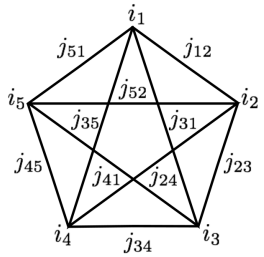

Figure 7: Boundary spin-network of a spin foam dual to a single 4-simplex

$$W[s] = \frac{\lambda}{5!}\prod_f \dim j_f \{10j\}_v\,. \tag{169}$$

The value of $\Psi_{\mathbf{q}}[s]$ on the spin-networks $s = (\Gamma_5, j_{nm})$ (here $n, m = 1, ..., 5$) can be determined by triangulating $\Sigma_{\mathbf{q}}$ with the 3d triangulation formed by the boundary of a *regular* four–simplex

[6]The normal is normalized to the area of the triangle.

of side L. The area of the triangles is $A_L = \sqrt{3}L^2/4$. Then (165) implies that $j^{(0)}_{nm} = j_L$ where $\kappa\hbar\sqrt{j_L(j_L+1)} = A_L$. In the large L limit we take $j_L = \kappa\hbar A_L$. The dihedral angles $\Phi^{(0)}_{nm} = \Phi$ of a regular tetrahedron are given by $\cos(\Phi) = -1/4$. Therefore (166) becomes

$$\Psi_{\mathbf{q}}[s] = C_5 \ \exp\left\{-\frac{1}{2j_L}\sum_{(nm)(p\,q)} \alpha_{(nm)(p\,q)}\ (j_{nm}-j_L)(j_{p\,q}-j_L) + i\Phi\sum_{(n,m)} j_{nm}\right\}. \tag{170}$$

To respect the symmetry of the sphere, the covariance matrix $\alpha_{(nm)(p\,q)}$ of the gaussian can depend only on three numbers

$$\alpha_{(nm)(p\,q)} = \alpha_1\ a_{(nm)(p\,q)} + \alpha_2\ \delta_{(nm)(p\,q)} + \alpha_3\ b_{(nm)(p\,q)} \tag{171}$$

where $\delta_{(nm)(p\,q)} = 1$ if $(nm) = (p\,q)$, $a_{(nm)(p\,q)} = 1$ if just two indices are the same, and $b_{(nm)(p\,q)} = 1$ if all four indices are different, and in all other cases these quantities vanish.

The component of the state (166) that matters at first order in λ is thus completely determined up to the three numbers $\alpha_1, \alpha_2, \alpha_3$, and the constant C_5. This amounts to select a vacuum state which is a coherent state peaked both on the background values of the spins (the extrinsic geometry of the boundary surface), *and* on the background values of the angles (the intrinsic geometry of the boundary surface). See (87) for a similar construction in 3d. For clarity, let us stress that we are *not* assuming that the boundary state has components *only* on the five-valent graph considered. What we are saying is that only this component of the boundary state enters the expansion to first order in λ that we are considering.

Now we can use the asymptotic formula for the $10j$-symbol (145) without the degenerete term, in fact it can be seen that expanding (145) around a background selected by the boundary state, the degenerate term D disappear (89). We can substitute the asymptotic formula for the $10j$-symbol with the simpler expression

$$\sum_{\sigma} e^{\mathrm{i}S[\sigma]} + e^{-\mathrm{i}S[\sigma]}, \tag{172}$$

where $S[\sigma] = \sum_t j_t\Phi_t(j_\sigma)$ and Φ_t is the dihedral angle between the two tetrahedra sharing the triangle t.

Now we have all the ingredients to compute the diagonal components

$$G(L)_{tt'} = G^{abcd}_{\mathbf{q}}(\mathbf{x},\mathbf{y}) n^t_a n^t_b n^{t'}_c n^{t'}_d, \tag{173}$$

where n^t_a is the normal to the triangle t living in the 3-dimensional space defined by the tetrahedron.

We do not perform the full calculation of the first order of the graviton propagator in (19) and report only the surprising final result:

$$G(L) = \frac{32\hbar G}{\pi L^2} M, \tag{174}$$

where M is a numerical matrix that can be fixed to be as in the linearized theory. This result is the manifestation of Newton law at large distance. The non diagonal terms have been calculated

in (21) and the result is that to obtain the Newton law we have to modify the dynamics, as we explain in the next section.
Now there is a technical point: the full structure of the propagator depends on which gauge has been chosen. Which gauge shall we use in order to compare LQG and perturbative quantum gravity propagators? LQG propagator is defined in a generalized temporal gauge ($h^{\mu\nu}$ has vanishing components along the normals to the 3d boundary sphere); this is called radial (or Fock-Schwinger) gauge (90; 91; 92). In addition we put the traceless condition $h^{\mu}{}_{\mu} = 0$. Perturbative quantum gravity is mostly known in harmonic gauge and one is tempted to take the radial (and traceless) components of the linearized quantum gravity propagator in harmonic gauge, then to take the harmonic (traverse) components of the Loop Quantum Gravity propagator, and finally to compare the two expressions. Fortunately it exists a radial-harmonic-traceless gauge in linearized General Relativity (20) and in the following we present this result in detail first illustrating an analogous result in Electromagnetism.

5.3 *Compatibility between of radial, Lorenz and harmonic gauges*

The radial gauge, or Fock-Schwinger gauge (90; 91), is defined by

$$x^{\mu} A_{\mu} = 0 \tag{175}$$

in Maxwell theory, and by

$$x^{\mu} h_{\mu\nu} = 0 \tag{176}$$

in linearized General Relativity. Here $x = (x^{\mu})$ are Lorentzian (or Euclidean) spacetime coordinates in $d+1$ spacetime dimensions, where $\mu = 0, 1, \ldots, d$; $A_{\mu}(x)$ is the electromagnetic potential. The radial gauge has been considered with various motivations. For instance, radial–gauge perturbation theory was studied in (93; 92; 94; 95), where an expression for the propagator and Feynman rules in this gauge were derived. A number of papers implicitly use this gauge in the context of nonperturbative Euclidean Loop Quantum Gravity (7; 84; 19; 86; 96). Here, indeed, consider a spherical region in 4d Euclidean spacetime, and identify the degrees of freedom on the 3d boundary Σ of this region with the degrees of freedom described by Hamiltonian Loop Quantum Gravity. The last is defined in a "temporal" gauge where the field components in the direction *normal to the boundary surface* Σ are gauge fixed. Since the direction normal to a sphere is radial, this procedure is equivalent to imposing the radial gauge (176) in the linearization around flat spacetime.

The radial gauge is usually viewed as an *alternative* to the commonly used Lorenz and harmonic gauges, defined respectively by

$$\partial_{\mu} A^{\mu} = 0 \tag{177}$$

in Maxwell theory and by

$$\partial_{\mu} h^{\mu}{}_{\nu} - \frac{1}{2}\, \partial_{\nu} h^{\mu}{}_{\mu} = 0 \tag{178}$$

in linearized General Relativity. Here we observe, instead, that the radial gauge is *compatible* with the Lorenz and the harmonic gauges. That is, if A_{μ} and $h_{\mu\nu}$ solve the Maxwell and the

linearized Einstein equations, then they can be gauge-transformed to fields A'_μ and $h'_{\mu\nu}$ satisfying (175,176) *and* (177,178). This is analogous to the well known fact (see for instance (32)) that the Lorenz and the harmonic gauges can be imposed simultaneously with the temporal gauge

$$A_0 = 0 \,, \tag{179a}$$

$$h_{0\mu} = 0 \,. \tag{179b}$$

We find convenient, below, to utilize the language of general covariant tensor calculus. To avoid confusion, let us point out that this does not mean that we work on a curved spacetime. We are only concerned here with Maxwell theory on flat space and with linearized General Relativity also on flat space. Tensor calculus is used below only as a tool for dealing in compact form with expressions in the hyperspherical coordinates that simplify the analysis of the radial gauge.

In the first paragraph is discussed Maxwell theory is discussed, in the second is discussed gravity. We work in an arbitrary number of dimensions, and we cover the Euclidean and the Lorentzian signatures at the same time. That is, we can take either $(\eta_{\mu\nu}) = \mathrm{diag}[1,1,1,1,...]$ or $(\eta_{\mu\nu}) = \mathrm{diag}[1,-1,-1,-1,...]$. The analysis is local in spacetime and disregards singular points such as the origin.

Maxwell theory In this paragraph we show the compatibility between Lorenz and radial gauge in electromagnetism. Maxwell vacuum equations are

$$\partial_\nu F^{\nu\mu} = 0 \,, \tag{180}$$

where $F_{\mu\nu} = \partial_\mu A_\nu - \partial_\nu A_\mu$. That is

$$\Box A_\mu - \partial_\mu \partial_\nu A^\nu = 0 \,, \tag{181}$$

where $\Box = \eta^{\mu\nu}\partial_\mu\partial_\nu$. This equation is of course invariant under the gauge transformation

$$A_\mu \to A'_\mu = A_\mu + \partial_\mu \lambda \,. \tag{182}$$

- **Temporal and Lorenz gauge**

  We begin by recalling how one can derive the well-know result that the Lorenz and *temporal* gauges are compatible. This is a demonstration that can be found in most elementary books on electromagnetism; we recall it here in a form that we shall reproduce below for the radial gauge.

  Let us write $(x^\mu) = (x^0, x^i) = (t, \vec{x}\,)$, where $i = 1, \ldots, d$. Let A_μ satisfy the Maxwell equations (181). We now show that there is a gauge equivalent field A'_μ satisfying the temporal as well as the Lorenz gauge conditions. That is, there exist a scalar function λ such that A'_μ defined in (182) satisfies (179a) and (177). The equation (179a) for A'_μ defined in (182) gives $A_0 + \partial_0\lambda = 0$, with the general solution

$$\lambda(t, \vec{x}\,) = -\int_{t_0}^{t} A_0(\tau, \vec{x}\,)\, \mathrm{d}\tau + \tilde{\lambda}(\vec{x}\,) \,, \tag{183}$$

where $\tilde{\lambda}(\vec{x}\,)$ is an integration "constant", which is an arbitrary function on the surface Σ defined by $t = t_0$. Can $\tilde{\lambda}(\vec{x}\,)$ (which is a function of d variables) be chosen in such a way that the Lorenz gauge condition (which is a function of $d+1$ variables) is satisfied? To show that this is the case, let us first fix $\tilde{\lambda}(\vec{x}\,)$ in such a way that the Lorenz gauge condition is satisfied *on* Σ. Inserting A'_μ in (177) and using (179a) we have

$$\partial_\mu A'^\mu = \partial_i A'^i = \partial_i A^i + \Delta\lambda = 0\,, \tag{184}$$

where $\Delta = \partial_i\partial^i$ is the Laplace operator[7] on Σ. The restriction of this equation to Σ gives the Poisson equation

$$\Delta\tilde{\lambda}(\vec{x}\,) = -\partial_i A^i(t_0, \vec{x}\,)\,, \tag{185}$$

which determines $\tilde{\lambda}(\vec{x}\,)$. With $\tilde{\lambda}(\vec{x}\,)$ satisfying this equation, A'_μ satisfies the temporal gauge condition everywhere and the Lorenz gauge condition on Σ. However, this implies immediately that A'_μ satisfies the Lorenz gauge condition everywhere as well, thanks to the Maxwell equations. In fact, the time component of (181) reads

$$\Box A'_0 - \partial_0\partial_\nu A'^\nu = -\partial_0(\partial_\nu A'^\nu) = 0\,. \tag{186}$$

That is: for a field in the temporal gauge, the Maxwell equations imply that if the Lorenz gauge is satisfied on Σ then it is satisfied everywhere.

- **Radial and Lorenz gauge**

We now show that the *radial* and Lorenz gauge are compatible, following steps similar to the ones above. We want to show that there exists a function λ such that A'_μ defined in (182) satisfies (175) and (177), assuming that A_μ satisfies the Maxwell equations.

Due to the symmetry of the problem, it is convenient to use polar coordinates. We write these as $(x^a) = (x^r, x^i) = (r, \vec{x}\,)$, where $r = \sqrt{|\eta_{\mu\nu}x^\mu x^\nu|}$ is the $(d+1)$-dimensional radius and $\vec{x} = (x^i)$ are three angular coordinates. In these coordinates the metric tensor $\eta_{\mu\nu}$ takes the simple form

$$\mathrm{d}s^2 = \gamma_{ab}(r, \vec{x}\,)\,\mathrm{d}x^a\,\mathrm{d}x^b = \mathrm{d}r^2 + r^2\xi_{ij}(\vec{x}\,)\,\mathrm{d}x^i\,\mathrm{d}x^j\,, \tag{187}$$

where $\xi_{ij}(\vec{x}\,)$ is independent from r and is the metric of a 3-sphere of unit radius in the Euclidean case, and the metric of an hyperboloid of unit radius in the Lorentzian case. It is easy to see that in these coordinates, the radial gauge condition (175) takes the simple form

$$A'_r = 0\,. \tag{188}$$

Inserting the definition of A'_μ gives

$$\partial_r\lambda = -A_r\,, \tag{189}$$

[7] Minus the Laplace operator in the Lorentzian case.

with the general solution

$$\lambda(r,\vec{x}\,) = -\int_{r_0}^{r} A_r(\rho,\vec{x}\,)\,\mathrm{d}\rho + \tilde{\lambda}(\vec{x}\,)\,, \tag{190}$$

where the integration constant $\tilde{\lambda}$ is now a function on the surface Σ defined by $r=r_0$. The surface Σ is a d-sphere in the Euclidean case and a d-dimensional hyperboloid in the Lorentzian case. As in the previous section, we fix $\tilde{\lambda}(\vec{x}\,)$ by requiring the Lorenz condition to be satisfied on Σ. It is convenient to use general covariant tensor calculus in order to simplify the expressions in polar coordinates. In arbitrary coordinates, the Lorenz condition reads

$$\nabla_a A'^a = \frac{1}{\sqrt{\gamma}}\partial_a\big(\sqrt{\gamma}A'^a\big) = 0\,, \tag{191}$$

where ∇_a is the covariant derivative, $A_b = A^a g_{ab}$, and γ is the determinant of γ_{ab}. This determinant has the form $\gamma = r^{2d}\xi$, where ξ is the determinant of ξ_{ij}. When the radial gauge is satisfied, (191) reduces to

$$\partial_i\big(\sqrt{\xi}A'^i\big) = 0\,. \tag{192}$$

Let us now require that A'_μ satisfies this equation on Σ. Using (182), this requirement fixes $\tilde{\lambda}$ to be the solution of a Poisson equation on Σ, that is

$$\Delta\tilde{\lambda} = -\frac{1}{\sqrt{\xi}}\partial_i\big(\sqrt{\xi}A^i\big)\,, \tag{193}$$

where the Laplace operator is $\Delta = \nabla_i\,\xi^{ij}\nabla_j$. In arbitrary coordinates, Maxwell equations read

$$\nabla_a F^{ab} = \frac{1}{\sqrt{\gamma}}\partial_a\big(\sqrt{\gamma}\,F^{ab}\big) = 0\,, \tag{194}$$

where

$$F^{ab} = \nabla^a A^b - \nabla^b A^a\,. \tag{195}$$

Consider the radial ($b=r$) component of (194); since $A'_r = 0$, using the form (187) of the metric, we have

$$\begin{aligned}\frac{1}{\sqrt{\gamma}}\partial_a(\sqrt{\gamma}F^{ar}) &= \frac{1}{\sqrt{\gamma}}\partial_a(\sqrt{\gamma}\gamma^{ab}F_{br}) = \frac{1}{\sqrt{\gamma}}\partial_a(\sqrt{\gamma}\gamma^{ab}(\partial_b A'_r - \partial_r A'_b)) = \\ &= -\frac{1}{\sqrt{\xi}}\partial_i\Big(\sqrt{\xi}\,\frac{\xi^{ij}}{r^2}\partial_r A'_j\Big) = -\frac{1}{r^2\sqrt{\xi}}\partial_r\partial_i(\sqrt{\xi}\xi^{ij}A'_j) = 0\,,\end{aligned} \tag{196}$$

which shows that the Lorenz gauge condition (192) is satisfied everywhere if it satisfied on Σ. This shows that we can find a function λ such that both the radial and the Lorenz gauge are satisfied everywhere.

Linearized General Relativity We now consider the compatibility between the radial gauge and the harmonic traceless gauge (also known as transverse traceless gauge (32)) in linearized General Relativity. Einstein equations in vacuum are given by the vanishing of the Ricci tensor. If $|h_{\mu\nu}(x)| \ll 1$, and we linearize these equations in $h_{\mu\nu}$, we obtain the linearized Einstein equations

$$\partial_\mu \partial_\nu h^\alpha{}_\alpha + \partial_\alpha \partial^\alpha h_{\mu\nu} - \partial_\mu \partial^\alpha h_{\alpha\nu} - \partial_\nu \partial^\alpha h_{\alpha\mu} = 0 \,. \tag{197}$$

Under infinitesimal coordinate transformations,

$$h_{\mu\nu} \to h'_{\mu\nu} = h_{\mu\nu} + \frac{1}{2}(\partial_\mu \lambda_\nu + \partial_\nu \lambda_\mu) \,, \tag{198}$$

where the factor $1/2$ is inserted for convenience. These are gauge transformations of the linearized theory. The harmonic gauge is defined by the condition

$$\nabla^\nu \nabla_\nu x^\mu = 0 \,, \tag{199}$$

where ∇_ν is the covariant partial derivative[8]; in the linearized theory (199) reduces to

$$\partial_\nu h^{\nu\mu} - \frac{1}{2}\partial^\mu h^\nu{}_\nu = 0 \,, \tag{200}$$

and in this gauge the Einstein equations (197) read simply

$$\Box h_{\mu\nu} = 0 \,. \tag{201}$$

- **Temporal and harmonic gauge**

  As we did for Maxwell theory, we begin by recalling how the compatibility between *temporal* and harmonic gauge can be proved. Start by searching a gauge parameter λ_μ that takes $h_{\mu\nu}$ to the temporal gauge $h'_{0\nu} = 0$. Equation (179b) gives

  $$h_{0\mu} + \frac{1}{2}(\partial_0 \lambda_\mu + \partial_\mu \lambda_0) = 0 \tag{202}$$

  with the general solution

  $$\lambda_0(t, \vec{x}\,) = -\int_{t_0}^{t} h_{00}(\tau, \vec{x}\,)\, \mathrm{d}\tau + \tilde{\lambda}_0(\vec{x}\,) \,, \tag{203a}$$

  $$\lambda_i(t, \vec{x}\,) = -\int_{t_0}^{t} \Big(2h_{0i}(\tau, \vec{x}\,) + \partial_i \lambda_0(\tau, \vec{x}\,)\Big)\, \mathrm{d}\tau + \tilde{\lambda}_i(\vec{x}\,) \,, \tag{203b}$$

  where the integration constants $\tilde{\lambda}_\mu(\vec{x}\,)$ are functions on the 3d surface Σ defined by $t = t_0$. Next, we fix $\tilde{\lambda}_i$ by imposing the harmonic gauge condition (200) on Σ. Since we are in temporal gauge, this gives

  $$\Delta \tilde{\lambda}_j = -2\partial_i h^i{}_j + \partial_j h^i{}_i \,, \tag{204}$$

[8] Notice that (199) means the covariant Laplacian of d+1 scalars (d+1 coordinates), not the covariant Laplacian of a $(d+1)$-vector.

which can be clearly solved on Σ. The time-time component of Einstein equations becomes

$$\partial_t^2 h'^i{}_i = 0 \,, \tag{205}$$

whose only well behaved solution is $h'^i{}_i = 0$; so in the temporal gauge the invariant trace of $h'_{\mu\nu}$ vanishes:

$$h'^\mu{}_\mu = \eta^{\mu\nu} h'_{\mu\nu} = 0 \,, \tag{206}$$

and the harmonic condition (200) takes the simpler form

$$\partial_\nu h'^{\nu\mu} = 0 \,, \tag{207}$$

similar to the Lorenz gauge. Now the (t, i) components of Einstein equations read

$$\partial_t \partial_j h'^j{}_i = 0 \,, \tag{208}$$

which gives $\partial_j h'^j{}_i = 0$ everywhere, once imposed on Σ.

- **Radial and harmonic gauge**

Let us finally come to the compatibility between the *radial* and harmonic gauges. We return to the polar coordinates used in the Maxwell case. In these coordinates, the radial gauge condition (176) reads

$$h'_{rr} = h'_{ri} = 0 \,. \tag{209}$$

Inserting the gauge transformation (198) gives

$$\partial_r \lambda_r = -h_{rr} \,, \tag{210a}$$

$$\partial_r \lambda_i + \partial_i \lambda_r - \frac{2}{r} \lambda_i = -2 h_{ri} \,, \tag{210b}$$

with the general solution

$$\lambda_r(r, \vec{x}\,) = -\int_{r_0}^{r} h_{rr}(\rho, \vec{x}\,)\, \mathrm{d}\rho + \tilde{\lambda}_r(\vec{x}\,) \,, \tag{211a}$$

$$\lambda_i(r, \vec{x}\,) = -r^2 \int_{r_0}^{r} \frac{2h_{ri}(\rho, \vec{x}\,) + \partial_i \lambda_r(\rho, \vec{x}\,)}{\rho^2}\, \mathrm{d}\rho + r^2\, \tilde{\lambda}_i(\vec{x}\,) \,, \tag{211b}$$

where $\tilde{\lambda}_r, \tilde{\lambda}_i$ are functions on the surface Σ given by $r = r_0$. We can then fix $\tilde{\lambda}_i$ by imposing the harmonic condition on Σ precisely as before. In the polar coordinates (187), we have easily the following rules for the Christoffel symbols:

$$\Gamma^a{}_{rr} = 0 \,, \qquad \Gamma^i{}_{jr} = \frac{1}{r} \delta^i{}_j \,, \qquad \Gamma^r{}_{ra} = 0 \,. \tag{212}$$

We note also that $\Gamma^i{}_{jk}$ is independent of r. Consider the (r,r) component of Einstein equations:

$$\nabla_r \nabla_r h'^a{}_a + \nabla_a \nabla^a h'_{rr} - \nabla_r \nabla^a h_{ar} - \nabla_r \nabla^a h'_{ar} = 0 \,. \tag{213}$$

Taking into account (187) and (212), it is verified after a little algebra that the previous equation becomes

$$\partial_r^2 h'^a{}_a + \frac{2}{r} \partial_r h'^a{}_a = 0 \,, \tag{214}$$

which is a differential equation for the trace $h'^a{}_a$. Its only solution well-behaved at the origin and at infinity is $h'^a{}_a = 0$. Using this, the (r,i) components of Einstein equations read:

$$\nabla_a \nabla^a h'_{ri} - \nabla_r \nabla^a h'_{ai} - \nabla_i \nabla^a h'_{ar} = -\partial_r \nabla_a h'^a{}_i = 0 \,, \tag{215}$$

and the harmonic condition is simply

$$\nabla_a h'^{ab} = 0 \,. \tag{216}$$

Equation (215) shows immediately that the $b=i$ components of the gauge condition (216) hold everywhere if they hold on Σ. The vanishing of the $b=r$ component of (216) follows immediately since, using (212), we have

$$\nabla_a h'^a{}_r = -\frac{1}{r} h'^a{}_a = 0 \,. \tag{217}$$

Therefore the harmonic gauge condition, the radial gauge condition and the vanishing of the trace are all consistent with one another.

6 Non diagonal components

In (21) a technique to compute the non diagonal components of LQG graviton propagator was developed; the construction of the non diagonal terms is very important because the graviton operators $\widehat{E}_n^{(i)} \cdot \widehat{E}_n^{(j)}$ call into play the dependence of the spin-networks on the *intertwiners* and, in turn, the dependence of the boundary state and the vertex from these variables. From this analysis it follows that the BC dynamics used to compute the diagonal terms has a trivial intertwiner dependence that jeopardize the correct behavior of the non diagonal terms. The key ingredients for the calculation of non diagonal terms are: the action of the field operators $\widehat{E}_n^{(i)} \cdot \widehat{E}_n^{(j)}$ on spin-networks, the boundary state and the implementation of the pairing independence.

6.1 *Action of field operators*

The field operators associated to the node n acts on the intertwiner space at the node n; the node is determined by five quantum numbers: the four spins j_l, $(l = 1 \dots 4)$ labeling the links adjacent to the node, and the value of the intertwiner i associated to the virtual link. The

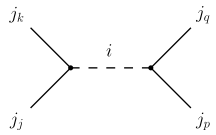

operator $\widehat{E}_n^{(k)}$ is defined as the projection of $\widehat{E}_i^a(x_n)$ along the normal to the triangle cut by the link k, and x_n is the node n. The action of the field operators $\widehat{E}^{(k)} \cdot \widehat{E}^{(j)}$ is a "double grasping" that inserts a virtual link "near" the node, connecting the links k and j. Once fixed the pairing at the node, say $(k, j)(p, q)$ like in figure (6.1), and the orientation (say clockwise for each of two trivalent vertices) there are three possible configurations for the grasping: $E^{(k)} \cdot E^{(j)}$, $E^{(k)} \cdot E^{(q)}$, $E^{(k)} \cdot E^{(p)}$; we can compute the action in every configuration using the graphic notation of $SU(2)$ recoupling theory.

6.2 *The boundary state*

The boundary state is a generalization of (170) with a non trivial intertwiner dependence:

$$\begin{aligned}\Phi(\mathbf{j}, \mathbf{i}) = C \exp\left\{ -\frac{1}{2j_0} \sum_{(ij)(mr)} \alpha_{(ij)(mr)} \ (j_{ij} - j_0)(j_{mr} - j_0) + \mathrm{i}\Phi \sum_{(ij)} j_{ij} \right\} \times \\ \times \exp\left\{ -\sum_n \left(\frac{(i_n - i_0)^2}{4\sigma} + \sum_{p \neq n} \phi(j_{np} - j_0)(i_n - i_0) + \mathrm{i}\chi(i_n - i_0) \right) \right\} .\end{aligned} \tag{218}$$

Here the exponential in the first line has precisely the spin dependence of the state (166); the second factor contains a Gaussian dependence on the intertwiner variables. More precisely, it includes a diagonal intetwiner-intertwiner Gaussian term, a nondiagonal Gaussian spin-intertwiner term, and a phase factor. The constants appearing in (218) can be fixed by requiring the state

to be peaked on the expected geometry. As in section 5.2 the constant j_0 determines the background area A_0 of the triangles; the constant Φ determines the background value of the angles between the normals to tetrahedra; we fix it to that of a regular four-simplex, namely $\cos\Phi = -1/4$. The constant i_0 is the background value of the intertwiner variables. As shown before, the spin of the virtual link i_n is the quantum number of the *angle* between the normals of two triangles. The five intertwiners i_n are the quantum numbers associated to the angles $\theta_n^{(nk,nj)}$ between the links (nk) and (nj). More precisely, we have the following action (with $\kappa\hbar\gamma = 1$):

$$\widehat{A}^2_{nk} + \widehat{A}^2_{nj} + 2\widehat{A}_{nk}\widehat{A}_{nj}\widehat{\cos\theta}_n^{(nk,nj)}$$

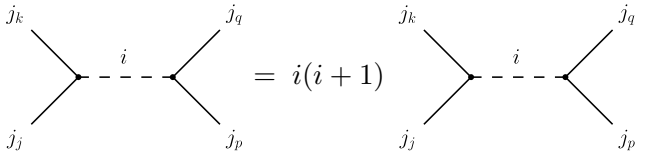

$$= i(i+1)$$

(219)

where k and j are the paired links at the node n and A_{nk} is the area of the triangle dual to the link (nk) . For each node, the state must therefore be peaked on a value i_0 such that

$$i_0(i_0+1) = A_0^2 + A_0^2 + 2A_0A_0\cos\theta_{ij}\,. \tag{220}$$

For the regular 4-simplex, in the large distance limit we have $A_{kj} \simeq j_0$, $\cos\theta_{kj} = -\frac{1}{3}$, which gives

$$i_0 = \frac{2}{\sqrt{3}}\,j_0\,. \tag{221}$$

Fixing i_0 in this manner determines only the mean value of the angle θ_{kj} between the two paired triangles. What about the mean value of the angles between triangles that are not paired together, such as θ_{kq} in (219)? It is shown in (97) that a state of the form $e^{-(i-i_0)^2/\sigma}$ is peaked on $\theta_{kq} = 0$, which is not what we want; but the mean value of θ_{kq}, can be modified by adding a phase to the state. This is the analog of the fact that a phase changes the mean value of the momentum of the wave packet of a non relativistic particle, without affecting the mean value of the position. In particular, it was shown in (97) that by choosing the phase and the width of the Gaussian to be

$$\chi = \frac{\pi}{2}, \qquad \sigma = \frac{4j_0}{3}\,, \tag{222}$$

we obtain a state whose mean value and variance for all angles is the same. Let us therefore adopt here these values.

Furthermore, here the spins can take arbitrary values around the peak symmetric configuration $j_{nm} = j_0$; as a consequence, one has to add a spin-intertwiner Gaussian terms. A detailed calculation, shows that choosing

$$\phi = -\mathrm{i}\frac{3}{4j_0}\,, \tag{223}$$

in the large j_0 limit, the state (218) transforms under change of pairing into a state with the same intertwiner mean value and the same variance σ. We assume this value of ϕ from now on. Now, introducing the perturbations $\delta i_n = i_n - i_0$ and $\delta j_{mr} = j_{mr} - j_0$, the wave functional given in (218) reads

$$\Phi(\mathbf{j},\mathbf{i}) \;= C\; e^{-\frac{1}{2j_0}\sum\alpha_{(ij)(mr)}\delta j_{ij}\delta j_{mr} + \mathrm{i}\Phi\sum_{ij}\delta j_{ij}}\, e^{-\sum_n\left(\frac{3(\delta i_n)^2}{4j_0} - \mathrm{i}\left(\sum_a \frac{3}{4j_0}\delta j_{an} - \frac{\pi}{2}\right)\delta i_n\right)}\,. \tag{224}$$

6.3 *Symmetrization of the state*

The state (224) presents a difficulty: it does not respect the symmetry of the four-simplex; to avoid this difficulties the simplest possibility is to choose an arbitrary pairing, and then to symmetrize *only* under the symmetries of the four-simplex.
Recall that there are three natural basis in each intertwiner space, determined by the three possible pairings of these links. Denote them as follows:

$i^x =$ 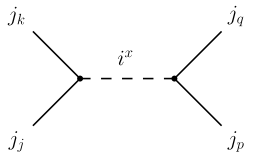

, $i^y =$ 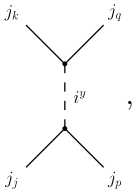

, $i^z =$ 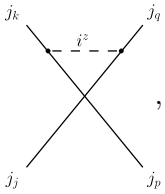

, (225)

where we conventionally denote $i^x \equiv i$ the basis in the pairing chosen as reference. These bases diagonalize the three non commuting operators $\widehat{E}^{(k)} \cdot \widehat{E}^{(j)}$, $\widehat{E}^{(k)} \cdot \widehat{E}^{(q)}$ and $\widehat{E}^{(k)} \cdot \widehat{E}^{(p)}$, respectively. The symmetries of a four-simplex are generated by the 5! permutations σ of the five vertices of the four-simplex. A permutation $\sigma : \{1,2,3,4,5\} \to \{\sigma(1), \sigma(2), \sigma(3), \sigma(4), \sigma(5)\}$ acts naturally on spin-networks:

$$\sigma |j_{nm}, i_{x_n}\rangle = |j_{\sigma(n)\sigma(m)}, i_{\sigma(x_n)}\rangle \,, \tag{226}$$

where the action $\sigma(x_n)$ of the permutation on a node is defined by

$$\sigma((ab)(cd)_n) = (\sigma(a)\sigma(b))(\sigma(c)\sigma(d))_{\sigma(n)} \tag{227}$$

and can therefore change the original pairing at the node.
We define the boundary state by replacing (224) with

$$|\Psi\rangle = \sum_\sigma \ \sigma|\Phi\rangle = \sum_\sigma \ \sum_{\mathbf{j},\mathbf{i}} \ \Phi(\mathbf{j},\mathbf{i}) \ \ \sigma|\mathbf{j},\mathbf{i}\rangle \,. \tag{228}$$

6.4 *Calculation of complete propagator*

The full calculation of the propagator is done in (21); we follow the main steps to give a sketch of the calculation. First of all we change the basis in order to diagonalize the action of the double grasping operators. The formula for a change of basis associated to a change of pairing (83), i.e. from the basis i_y to i_x in the node $n = 1$, is for large j_0's the following:

$$\Phi'_{\mathbf{q}}(\mathbf{j}, i_1^y, i_2, ..., i_5) \simeq \Phi(\mathbf{j}, i_1^x, i_2, ..., i_5) N_1 \ e^{-\mathrm{i}S[j_{1a}]} e^{-2\mathrm{i}\left(\sum_a \frac{3}{4j_0}\,\delta j^{a1}\right)\delta i_1^x} \,, \tag{229}$$

where N_1 is a constant phase, and $S[j_{1a}]$ is the expansion of the Regge Action (120) for the tetrahedron associated with the $6j$-symbol, up to second order *only in the link variables*, that is

$$S[j_{1a}] = \sum_{a\neq 1} \left(\frac{\partial S_R}{\partial j_{1a}}\bigg|_{j_0,i_0} \delta j_{1a} + \frac{\partial^2 S_R}{\partial j_{1a}\partial j_{1a'}}\bigg|_{j_0,i_0} \delta j_{1a}\delta j_{1a'} + \frac{1}{2}\,\frac{\partial^2 S_R}{\partial^2 j_{1a}}\bigg|_{j_0,i_0} (\delta j_{1a})^2 \right) . \tag{230}$$

The second step is to use the asymptotic formula of the Barret-Crane vertex (169) as in section (5.2).
Finally, after a long calculation, inserting the explicit form of the state and the asymptotic expression for the BC vertex we obtain for large j_0's

$$\begin{aligned}\mathbf{G}^{ij,kl}_{\mathbf{q}\,n,m} \simeq \mathcal{N}' j_0^2 \sum_{\delta\mathbf{j},\,\delta\mathbf{i}} \left(\frac{2}{\sqrt{3}}\,\delta i_n - \delta j_{nj} - \delta j_{nk}\right)\left(\frac{2}{\sqrt{3}}\,\delta i_m - \delta j_{mk} - \delta j_{ml}\right)\times \\ \times\ e^{-\frac{1}{2j_0}(\alpha+iGj_0)_{(ij)(mn)}\ \delta j_{ij}\delta j_{mn}} e^{-\sum_n\left(\frac{3(\delta i_n)^2}{4j_0}-\mathrm{i}\left(\sum_a \frac{3}{4j_0}\,\delta j_{an}+\frac{\pi}{2}\right)\delta i_n\right)}\,;\end{aligned} \tag{231}$$

here G is the matrix of the second derivatives of the Regge action (see (84; 19)). To evaluate this expression we can approximate the sum with an integral and rearrange it introducing the 15 component vector $\delta I^\alpha = (\delta j^{ab}, \delta i_n)$ and $\Theta^\alpha = (0, \chi_{i_n})$ and the 15×15 correlation matrix

$$M = \begin{pmatrix} \mathrm{A}_{10\times 10} & \mathrm{C}_{10\times 5} \\ \mathrm{C}^T_{5\times 10} & \mathrm{S}_{5\times 5}\end{pmatrix}, \tag{232}$$

where $A_{ab\,cd} = \frac{1}{2}(\alpha + iGj_0)_{ab\,cd}$ is a 10×10 matrix and $S_{nm} = I_{nm}\frac{3}{4}$ is a diagonal 5×5 matrix and C is a 10×5 matrix. We have:

$$\mathbf{G}^{ij,kl}_{\mathbf{q}\,n,m} = \mathcal{N}' j_0^2 \int \mathrm{d}\delta I^\alpha \left(\frac{2}{\sqrt{3}}\,\delta i_n - \delta j_{ni} - \delta j_{nj}\right)\left(\frac{2}{\sqrt{3}}\,\delta i_m - \delta j_{mk} - \delta j_{ml}\right)\ e^{-\frac{M_{\alpha\beta}}{j_0}\delta I^\alpha \delta I^\beta}\ e^{i\Theta_\alpha \delta I^\alpha}. \tag{233}$$

The matrix M is invertible and independent from j_0. A direct calculation gives a sum of terms of the kind

$$\frac{e^{-j_0\Theta M^{-1}\Theta}}{\sqrt{\det M}}\left(j_0^3 M^{-1}_{\alpha\beta} - j_0^4 M^{-1}_{\alpha\gamma}\Theta^\gamma M^{-1}_{\beta\delta}\Theta^\delta\right). \tag{234}$$

These terms go to zero fast in the $j_0\to\infty$ limit, and therefore do not match the expected large distance behavior of the propagator. There is no way to avoid this problem even changing the normalization factor.
This difficulty stresses the inadequacy of the Barret Crane model: the vertex freezes the intertwiners d.o.f. by projecting on the BC intertwiner. Now we explain the problem in more detail (98).
The propagator depends only on the asymptotic behavior of the vertex. This has the structure (75)

$$W_{BC}(\mathbf{j}) \sim e^{\frac{i}{2}(\delta\mathbf{j}G\delta\mathbf{j})}e^{i\Phi\cdot\delta\mathbf{j}} + e^{-\frac{i}{2}(\delta\mathbf{j}G\delta\mathbf{j})}e^{-i\Phi\cdot\delta\mathbf{j}}, \tag{235}$$

where G is the 10×10 matrix given by the second derivatives of the 4d Regge action around the symmetric state, $\delta\mathbf{j}$ is the difference between the ten spins $\mathbf{j}$ and their background value j_0, and Φ is a 10d vector with all equal components, which were shown in (80; 19) to precisely match those determined by the background extrinsic curvature.

The problem with the BC vertex is that it does not cancel the phase in the intertwiner variables of the boundary state and so this makes the non diagonal components vanish. In

Quantum Mechanics there is an analogous mechanism through which the dynamical kernel reproduces the semiclassical dynamics: there is a cancellation of the phases between the propagation kernel and the boundary state. If this does not happen, the rapidly oscillating phases suppress the amplitude. For instance, in non-relativistic Quantum Mechanics, the propagation kernel $K(x,y)$ of a free particle, has a phase dependence on small fluctuations $\delta x = x - x_0$ and $\delta y = y - y_0$ of the form

$$K(x_0+\delta x, y_0+\delta y) = \langle x_0+\delta x | e^{-\frac{\mathrm{i}}{\hbar}\frac{p^2}{2m}t} | y_0+\delta y\rangle \sim C\ e^{-\mathrm{i}p_0\delta x}\ e^{\mathrm{i}p_0\delta y}. \tag{236}$$

where $p_0 = m(y_0 - x_0)/t$. This phase cancels precisely the phase of the initial and final wave packets ψ_i and ψ_f centered on x_0 and y_0, only if these have the correct momentum. That is

$$\langle \psi_f | e^{-\frac{\mathrm{i}}{\hbar}Ht} | \psi_i\rangle = \int \mathrm{d}x \int \mathrm{d}y\ e^{-\frac{(x-x_0)^2}{2\sigma} - \frac{\mathrm{i}}{\hbar}p_f x}\ K(x,y)\ e^{-\frac{(y-y_0)^2}{2\sigma} + \frac{\mathrm{i}}{\hbar}p_i y} \tag{237}$$

is suppressed by the oscillating phases unless $p_i = p_f = p_0$. This is the standard mechanism through which a quantum theory reproduces the classical behavior. In quantum gravity, it is reasonable to expect the same to happen if we have to recover the Einstein equations in the semiclassical limit. That is, the propagation kernel W, must have a phase dependence that matches the one in the semiclassical boundary state. It is interesting, for future investigations, to see if we can obtain the correct non diagonal terms putting by hands the missing phase into the vertex: the answer is yes.

To this purpose we choose a vertex W with an asymptotic form that includes a Gaussian intertwiner-intertwiner and spin-intertwiner dependence, and –most crucially– a phase dependence on the intertwiner variables. To write this, introduce a 15d vector $\delta\mathbf{I} = (\delta\mathbf{j}, \delta\mathbf{i})$, where $\delta I_\alpha = (\delta j_{nm}, \delta i_n) = (j_{nm} - j_0, i_n - i_0)$, and consider the vertex amplitude

$$W(\mathbf{j},\mathbf{i}) = e^{\frac{i}{2}(\delta\mathbf{I}G\delta\mathbf{I})} e^{\mathrm{i}\phi\cdot\delta\mathbf{I}} + e^{-\frac{\mathrm{i}}{2}(\delta\mathbf{I}G\delta\mathbf{I})} e^{-\mathrm{i}\phi\cdot\delta\mathbf{I}}\,. \tag{238}$$

Here G is now a 15×15 matrix and $\phi = (\phi_{nm}, \phi_n)$ is a 15d vector. Its 10 spin components ϕ_{nm} just reproduce the spin phase dependence of (235), while its five intertwiner components are equal and we fix them to have value $\phi_n = \pi/2$. This phase dependence is the crucial detail that makes the calculation work and we obtain the correct behavior of the non diagonal terms of graviton propagator.

7 A new model: EPRL vertex

In (15) J. Engle, R. Pereira and C. Rovelli have introduced a new spinfoam model to correct the BC model. The difficulties with the BC model are related to the fact that the intertwiner quantum numbers are fully constrained; this is due to the mistake of imposing the simplicity constraints as strong operator equations, even though they are second class constraints. In fact it is well known that imposing second class constraints strongly may lead to the incorrect elimination of physical degrees of freedom. The advantages of the new model are:

- Its boundary quantum state space matches *exactly* the one of $SO(3)$ LQG: no degrees of freedom are lost.
- As the degrees of freedom missing in BC are recovered, the vertex may yield the correct low-energy n-point functions.
- The vertex can be seen as a vertex over $SO(3)$ spin-networks or $SO(4)$ spin-networks, and it is both $SO(3)$ and $SO(4)$ covariant.

The generalization of this model to arbitrary values of γ is performed by J. Engle, E.R. Livine, R. Pereira and C. Rovelli in (22). Here we describe this more general model (EPRL model).

7.1 *The goal of the model: imposing weakly the simplicity constraints*

The Barrett-Crane theory constrains entirely the intertwiner degrees of freedom. The reduction of the intertwiner space to the sole i_{BC} vector comes from the strong imposition of the off-diagonal simplicity constraints, as we have seen in section 4.5. But these constraints do not commute with one another, and are therefore second class. Imposing second class constraints strongly is a well-known way of erroneously killing physical degrees of freedom in a theory.

In order to illustrate the problems that follow from imposing second class constraints strongly, and a possible solutions to this problem, consider a simple system that describes a single particle, but using twice as many variables as needed. The phase space is the doubled phase space for one particle, i.e., $((q_1, p_1), (q_2, p_2))$, and the symplectic structure is the one given by the commutator $\{q_a, p_b\} = \delta_{ab}$. We set the constraints to be

$$\begin{aligned} q_1 - q_2 &= 0\,, \\ p_1 - p_2 &= 0\,. \end{aligned} \tag{239}$$

To simplify the constraints we perform a change of variables $q_\pm = (q_1 \pm q_2)/2$ and $p_\pm = (p_1 \pm p_2)/2$, now the system (239) reads: $q_- = p_- = 0$. They are clearly second class constraints. Suppose we quantize this system on the Schrödinger Hilbert space $L^2[\mathbb{R}^2]$ formed by wave functions of the form $\psi(q_+, q_-)$. If we impose the two constraints strongly we obtain the set of two equations

$$\begin{aligned} q_-\ \psi(q_+, q_-) &= 0, \\ i\hbar\frac{\partial}{\partial q_-}\ \psi(q_+, q_-) &= 0 \end{aligned} \tag{240}$$

which has no solutions. We have lost entirely the system.

There are several ways of dealing with second class systems. One possibility, which is employed for instance in the Gupta-Bleuler formalism for electromagnetism and in string theory, can be illustrated as follows in the context of the simple model above. Define the creation and annihilation operators $a_-^\dagger = (p_- + iq_-)/\sqrt{2}$ and $a_- = (p_- - iq_-)/\sqrt{2}$. The constraints now read $a_- = a_-^\dagger = 0$. Impose only one of these strongly: $a_-|\psi\rangle = 0$ and call the space of states solving this $\mathcal{H}_{ph}$. Notice that the other one holds weakly, in the sense that

$$\langle\phi|a_-^\dagger|\psi\rangle = 0 \qquad \forall\ \phi,\psi \in \mathcal{H}_{ph}\,. \tag{241}$$

That is, $a_-^\dagger$ maps the physical Hilbert space $\mathcal{H}_{ph}$ into a subspace orthogonal to $\mathcal{H}_{ph}$. Similarly, in the Gupta-Bleuler formalism the Lorenz condition (which forms a second class system with the Gauss constraint) holds in the form

$$\langle\phi|\partial^\mu A_\mu|\psi\rangle = 0 \qquad \forall\ \phi,\psi \in \mathcal{H}_{ph}\,. \tag{242}$$

A general strategy to deal with second class constraints is therefore to search for a decomposition of the Hilbert space of the theory $\mathcal{H}_{kin} = \mathcal{H}_{phys} \oplus \mathcal{H}_{sp}$ (sp. for spurious) such that the constraints map $\mathcal{H}_{phys} \to \mathcal{H}_{sp}$. We then say that the constraints vanish weakly on $\mathcal{H}_{phys}$. This is the strategy we employ below for the off-diagonal simplicity constraints. Since the decomposition may not be unique, we will have to select the one which is best physically motivated.

7.2 *Description of the model*

As in the BC model we discretize spacetime using as configuration variables the bivectors $B_f(t)^{IJ}$ associated to faces f, and the holonomy $U_f(t,t')$ along the tetrahedra sharing f, starting from the tetrahedron t and ending at t'; $U_f(t) \equiv U_f(t,t)$ is the holonomy around the full loop of tetrahedra. Discretized GR results from imposing constraints on the B variables as seen for the BC model. They are:
1) simplicity constraints (diagonal (136), off-diagonal (137), dynamical (138));
2) closure constraint.
The dynamical simplicity constraint is automatically satisfied when the other constraints are satisfied. The closure constraint will be automatically implemented in the quantum theory; its effect, as known, is to restrict the states of the quantum theory to the gauge invariant ones.
Recall that in the LQG approach the action that is quantized is the Holst action (28), obtained adding to the original action a term that does not change the equations of motion. The classical discretized version of the Holst action is (99)

$$\begin{aligned} S \;=\; & -\frac{1}{\kappa}\sum_{f\in int\Delta} \mathrm{Tr}\Big[B_f(t)U_f(t) + \frac{1}{\gamma}{}^*B_f(t)U_f(t)\Big] \\ & -\frac{1}{\kappa}\sum_{f\in\partial\Delta} \mathrm{Tr}\Big[B_f(t)U_f(t,t') + \frac{1}{\gamma}{}^*B_f(t)U_f(t,t')\Big]\,. \end{aligned} \tag{243}$$

The constraints (136) and (137) have two sectors of solutions, one in which $B = {}^*e \wedge e$, and one in which $B = e \wedge e$. For finite Immirzi parameter both sectors in fact yield GR, but the value of the Newton constant and Immirzi parameter are different in each sector. In the $B = {}^*e \wedge e$ sector, the discrete Holst action becomes the Holst formulation of GR (35) with Newton constant G and Immirzi parameter γ. In the $B = e \wedge e$ sector, one *also* obtains the Holst formulation of GR, but this time with Newton constant $G\gamma$, and Immirzi parameter s/γ, where the signature s is $+1$ in the euclidean theory and -1 in the lorentzian theory. In order to select a single sector, we reformulate the simplicity constraints in such a way that these two sectors are distinguished. To this purpose, we replace the off-diagonal constraint (137) with the following stronger constraint: for each tetrahedron t there exists a (timelike in the Lorentzian case) vector n^I such that

$$n_I B_f^{IJ}(t) = 0 \tag{244}$$

for every triangle f of the tetrahedron. This condition is stronger than (137) since it selects only the desired $B = e \wedge e$ sector.
The relevant classical variables are the ones canonically conjugate; the variable conjugate to $U_f(t, t')$ is

$$J_f(t) = \frac{1}{k}(B_f(t) + \frac{1}{\gamma}{}^*B_f(t))\,. \tag{245}$$

We define also the spatial and temporal components of J as its contraction with n^I; choosing coordinates such that $(n^I) = (1, 0, 0, 0)$

$$L^i \equiv \frac{1}{2}\epsilon^i_{jk}J^{ik} \tag{246}$$

$$K^i \equiv J^{0i} \qquad i, j, k = 1, 2, 3\,. \tag{247}$$

In terms of the new variable J_f, the diagonal and off-diagonal simplicity constraints (136)-(244) read

$$\mathcal{C}_{ff} \equiv \big(1 + \frac{s}{\gamma^2}\big){}^*J_f \cdot J_f - \frac{2s}{\gamma}J_f \cdot J_f \approx 0 \tag{248}$$

$$\mathcal{C}^J_f \equiv n_I\big({}^*J_f^{IJ} - \frac{s}{\gamma}J_f^{IJ}\big) \approx 0 \Leftrightarrow \mathcal{C}^j_f \equiv L^j_f - \frac{s}{\gamma}K^j_f \approx 0\,. \tag{249}$$

The first constraint (248) commutes with the others, while the system of off-diagonal constraints (249) does not close a Poisson algebra. Thus we will impose strongly (248) and more weakly (249).
As in lattice QFT we choose the unconstrained kinematical quantum state space to be $\mathcal{H} = L^2(G^L)$, where L is the number of links in the boundary of the dual triangulation, and quantize the quantities $J_f^{IJ}(t_{\text{start}})$ as the right invariant vector fields, and the quantities $J_f^{IJ}(t_{\text{end}})$ as the left invariant vector fields over the space $L^2(G)$ associated to the boundary face f. So the quantum diagonal and off-diagonal constraints read

$$\widehat{\mathcal{C}}_{ff} \equiv (1 + \frac{s}{\gamma^2})^*\widehat{J}_f \cdot \widehat{J}_f - \frac{2s}{\gamma}\widehat{J}_f \cdot \widehat{J}_f \approx 0\,, \tag{250}$$

$$\widehat{\mathcal{C}}^j_f \equiv \widehat{L}^j_f - \frac{s}{\gamma}\widehat{K}^j_f \approx 0\,. \tag{251}$$

Euclidean The $SO(4)$ scalar Casimir $J \cdot J$ acts diagonally on the (j_+, j_-) component of $L^2(SO(3))$ in the Peter-Weyl decomposition, giving the eigenvalue $j_+(j_+ + 1) + j_-(j_- + 1)$, while the pseudo-scalar Casimir ${}^*J \cdot J$ gives $j_+(j_+ + 1) - j_-(j_- + 1)$. Hence from equation (248) the quantum diagonal simplicity constraint restricts the self dual and anti-self dual quantum numbers to be related by

$$j_+ = \frac{\gamma + 1}{\mid \gamma - 1 \mid} j_- \,. \tag{252}$$

Also in the BC model the diagonal constraint gives the relation between the two sectors, but here the two sectors are not balanced because of the finite value of γ. The system of off-diagonal constraints (251) must be imposed weakly. Alternatively it can be replaced by the single "master" constraint

$$\sum_i (\mathcal{C}^i)^2 = \sum_i (L^i - \frac{s}{\gamma} K^i)^2 \approx 0 \,. \tag{253}$$

Using (250) the "master" off-diagonal constraint becomes

$${}^*\widehat{J} \cdot \widehat{J} - 4\gamma \widehat{L}^2 \approx 0 \,. \tag{254}$$

The (j_+, j_-) subspace of $L^2(SO(4))$ decomposes into $SO(3)$ irreducible subspaces

$$\mid j_+ - j_- \mid \oplus \ldots \oplus (j_+ + j_-)$$

. On those subspaces (254) acts diagonally giving the relation

$$k = \begin{cases} j^+ + j^- & 0 < \gamma < 1 \\ j^+ - j^- & \gamma > 1 \,, \end{cases} \tag{255}$$

where k labels the $SO(3)$ irreducible representations in the decomposition.
For $\gamma < 1$ the constraint selects the highest $SO(3)$ irreducible, for $\gamma > 1$ the lowest. The set of closure, diagonal, and "master" off-diagonal constraints select our physical state space $\mathcal{H}_{phys}$, which is spanned by $SO(4)$ spin-networks (viewed as functions of holonomies, not of the connection) labeled by (j_+, j_-) satisfying (252) and intertwiners living in $Inv[\mathcal{H}_{|j_{1+} \pm j_{1-}|} \otimes \ldots \mathcal{H}_{|j_{4+} \pm j_{4-}|}]$, where the sign depends on γ as we have seen. Remarkably, $\mathcal{H}_{phys}$ is isomorphic to the boundary state space given by $SO(3)$ spin-networks, which is *exactly* the LQG state space! The isomorphism is realized sending a link in the k representation into a link labeled by the couple (j_+, j_-), where $j_\pm = \frac{|\gamma \pm 1|}{2} k$, and the $SO(3)$ intertwiner i is mapped in an $SO(4)$ intertwiner as follows

$$\mid i \rangle \longmapsto \sum_{i_+ i_-} f^i_{i_+ i_-} \mid i_+ \, i_- \rangle \tag{256}$$

where

$$f^i_{i_+ i_-}(j_1, j_2, j_3, j_4) \equiv \langle i_+ \, i_- \mid f \mid i \rangle = i^{abcd} \, C_a^{a_+ a_-} C_b^{b_+ b_-} C_c^{c_+ c_-} C_d^{d_+ d_-} \, i^+_{a_+ b_+ c_+ d_+} i^-_{a_- b_- c_- d_-} \,. \tag{257}$$

The tensors $\mid i\rangle$, $\mid i_+\, i_-\rangle$ are $SO(3)$ and $SO(4)$ orthonormal intertwiners and

$$C_a^{a_+a_-} \equiv \langle j_1^+ j_2^-, a_+a_-|j_1\, a\rangle \tag{258}$$

are Clebsh-Gordan coefficients. The coefficients (257), called fusion coefficients, define a map

$$f : \mathrm{Inv}[\mathcal{H}_{j_1} \otimes \ldots \otimes \mathcal{H}_{j_4}] \longrightarrow \mathrm{Inv}[\mathcal{H}_{(\frac{|1-\gamma|j_1}{2}, \frac{(1+\gamma)j_1}{2})} \otimes \ldots \otimes \mathcal{H}_{(\frac{|1-\gamma|j_4}{2}, \frac{(1+\gamma)j_4}{2})}] \tag{259}$$

from $SO(3)$ to $SO(4)$ intertwiners. The vertex amplitude is the $SO(4)$ $15j$-symbol labeled by representations satisfying (252) and intertwiners of the form (256). In terms of the LQG boundary variables it is:

$$A(\{j_{ab}\}, \{i^a\}) = \sum_{i_+^a i_-^a} 15j\left(\frac{j_{ab}(1+\gamma)}{2}; i_+^a\right) 15j\left(\frac{j_{ab} \mid 1-\gamma \mid}{2}; i_-^a\right) \prod_a f_{i_+^a i_-^a}^{i^a}(j_{ab})\,. \tag{260}$$

Lorentzian The $SL(2,\mathbb{C})$ Casimir operators for a representation of the Lorentz group in the principal series (n,ρ) are given by

$$J\cdot J = 2(L^2 - K^2) = \frac{1}{2}(n^2 - \rho^2 - 4)\,, \tag{261}$$

$$^*J\cdot J = -4L\cdot K = n\rho\,. \tag{262}$$

Solutions of (250) are given by either $\rho = \gamma n$ or $\rho = -n/\gamma$. The existence of these two solutions reflects the two sectors mentioned previously with Immirzi parameter γ and $-1/\gamma$. BF theory cannot a priori distinguish between these two sectors. However, in our framework, the master constraint (253) breaks this symmetry and selects the first branch $\rho = \gamma n$. It further imposes that $k = n/2$, where k again labels the subspaces diagonalizing L^2. Therefore the constraints select the lowest $SU(2)$ irreducible representation in the decomposition of $\mathcal{H}_{(n,\rho)} = \bigoplus_{k\geq n/2}\mathcal{H}_k$. Notice that there is no restriction on the value of γ as there was in the Euclidean case.

Notice also that the continuous label ρ becomes quantized, because n is discrete. It is because of this fact that any continuous spectrum depending on ρ comes out effectively discrete on the subspace satisfying the simplicity constraints.

As before, the embedding of intertwiners is given by:

$$f: \quad \mathrm{Inv}[\mathcal{H}_{j_1}\otimes ...\otimes \mathcal{H}_{j_4}] \longrightarrow \mathrm{Inv}[\mathcal{H}_{(n_1,\rho_1)}\otimes ...\otimes \mathcal{H}_{(n_4,\rho_4)}],$$

$$|i\rangle \longmapsto \sum_n \int \mathrm{d}\rho\,(n^2+\rho^2) f^i_{n\,\rho}|n\,\rho\rangle \tag{263}$$

where

$$f^i_{n\rho} \equiv i^{abcd}\overline{v}^{(n,\rho)}_{j_1 m_1,\ldots,j_4 m_4}\,. \tag{264}$$

Here $j_1 ... j_4$ are the representations meeting at the node, (j_a, m_a) are indices in the representation (n_a,ρ_a) of $SL(2,\mathbb{C})$, and $v^{(n,\rho)}$ is an $SL(2,\mathbb{C})$ 4-valent intertwiner labeled by the virtual link (n,ρ).
The boundary space is once again just given by the $SU(2)$ spin networks.

We are now ready to define the vertex. As before, we obtain

$$A(j_{ab}, i_a) = \sum_{n_a} \int d\rho_a (n_a^2 + \rho_a^2) \left(\prod_a f^{i_a}_{n_a \rho_a}(j_{ab}) \right) 15j_{SL(2,\mathbb{C})} \left((2j_{ab}, 2j_{ab}\gamma); (n_a, \rho_a) \right) . \quad (265)$$

The final partition function, for an arbitrary triangulation, is given by gluing these amplitudes together with suitable edge and face amplitudes:

$$Z = \sum_{j_f, i_e} \prod_f (2j_f)^2 (1+\gamma^2) \prod_v A(j_f, i_e) . \quad (266)$$

One important result achived by the EPRL model is that the spectrum of the operator related to the area of a triangle dual to the face f

$$\text{Area}^2 \equiv \frac{1}{2} ({}^\star B)^{ij} ({}^\star B)_{ij} = \frac{1}{4} \kappa^2 \gamma^2 L^2 \quad (267)$$

is *exactly* the spectrum of LQG, for both Euclidean and Lorentzian signatures:

$$\text{Area} = 8\pi\hbar G \gamma \sqrt{k(k+1)} . \quad (268)$$

This spectrum can be compared with the continuous spectrum

$$\text{Area} \sim \frac{1}{2} \sqrt{4k(k+1) - n^2 + \rho^2 + 4} \quad (269)$$

that was previously obtained in covariant LQG, before imposing the second class constraints (see (100)). Remarkably, imposing the simplicity constraints (248) and (254) reduces the continuous spectrum (269) to the exact discrete LQG spectrum (268).

7.3 *Outlook and summary*

E. Livine and S. Speziale have found an independent derivation of the vertex proposed here, based on the use of the coherent intertwiners they have introduced in (23). There is a relation between the $SO(4)$ states of this model and the projected spin-network states studied by L. Livine in (101). (A similar approach is developed by Alexandrov in (102).) The constrained $SO(4)$ states that form the physical Hilbert space of the EPRL model can be constructed from (the Euclidean analog of) these projected spin-networks. The Euclidean analog of the projected spin-networks defined in (101) are wavefunctions $\Psi[U_l, \chi_n]$ depending on an $SO(4)$ group element for each link, and a vector $\chi_n \in SO(4)/SO(3)$ at each node. The wavefunctions are labeled by an $SO(4)$ representation (j_l^+, j_l^-) for each link, an $SU(2)$ representation j_{nl} for each node and link based at that node, and an $SU(2)$ intertwiner at each node. The $SO(4)$ spin-networks in the EPR model can be obtained from the projected spin-networks by (i) setting $j_l^+ = j_l^- \equiv j_l$, (ii) setting $j_{nl} = j_l^+ + j_l^- = 2j_l$, and (iii) averaging over χ_n at each node (concretely this averaging can be done by acting on each χ_n with an $SO(4)$ element U_n, and then averaging over the U_n's independently using the Haar measure). Each of these three steps corresponds directly to solving (i) the diagonal simplicity constraints, (ii) the off-diagonal

simplicity constraints, and (iii) the Gauss constraint.
In this section we have described only the EPRL model, but there is also another model for the spin foam vertex proposed by L. Freidel and K. Krasnov (24).

In summary. The EPRL model extends the definition of the "flipped" loop-quantum-gravity vertex in (15) to the case of finite Immirzi parameter γ. It covers both the Euclidean and Lorentzian cases. The off-diagonal simplicity constraints are imposed weakly. This weakening of the constraints is motivated by the observation that they do not form a closed algebra, as well as by the realization that a richer boundary space is needed. The theory we have obtained is characterized by the fact that its boundary state space exactly matches that of Loop Quantum Gravity. This can be seen as an independent derivation of the LQG kinematics, and, in particular, of the fact that geometry is quantized. A vertex amplitude has then been derived from the discrete action, leading to a spinfoam model giving transition amplitudes for LQG states. The spectrum of the area operator too is the same as in LQG, both for the Euclidean *and* the Lorentzian sectors; the fact that the spectrum is discrete also in the Lorentzian case is remarkable; in fact it is non trivial that a non-compact gauge group, such as the Lorentz group, whose representations have continuous labels, may give rise to geometric observables with discrete spectrum.

We expect that the model considered here will admit a group field theory formulation and that its vertex can be used to generate the dynamics of Loop Quantum Gravity. The problem of calculating n-point functions is to derive the asymptotic formula for the new vertex at large spins. This is still missing, but in a recent work (25) we find the first ingredient: the asymptotics of the fusion coefficients. This is illustrated in the next section. From now on to avoid confusion we change notation and replace the label $+, -$ with R, L.

8 Asymptotics of LQG fusion coefficients

In the last section we have described the new spinfoam model Engle-Pereira-Rovelli-Livine (EPRL), here we present a careful analysis of the asymptotics of fusion coefficients $f^{i^a}_{i^a_L i^a_R}$ in the vertex amplitude (260); this is a step needed for the study of the semiclassical properties of the model and expecially to check if the new vertex has the right dependence in the intertwiners variables. The region of parameter space of interest is large spins j_{ab} and intertwiners i_a of the same order of magnitude of the spins. As a result, the fusion coefficients for the node $\bar{a}$, $f^{i_{\bar{a}}}_{i^L_{\bar{a}} i^R_{\bar{a}}}(j_{\bar{a}b})$, can be seen as a function of the two bare variables $i^L_{\bar{a}}$, $i^R_{\bar{a}}$, of the fluctuation of the intertwiner $i_{\bar{a}}$ and of the fluctuation of the four spins $j_{\bar{a}b}$. For different approaches to the semiclassical limit, see (103) and (104).

This section is organized as follows: in the first part 8.1 we show a simple analytic expression for the EPRL fusion coefficients; in the second 8.2 we use this expression for the analysis of the asymptotics of the coefficients in the region of parameter space of interest, and in third part 8.3 we show that the fusion coefficients map $SO(3)$ semiclassical intertwiners into $SU(2)_L \times SU(2)_R$ semiclassical intertwiners. We conclude discussing the relevance of this result for the analysis of the semiclassical behavior of the model. In the appendix we collect some useful formula involving Wigner coefficients.

8.1 *Analytical expression for the fusion coefficients*

The fusion coefficients provide a map from four-valent $SO(3)$ intertwiners to four-valent $SO(4)$ intertwiners. They can be defined in terms of contractions of $SU(2)$ $3j$-symbols. In the following we use a planar diagrammatic notation for $SU(2)$ recoupling theory (105). We represent the $SU(2)$ Wigner metric and the $SU(2)$ three-valent intertwiner respectively by an oriented line and by a node with three links oriented counter-clockwise[9]. As we have seen before, a four-valent $SO(3)$ intertwiner $|i\rangle$ can be represented in terms of the recoupling basis as

$$|i\,\rangle = \sqrt{2i+1}$$

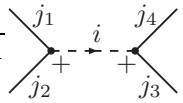

(270)

where a dashed line has been used to denote the virtual link associated to the coupling channel. Similarly a four-valent $SO(4)$ intertwiner can be represented in terms of an $SU(2)_L \times SU(2)_R$ basis as $|i_L\rangle|i_R\rangle$.

Using this diagrammatic notation, the EPRL fusion coefficients for given Immirzi parameter

[9] A minus sign in place of the + will be used to indicate clockwise orientation of the links.

γ are given by

$$f^i_{i_L i_R}(j_1,j_2,j_3,j_4) = (-1)^{j_1-j_2+j_3-j_4}\sqrt{(2i+1)(2i_L+1)(2i_R+1)\Pi_{n=1}^4(2j_n+1)} \quad \times \qquad (271)$$

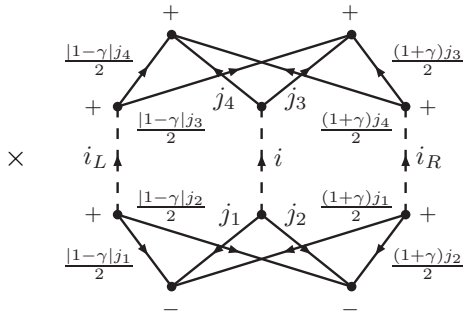

These coefficients define a map

$$f : Inv[H_{j_1}\otimes\ldots\otimes H_{j_4}] \longrightarrow Inv[H_{(\frac{|1-\gamma|j_1}{2},\frac{(1+\gamma)j_1}{2})}\otimes\ldots\otimes H_{(\frac{|1-\gamma|j_4}{2},\frac{(1+\gamma)j_4}{2})}] \qquad (272)$$

from $SO(3)$ to $SO(4)$ intertwiners. Using the identity

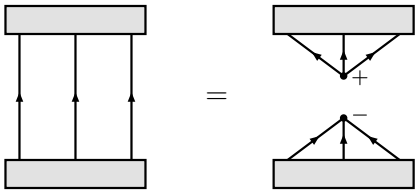

(273)

where the shaded rectangles represent arbitrary closed graphs, we have that the diagram in (271) can be written as the product of two terms

$$f^i_{i_L i_R}(j_1,j_2,j_3,j_4) = \qquad (274)$$

$$= (-1)^{j_1-j_2+j_3-j_4}\sqrt{(2i+1)(2i_L+1)(2i_R+1)\Pi_n(2j_n+1)}\ q^i_{i_L i_R}(j_1,j_2)\ q^i_{i_L i_R}(j_3,j_4) \qquad (275)$$

where $q^i_{i_L i_R}$ is given by the following $9j$-symbol

$$q^i_{i_L i_R}(j_1,j_2) \quad = \quad$$

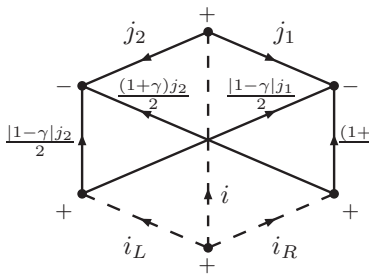

$$= \begin{Bmatrix} \frac{|1-\gamma|}{2}j_1 & i_L & \frac{|1-\gamma|}{2}j_2 \\ \frac{1+\gamma}{2}j_1 & i_R & \frac{1+\gamma}{2}j_2 \\ j_1 & i & j_2 \end{Bmatrix} . \qquad (276)$$

From the form of $q^i_{i_L i_R}$ we can read a number of properties of the fusion coefficients. First of all, the diagram in expression (276) displays a node with three links labelled i, i_L, i_R. This

corresponds to a triangular inequality between the intertwiners i, i_L, i_R which is not evident from formula (271). As a result we have that the fusion coefficients vanish outside the domain

$$|i_L - i_R| \leq i \leq i_L + i_R \ . \tag{277}$$

Moreover in the monochromatic case, $j_1 = j_2 = j_3 = j_4$, we have that the fusion coefficients are non-negative (as follows from (275)) and, for $i_L + i_R + i$ odd, they vanish (because the first and the third column in the $9j$-symbol are identical).

As discussed in (24; 23), the fact that the spins labeling the links in (271) have to be half-integers imposes a quantization condition on the Immirzi parameter γ. In particular γ has to be rational and a restriction on spins may be present. Such restrictions are absent in the Lorentzian case. Now notice that for $0 \leq \gamma < 1$ we have that $\frac{1+\gamma}{2} + \frac{|1-\gamma|}{2} = 1$, while for $\gamma > 1$ we have that $\frac{1+\gamma}{2} - \frac{|1-\gamma|}{2} = 1$ (with the limiting case $\gamma = 1$ corresponding to a selfdual connection). As a result, in the first and the third column of the $9j$-symbol in (276), the third entry is either the sum or the difference of the first two. In both cases the $9j$-symbol admits a simple expression in terms of a product of factorials and of a $3j$-symbol (see appendix A). Using this result we have that, for $0 \leq \gamma < 1$, the coefficient $q^i_{i_L i_R}(j_1, j_2)$ can be written as

$$q^i_{i_L i_R}(j_1, j_2) = (-1)^{i_L - i_R + (j_1 - j_2)} \begin{pmatrix} i_L & i_R & i \\ \frac{|1-\gamma|(j_1-j_2)}{2} & \frac{(1+\gamma)(j_1-j_2)}{2} & -(j_1 - j_2) \end{pmatrix} \ A^i_{i_L i_R}(j_1, j_2) \tag{278}$$

with $A^i_{i_L i_R}(j_1, j_2)$ given by

$$\begin{aligned} A^i_{i_L i_R}(j_1, j_2) = & \sqrt{\frac{(j_1 + j_2 - i)!\,(j_1 + j_2 + i + 1)!}{(2j_1 + 1)!\,(2j_2 + 1)!}} \ \times \\ & \times \sqrt{\frac{(|1-\gamma|j_1)!\,(|1-\gamma|j_2)!}{(\frac{|1-\gamma|j_1}{2} + \frac{|1-\gamma|j_2}{2} - i_L)!\,(\frac{|1-\gamma|j_1}{2} + \frac{|1-\gamma|j_2}{2} + i_L + 1)!}} \ \times \\ & \times \sqrt{\frac{((1+\gamma)j_1)!\,((1+\gamma)j_2)!}{(\frac{(1+\gamma)j_1}{2} + \frac{(1+\gamma)j_2}{2} - i_R)!\,(\frac{(1+\gamma)j_1}{2} + \frac{(1+\gamma)j_2}{2} + i_R + 1)!}} \ . \end{aligned} \tag{279}$$

A similar result is available for $\gamma > 1$. The Wigner $3j$-symbol in expression (278) displays explicitly the triangle inequality (277) among the intertwiners. Notice that the expression simplifies further in the monochromatic case as we have a $3j$-symbol with vanishing magnetic indices.

The fact that the fusion coefficients (271) admit an analytic expression which is so simple is certainly remarkable. The algebraic expression (275),(278),(279) involves no sum over magnetic indices. On the other hand, expression (271) involves ten $3j$-symbols (one for each node in the graph) and naively fifteen sums over magnetic indices (one for each link). In the following we will use this expression as starting point for our asymptotic analysis.

8.2 *Asymptotic analysis*

The new analytic formula (275),(278),(279) is well suited for studying the behavior of the EPRL fusion coefficients in different asymptotic regions of parameter space. Here we focus on the region of interest in the analysis of semiclassical correlations as discussed in the introduction. This region is identified as follows: let us introduce a large spin j_0 and a large intertwiner (i.e. virtual spin in a coupling channel) i_0; let us also fix the ratio between i_0 and j_0 to be of order one – in particular we will take $i_0 = \frac{2}{\sqrt{3}} j_0$; then we assume that

- the spins j_1, j_2, j_3, j_4, are restricted to be of the form $j_e = j_0 + \delta j_e$ with the fluctuation δj_e small with respect to the background value j_0. More precisely we require that the relative fluctuation $\frac{\delta j_e}{j_0}$ is of order $o(1/\sqrt{j_0})$;
- the $SO(3)$ intertwiner i is restricted to be of the form $i = i_0 + \delta i$ with the relative fluctuation $\frac{\delta i}{i_0}$ of order $o(1/\sqrt{j_0})$;
- the intertwiners for $SU(2)_L$ and $SU(2)_R$ are studied in the region close to the background values $i_L^0 = \frac{|1-\gamma|}{2} i_0$ and $i_R^0 = \frac{1+\gamma}{2} i_0$. We study the dependence of the fusion coefficients on the fluctuations of these background values assuming that the relative fluctuations $\delta i_L / i_0$ and $\delta i_R / i_0$ are of order $o(1/\sqrt{j_0})$.

A detailed motivation for these assumptions is provided in subsection 8.3. Here we notice that, both for $0 \leq \gamma < 1$ and for $\gamma > 1$, the background value of the intertwiners i_L, i_R, i, saturate one of the two triangular inequalities (277). As a result, we have that the fusion coefficients vanish unless the perturbations on the background satisfy the following inequality

$$\delta i \leq \delta i_L + \delta i_R \qquad 0 \leq \gamma < 1 \tag{280}$$

$$\delta i_R \leq \delta i + \delta i_L \qquad \gamma > 1 \, . \tag{281}$$

In order to derive the asymptotics of the EPRL fusion coefficients in this region of parameter space we need to analyze both the asymptotics of the $3j$-symbol in (278) and of the coefficients $A^i_{i_L i_R}(j_1, j_2)$. This is done in the following two paragraphs

Asymptotics of $3j$-symbols The behavior of the $3j$-symbol appearing in equation (278) in the asymptotic region described above is given by Ponzano-Regge asymptotic expression (equation 2.6 in (72); see also appendix B):

$$\begin{pmatrix} i_L & i_R & i \\ \frac{|1-\gamma|(j_1-j_2)}{2} & \frac{(1+\gamma)(j_1-j_2)}{2} & -(j_1-j_2) \end{pmatrix} \sim \frac{(-1)^{i_L+i_R-i+1}}{\sqrt{2\pi A}} \times \tag{282}$$

$$\times \cos\left((i_L + \frac{1}{2})\theta_L + (i_R + \frac{1}{2})\theta_R + (i + \frac{1}{2})\theta + \tfrac{|1-\gamma|(j_1-j_2)}{2}\phi_- - \tfrac{(1+\gamma)(j_1-j_2)}{2}\phi_+ + \frac{\pi}{4} \right) .$$

The quantities A, θ_L, θ_R, θ, ϕ_-, ϕ_+ admit a simple geometrical representation: let us consider a triangle with sides of length $i_L + \frac{1}{2}$, $i_R + \frac{1}{2}$, $i + \frac{1}{2}$ embedded in 3d Euclidean space as shown

below

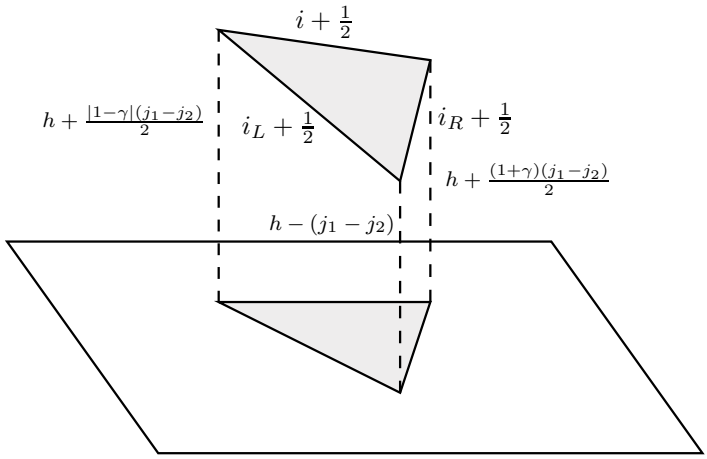

(283)

In the figure the height of the three vertices of the triangle with respect to a plane are given; this fixes the orientation of the triangle and forms an orthogonal prism with triangular base. The quantity A is the area of the base of the prism (shaded in picture). The quantities θ_L, θ_R, θ are dihedral angles between the faces of the prism which intersect at the sides i_L, i_R, i of the triangle. The quantities ϕ_-, ϕ_+ are dihedral angles between the faces of the prism which share the side of length $h+|1-\gamma|(j_1-j_2)/2$ and the side of length $h+(1+\gamma)(j_1-j_2)/2$, respectively. For explicit expressions we refer to the appendix.

In the monochromatic case, $j_1 = j_2$, we have that the triangle is parallel to the plane and the formula simplifies a lot; in particular we have that the area A of the base of the prism is simply given by Heron formula in terms of i_L, i_R, i only, and the dihedral angles θ_L, θ_R, θ are all equal to $\pi/2$. As a result the asymptotics is given by

$$\begin{pmatrix} i_L & i_R & i \\ 0 & 0 & 0 \end{pmatrix} \sim \frac{1}{\sqrt{2\pi A}} \frac{1+(-1)^{i_L+i_R+i}}{2} (-1)^{\frac{i_L+i_R+i}{2}} \ . \tag{284}$$

Notice that the sum $i_L + i_R + i$ is required to be integer and that the asymptotic expression vanishes if the sum is odd and is real if the sum is even. Now, the background configuration of i_L, i_R and i we are interested in corresponds to a triangle which is close to be degenerate to a segment. This is due to the fact that $\frac{(1-\gamma)}{2} i_0 + \frac{(1+\gamma)}{2} i_0 = i_0$ for $0 \leq \gamma < 1$, and $\frac{(\gamma+1)}{2} i_0 - \frac{(\gamma-1)}{2} i_0 = i_0$ for $\gamma > 1$. In fact the triangle is not degenerate as an offset $\frac{1}{2}$ is present in the length of its edges. As a result the area of this almost-degenerate triangle is non-zero and scales as $i_0^{3/2}$ for large i_0. When we take into account allowed perturbations of the edge-lengths of the triangle we find

$$A = \begin{cases} \frac{1}{4}\sqrt{1-\gamma^2}\, i_0^{3/2} \left(\sqrt{1 + 2(\delta i_L + \delta i_R - \delta i)} + o(i_0^{-3/4}) \right) & 0 \leq \gamma < 1 \\ \frac{1}{4}\sqrt{\gamma^2-1}\, i_0^{3/2} \left(\sqrt{1 + 2(\delta i + \delta i_L - \delta i_R)} + o(i_0^{-3/4}) \right) & \gamma > 1 \quad . \end{cases} \tag{285}$$

This formula holds both when the respective sums $\delta i_L + \delta i_R - \delta i$ and $\delta i + \delta i_L - \delta i_R$ vanish and when they are positive and at most of order $O(\sqrt{i_0})$. As a result we have that, when

$\delta i_L + \delta i_R - \delta i$, or $\delta i + \delta i_L - \delta i_R$ respectively, is even the perturbative asymptotics of the square of the $3j$-symbol is

$$\begin{pmatrix} \frac{|1-\gamma|}{2} i_0 + \delta i_L & \frac{(1+\gamma)}{2} i_0 + \delta i_R & i_0 + \delta i \\ 0 & 0 & 0 \end{pmatrix}^2 \sim \tag{286}$$

$$\sim \begin{cases} \frac{2}{\pi} \frac{1}{\sqrt{1-\gamma^2}} \; \frac{i_0^{-3/2}}{\sqrt{1+2(\delta i_L + \delta i_R - \delta i)}} \; \theta(\delta i_L + \delta i_R - \delta i) & 0 \leq \gamma < 1 \\ \frac{2}{\pi} \frac{1}{\sqrt{\gamma^2-1}} \; \frac{i_0^{-3/2}}{\sqrt{1+2(\delta i + \delta i_L - \delta i_R)}} \; \theta(\delta i + \delta i_L - \delta i_R) & \gamma > 1 \quad . \end{cases}$$

The theta functions implement the triangular inequality on the fluctuations. In the more general case when $j_1 - j_2$ is non-zero but small with respect to the size of the triangle, we have that the fluctuation in δj_e can be treated perturbatively and, to leading order, the asymptotic expression remains unchanged.

Gaussians from factorials In this paragraph we study the asymptotics of the function $A^i_{i_L i_R}(j_1, j_2)$ which, for $0 \leq \gamma < 1$, is given by expression (279). The proof in the case $\gamma > 1$ goes the same way. In the asymptotic region of interest all the factorials in (279) have large argument, therefore Stirling's asymptotic expansion can be used:

$$j_0! \; = \; \sqrt{2\pi j_0} \; e^{+j_0(\log j_0 \, - 1)} \; \big(1 + \sum_{n=1}^{N} a_n j_0^{-n} \, + \, O(j_0^{-(N+1)})\big) \qquad \text{for all } N > 0, \tag{287}$$

where a_n are coefficients which can be computed; for instance $a_1 = \frac{1}{12}$. The formula we need is a perturbative expansion of the factorial of $(1+\xi)j_0$ when the parameter ξ is of order $o(1/\sqrt{j_0})$. We have that

$$\big((1+\xi)j_0\big)! = \; \sqrt{2\pi j_0} \; \exp\Big(+ j_0(\log j_0 \, - 1) + \xi j_0 \log j_0 + j_0 \sum_{k=1}^{\infty} c_k \xi^k \Big) \times \tag{288}$$

$$\times \; \big(1 + \sum_{n=1}^{N} \sum_{m=1}^{M} a_n b_m j_0^{-n} \, \xi^m \, + \, O(j_0^{-(N+\frac{M}{2}+1)})\big) \tag{289}$$

where the coefficients b_m and c_k can be computed explicitly. We find that the function $A^i_{i_L i_R}(j_1, j_2)$ has the following asymptotic behavior

$$A^{i_0+\delta i}_{\frac{|1-\gamma| i_0}{2} + \delta i_L \, , \, \frac{(1+\gamma) i_0}{2} + \delta i_R}(j_0 + \delta j_1, j_0 + \delta j_2) \; \sim \; A_0(j_0) \, e^{-H(\delta i_L, \delta i_R, \delta i, \delta j_1, \delta j_2)} \tag{290}$$

where $A_0(j_0)$ is the function evaluated at the background values and $H(\delta i_L, \delta i_R, \delta i, \delta j_1, \delta j_2)$ is given by

$$\begin{aligned} H(\delta i_L, \delta i_R, \delta i, \delta j_1, \delta j_2) = \; & \frac{1}{2}(\text{arcsinh}\sqrt{3})\,\big(\delta i_L + \delta i_R - \delta i\big) + \\ & + \frac{\sqrt{3}}{2}\frac{(\delta i_L)^2}{|1-\gamma| i_0} + \frac{\sqrt{3}}{2}\frac{(\delta i_R)^2}{(1+\gamma) i_0} - \frac{\sqrt{3}}{4}\frac{(\delta i)^2}{i_0} + \\ & - \frac{1}{2}\frac{\delta i_L + \delta i_R - \delta i}{i_0}(\delta j_1 + \delta j_2) \; + \; O(\frac{1}{\sqrt{j_0}}) \end{aligned} \tag{291}$$

for $0 \leq \gamma < 1$, while for $\gamma > 1$ it is given by

$$\begin{aligned} H(\delta i_L, \delta i_R, \delta i, \delta j_1, \delta j_2) = \; & \frac{1}{2}(\text{arcsinh}\sqrt{3})\,\big(\delta i + \delta i_L - \delta i_R\big) + \\ & + \frac{\sqrt{3}}{2}\frac{(\delta i_L)^2}{|1-\gamma| i_0} + \frac{\sqrt{3}}{2}\frac{(\delta i_R)^2}{(1+\gamma) i_0} - \frac{\sqrt{3}}{4}\frac{(\delta i)^2}{i_0} + \\ & - \frac{1}{2}\frac{\delta i + \delta i_L - \delta i_R}{i_0}(\delta j_1 + \delta j_2) \; + \; O(\frac{1}{\sqrt{j_0}}) \; . \end{aligned} \tag{292}$$

Perturbative asymptotics of the fusion coefficients Collecting the results of the previous two subsections we find for the fusion coefficients the asymptotic formula

$$\begin{aligned} f^{i_0+\delta i}_{\frac{|1-\gamma| i_0}{2}+\delta i_L\,,\,\frac{(1+\gamma) i_0}{2}+\delta i_R}(j_0 + \delta j_e) \; \sim \; & f_0(j_0)\,\frac{1}{\sqrt{1 + 2(\delta i_L + \delta i_R - \delta i)}}\,\theta(\delta i_L + \delta i_R - \delta i) \times \\ & \times \exp\big(-\text{arcsinh}(\sqrt{3})\,(\delta i_L + \delta i_R - \delta i)\big) \times \\ & \times \exp\big(-\sqrt{3}\frac{(\delta i_L)^2}{|1-\gamma|\, i_0} - \sqrt{3}\frac{(\delta i_R)^2}{(1+\gamma)\, i_0} + \frac{\sqrt{3}}{2}\frac{(\delta i)^2}{i_0}\big) \times \\ & \times \exp\big(\frac{1}{2}\frac{\delta i_L + \delta i_R - \delta i}{i_0}(\delta j_1 + \delta j_2 + \delta j_3 + \delta j_4)\big) \end{aligned} \tag{293}$$

for $0 \leq \gamma < 1$, and

$$\begin{aligned} f^{i_0+\delta i}_{\frac{|1-\gamma| i_0}{2}+\delta i_L\,,\,\frac{(1+\gamma) i_0}{2}+\delta i_R}(j_0 + \delta j_e) \; \sim \; & f_0(j_0)\,\frac{1}{\sqrt{1 + 2(\delta i + \delta i_L - \delta i_R)}}\,\theta(\delta i + \delta i_L - \delta i_R) \times \\ & \times \exp\big(-\text{arcsinh}(\sqrt{3})\,(\delta i + \delta i_L - \delta i_R)\big) \times \\ & \times \exp\big(-\sqrt{3}\frac{(\delta i_L)^2}{|1-\gamma|\, i_0} - \sqrt{3}\frac{(\delta i_R)^2}{(1+\gamma)\, i_0} + \frac{\sqrt{3}}{2}\frac{(\delta i)^2}{i_0}\big) \times \\ & \times \exp\big(\frac{1}{2}\frac{\delta i + \delta i_L - \delta i_R}{i_0}(\delta j_1 + \delta j_2 + \delta j_3 + \delta j_4)\big) \end{aligned} \tag{294}$$

for $\gamma > 1$, where $f_0(j_0)$ is the value of the fusion coefficients at the background configuration. As we will show in next section, this asymptotic expression has an appealing geometrical interpretation and plays a key role in the connection between the semiclassical behavior of the spinfoam vertex and simplicial geometries.

8.3 *Semiclassical behavior*

To illustrate some important features of the semiclassical behavior of the fusion coefficients, we must first anticipate the principal idea of the next section: the propagation of boundary wave packets as a way to test the semiclassical behavior of a spinfoam model. Consider an "initial" state made by the product of four intertwiner wavepackets; this state has the geometrical interpretation of four semiclassical regular tetrahedra in the boundary of a 4-simplex of linear size of order $\sqrt{j}_0$. Then we can evolve this state (numerically) by contraction with the flipped vertex amplitude to give the "final" state, which in turn is an intertwiner wavepacket. While in (17) we considered only very small j_0's, in (26) we make the same calculation for higher spins both numerically and semi-analitically, and the results are clear: the "final" state is a semiclassical regular tetrahedron with the same size as the incoming ones. This is exactly what we expect from the classical equations of motion.

The evolution is defined by

$$\sum_{i_1 \dots i_5} W(j_0, i_1, \dots, i_5)\, \psi(i_1, j_0) \dots \psi(i_5, j_0) \equiv \phi(i_5, j_0), \tag{295}$$

where

$$\psi(i, j_0) = C(j_0)\, \exp\big(-\frac{\sqrt{3}}{2} \frac{(i - i_0)^2}{i_0} + \mathrm{i}\frac{\pi}{2}(i - i_0)\big) \tag{296}$$

is a semiclassical $SO(3)$ intertwiner (actually its components in the base $|i\rangle$), or a semiclassical tetrahedron, in the equilateral configuration, with $C(j_0)$ a normalization constant, and $W(j_0, i_1, \dots, i_5)$ is the vertex (260) with $\gamma = 0$ evaluated in the homogeneous spin configuration (the ten spins equal to j_0). In (295), if we want to make the sum over intertwiners, for fixed j_0, then we have to evaluate the function g defined as follows:

$$g(i_L, i_R, j_0) = \sum_i f^i_{i_L\, i_R}(j_0)\, \psi(i, j_0)\ . \tag{297}$$

The values of g are the components of an $SO(4)$ intertwiner in the basis $|i_L\rangle|i_R\rangle$, where $|i_L\rangle$ is an intertwiner between four $SU(2)$ irreducible representations of spin $j_0^L \equiv \frac{|1-\gamma|}{2} j_0$, and $|i_R\rangle$ is an intertwiner between representations of spin $j_0^R \equiv \frac{1+\gamma}{2} j_0$.

We show that EPRL fusion coefficients map $SO(3)$ semiclassical intertwiners into $SU(2)_L \times SU(2)_R$ semiclassical intertwiners. The sum over the intertwiner i of the fusion coefficients times the semiclassical state can be computed explicitly at leading order in a stationary phase

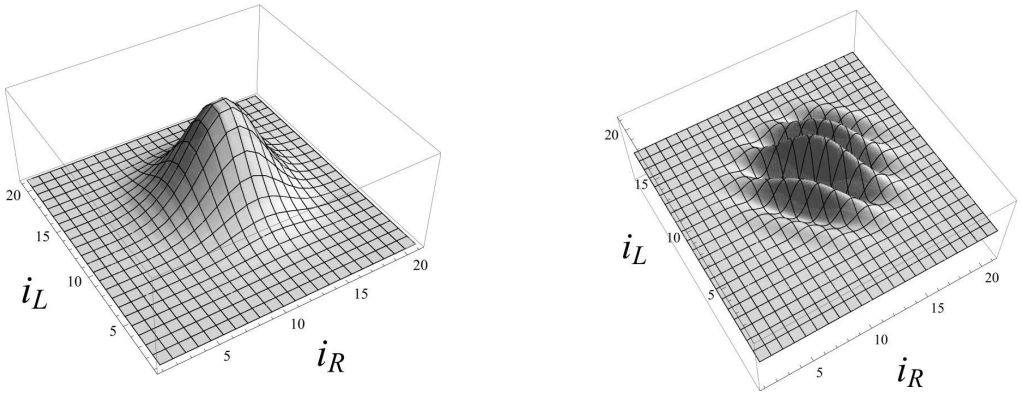

(a) (b)

Figure 8: (a) Interpolated plot of the modulus of $g(i_L, i_R, j_0)$ for $j_0 = 20$ and $\gamma = 0$ computed using the exact formula of the fusion coefficients. (b) Top view of the imaginary part.

approximation, using the asymptotic formula (293)(294). The result is

$$\sum_i f^i_{i_L\, i_R}(j_0)\, \psi(i, j_0) \;\approx\; \alpha_0\; f_0(j_0)\, C(j_0) \;\times\; \exp\Big(-\sqrt{3}\frac{(i_L - \frac{|1-\gamma|}{2}\, i_0)^2}{|1-\gamma|\, i_0} \pm \mathsf{i}\frac{\pi}{2}(i_L - \tfrac{|1-\gamma|}{2}\, i_0)\Big) \times \tag{298}$$

$$\times\; \exp\Big(-\sqrt{3}\frac{(i_R - \frac{(1+\gamma)}{2}\, i_0)^2}{(1+\gamma)\, i_0} + \mathsf{i}\frac{\pi}{2}(i_R - \tfrac{(1+\gamma)}{2} i_0)\Big)$$

where

$$\alpha_0 = \sum_{k\in 2\mathbb{N}} \frac{e^{-\mathrm{arcsinh}(\sqrt{3})k}}{\sqrt{1+2k}} e^{\mp \mathsf{i}\frac{\pi}{2}k} \simeq 0.97\;; \tag{299}$$

the plus-minus signs both in (298) and (299) refer to the two cases $\gamma < 1$ (upper sign) and $\gamma > 1$ (lower sign). The r.h.s. of (298), besides being a very simple formula for the asymptotical action of the map f on a semiclassical intertwiner, is asymptotically invariant under change of pairing of the virtual spins i_L and i_R (up to a normalization N). Recalling that the change of pairing is made by means of $6j$-symbols, we have

$$\sum_{i_L}\sum_{i_R} \sqrt{\dim(i_L)\dim(i_R)}(-1)^{i_L+k_L+i_R+k_R} \begin{Bmatrix} \frac{|1-\gamma|}{2}j_0 & \frac{|1-\gamma|}{2}j_0 & i_L \\ \frac{|1-\gamma|}{2}j_0 & \frac{|1-\gamma|}{2}j_0 & k_L \end{Bmatrix} \times \tag{300}$$

$$\times \begin{Bmatrix} \frac{1+\gamma}{2}j_0 & \frac{1+\gamma}{2}j_0 & i_R \\ \frac{1+\gamma}{2}j_0 & \frac{1+\gamma}{2}j_0 & k_R \end{Bmatrix}\; g(i_L, i_R) \approx N(j_0)\, g(k_L, k_R, j_0)\;.$$

This result holds because each of the two exponentials in (298) is of the form

$$\exp\big(-\frac{\sqrt{3}}{2}\frac{(k-k_0)^2}{k_0} \pm \mathsf{i}\frac{\pi}{2}(k-k_0)\big), \tag{301}$$

which is a semiclassical equilateral tetrahedron with area quantum numbers k_0; it follows that g is (asymptotically) an $SO(4)$ semiclassical intertwiner. The formula (298) can be checked against plots of the exact formula for large j_0's; a particular case is provided in fig.8.

In addition, we can ask whether the inverse map f^{-1} has the same semiclassical property. Remarkably, the answer is positive: f^{-1} maps semiclassical $SO(4)$ intertwiners into semiclassical $SO(3)$ intertwiners. The calculation, not reported here, involves error functions (because of the presence of the theta function) which have to be expanded to leading order in $1/j_0$.

A final remark on our choice for the asymptotic region is needed. The goal we have in mind is to apply the asymptotic formula for the fusion coefficients to the calculation of observables like the semiclassical correlations for two local geometric operators $\hat{\mathcal{O}}_1$, $\hat{\mathcal{O}}_2$

$$\langle \hat{\mathcal{O}}_1 \, \hat{\mathcal{O}}_2 \rangle_q = \frac{\sum_{j_{ab} i_a} W(j_{ab}, i_a) \, \hat{\mathcal{O}}_1 \, \hat{\mathcal{O}}_2 \, \Psi_q(j_{ab}, i_a)}{\sum_{j_{ab} i_a} W(j_{ab}, i_a) \, \Psi_q(j_{ab}, i_a)} \tag{302}$$

in the semiclassical regime (at the single-vertex level). If the classical (intrinsic and the extrinsic) geometry q over which the boundary state is peaked is the geometry of the boundary of a regular 4-simplex, then the sums in (302) are dominated by spins of the form $j_{ab} = j_0 + \delta j_{ab}$ and intertwiners of the form $i_a = i_0 + \delta i_a$, with $i_0 = 2j_0/\sqrt{3}$, where the fluctuations must be such that the relative fluctuations $\delta j/j_0, \delta i/j_0$ go to zero in the limit $j_0 \to \infty$. More precisely, the fluctuations are usually chosen to be at most of order $O(\sqrt{j_0})$. This is exactly the region we study here. As to the region in the (i_L, i_R) parameter space, the choice of the background values $\frac{|1-\gamma|}{2} i_0, \frac{1+\gamma}{2} i_0$ and the order of their fluctuations is made *a posteriori* both by numerical investigation and by the form of the asymptotic expansion. It is evident that the previous considerations hold in particular for the function g analyzed in this section.

8.4 *The case* $\gamma = 1$

When $\gamma = 1$ we have that $j_L \equiv \frac{|1-\gamma|}{2} j = 0$ and we can read from the graph (271) that the fusion coefficients vanish unless $i_L = 0$. Furthermore it is easy to see that for $\gamma = 1$ the fusion coefficients vanish also when i_R is different from i. This can be seen, for instance, applying the identity

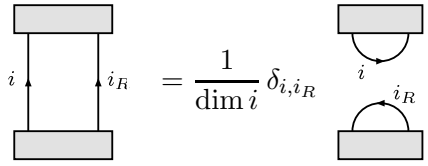

(303)

to the graph (271) with $i_L = 0$. As a result, we have simply

$$f^{i}_{i_L \, i_R}(j_1, j_2, j_3, j_4) = \delta_{i_L, 0} \delta_{i_R, i} \tag{304}$$

and the asymptotic analysis is trivial. The previous equation can be also considered as a normalization check; in fact, with the definition (271) for the fusion coefficients, the EPRL vertex amplitude (260) reduces for $\gamma = 1$ to the usual $SO(3)$ BF vertex amplitude.

9 Numerical investigations on the semiclassical limit

In this section we introduce a new technique to test the spinfoam dynamics, which is complementary to the calculation of n-point functions. This technique, presented for the first time in (17), and improved in (26), is the propagation of semiclassical wavepackets: as in ordinary Quantum Mechanics, if the theory has the correct semiclassical limit, then semiclassical wavepackets must follow the trajectory predicted by classical equations of motion. In (17), the wavepacket propagation in the intertwiner sector, was studied numerically in the case of EPR vertex (EPRL with $\gamma = 0$), finding a good semiclassical behavior. In brief, we considered the solution of discretized Einstein equations given by a single flat 4-simplex with boundary constituted by five regular tetrahedra. In the dual LQG picture this boundary is represented by a pentagonal 4-valent spin-network, labeled by ten spins and five intertwiners; but in order to have a semiclassical state one has to construct some (infinite) linear combination of spin-networks of this kind. It is known from (97) that basis 4-valent intertwiners with some choice of pairing can be superposed with Gaussian weight to be able to catch the classical geometry: since in a quantum tetrahedron the angles do not commute, one has to consider semiclassical superpositions to peak all angles on the same classical value. We chose an initial state formed by four coherent intertwiners at four nodes, and made the drastic approximation of taking the ten spins fixed to be equal to some j_0. Then we calculated numerically its evolution, here called 4-to-1-evolution, that is its contraction with the propagation kernel of the EPR spinfoam model. Classical Einstein equations impose the final state to be a coherent intertwiner with the same geometrical properties (mean and phase). We found good indications but, due to the very low j_0's, we couldn't conclude much about the analytical properties of the evolved state.
In the second paper (26) we conjecture the general behavior of the evolution at high j_0's which is very well supported numerically. In fact, as we shall argue, the propagation is perfectly "rigid": four gaussian wavepackets evolve into one gaussian wavepacket with the same parameters, except for a flip in the phase. The phase of the evolved phase, and in particular its flipping, will have a major role when considering physical expectation values. The support to our conjecture is made in two independent ways: the first is semi-analytical and is based on a numerical result on the $15j$-symbol viewed as a propagation kernel, and the asymptotic properties of the fusion coefficients already studied in the last section; the second is purely numerical. The first has the advantage of giving a nice picture of the dynamics in terms of wavepackets evolving separately in the left and right $SO(4)$ sectors, and it also pave the way for the completely analytical approach (to do this, one should have an asymptotic formula for the $15j$-symbol). We also explore the possibility of propagating three coherent intertwiners into two (we will refer to as the 3-to-2-evolution), finding similar results. Then we present the results from another point of view, namely as intertwiner physical expectation values, finding that these are asymptotically the predicted ones. Though we use the drastic approximation of fixing all spins, we regard our results as a strong indication that the EPRL model has the good semiclassical limit. In the end we present the numerical calculation of the intertwiner correlation function, finding a scaling law which is not the Newtonian one; we believe that this is due to the drastic approximation of freezing the spin variables in the boundary state, and not to pathologies of the model.

9.1 *Wave packets propagation*

Suppose you are explicitly given the propagation kernel $W_t(x, y)$ of a one-dimensional nonrelativistic quantum system defined by a Hamiltonian operator H

$$W_t(x, y) = \langle x|e^{-\frac{\mathrm{i}}{\hbar}Ht}|y\rangle \tag{305}$$

and you want to study whether the classical ($\hbar \to 0$) limit of this quantum theory yields a certain given classical evolution. One of the (many) ways of doing so is to propagate a wave packet $\psi_{x,p}(x)$ with $W_t(x, y)$. Suppose that in the time interval t the classical theory evolves the initial position and momentum x_i, p_i to the final values x_f, p_f. Then you can consider a semiclassical wave packet $\psi_{x_i,p_i}(y)$ centered on the initial values x_i, p_i, compute its evolution under the kernel

$$\phi(x) \equiv \int \mathrm{d}y \; W_t(x, y) \; \psi_{x_i,p_i}(y) \tag{306}$$

and ask whether or not this state is a semiclassical wave packet centered on the correct final values x_f, p_f. Here, we consider the possibility of using this method for exploring the semiclassical limit of the dynamics of nonperturbative quantum gravity.

We are interested in investigating the intertwiner dependence of the EPR vertex. The derivation of the vertex amplitude presented in (99) indicates that the process described by one vertex can be seen as the dynamics of a single cell in a Regge triangulation of General Relativity. This is a fortunate situation, because it allows us to give a simple and direct geometrical interpretation to the dynamical variables entering the vertex amplitude, and a simple formulation of the dynamical equations.

In section (5.2) we stressed that the areas and the angle between the normals to the tetrahedra code respectively the intrinsic and the extrinsic geometry of the boundary surface. Here we consider the boundary of a Regge cell that is formed by five tetrahedra joined along all their faces, thus forming a closed space with the topology of a 3-sphere. Recall that the ten spins j_{nm} ($n, m = 1, \dots, 5$) are the quantum numbers of the areas A_{nm} that separates the tetrahedra n and m, and the five intertwiners i_n are the quantum numbers associated to the angles $\theta_n^{(mp,qr)}$ between the triangles (mp) and (qr) in the tetrahedron n. These quantities determine entirely the intrinsic $(A_{nm}, \theta_n^{(mp,qr)})$ and extrinsic (Θ_{nm}) classical geometry of the boundary surface. Each tetrahedron has six such angles, of which only two are independent (at given values of the areas); but the corresponding quantum operators do not commute (97) and a basis of the Hilbert space on which they act can be obtained by diagonalizing just a single arbitrary one among these angles. Therefore the intrinsic geometry of the boundary of a classical Regge cell is determined by twenty numbers, but the the corresponding quantum numbers are only fifteen: the fifteen quantities j_{nm}, i_n. These are the fifteen arguments of the vertex. When using the intertwiners i_n, we have of course to specify to which pairing $i_n^{(mp,qr)}$ we are referring.

The equations of motion of any dynamical system can be expressed as constraints on the set formed by the initial, final and (if it is the case) boundary variables. For instance, in the case of the evolution of a free particle in the time interval t, the equations of motion can be expressed as constraints on the set (x_i, p_i, x_f, p_f). These constraints are of course $m(x_f - x_i)/t = p_i = p_f$.

(For the general logic of this approach to dynamics, see (7)). In General Relativity, the Einstein equations can be seen as constraints on boundary variables $A_{nm}, \theta_n^{(mp,qr)}$ and Θ_{nm}. These, in fact, can be viewed as the ensemble of the initial, boundary and final data for a process happening inside the boundary 3-sphere. Such constraints are a bit difficult to write explicitly, but one solution is easy: the one that corresponds to flat space and to the boundary of a *regular* 4-simplex. This is given by all equal areas $A_{nm} = j_0$, all equal angles $i_n = i_0$, and $\Theta_{nm} = \Theta$, where, as we have seen in section (6.2), elementary geometry gives

$$i_0 = \frac{2}{\sqrt{3}}\, j_0, \qquad \cos\Theta = -\frac{1}{4}. \tag{307}$$

It follows immediately from these considerations that a boundary wave packet centered on these values must be correctly propagated by the vertex amplitude, if the vertex amplitude is to give the Einstein equations in the classical limit.

The simplest wave packet we may consider is a simplified version of (224): a diagonal Gaussian wave packet

$$\Psi(j_{nm}, i_n) = \prod_{nm} \tilde{\psi}(j_{nm}) \prod_n \psi(i_n) \tag{308}$$

where

$$\tilde{\psi}(j_{nm}) = e^{-\frac{1}{\tau}(j_{nm}-j_0)^2 + \mathrm{i}\theta j_{nm}} \tag{309}$$

and

$$\psi(i) = N\sqrt{\dim(i)}\; e^{-\frac{3}{4j_0}(i-i_0)^2 + \mathrm{i}\frac{\pi}{2}i}. \tag{310}$$

In other words, the state considered is formed by a Gaussian state on the spins, with phase θ given by the extrinsic curvature and by a "coherent tetrahedron" state (see (97)) for each tetrahedron.

Let us write the wave packet (308) as an "initial state" times a "final state" by viewing the process represented by the spacetime region described by the Regge cell as a process evolving four tetrahedra into one. That is, let us write this state in the form

$$\Psi(j_{nm}, i_n) = \psi_{init}(j_{nm}, i'_n)\psi(i_5) \tag{311}$$

where $i'_n = (i_1, ..., i_4)$. Then we can test the classical limit of the vertex amplitude by computing the evolution of the four "incoming" tetrahedra generated by the vertex amplitude

$$\phi(i) = \sum_{j_{nm}, i'_n} W(j_{nm}, i'_n, i)\psi_{init}(j_{nm}, i'_n) \tag{312}$$

where i is i_5, and comparing $\phi(i)$ with $\psi(i)$. If the vertex amplitude has general relativity as its classical limit, then we expect that in the semiclassical limit, namely for large j_0, the evolution should evolve the "initial" boundary state $\psi_i(j_{nm}, i'_n)$ into a final state $\phi(i)$ which is still a wave packet centered on the same classical tetrahedron as the state $\psi(i)$ given in (310). That is, $\phi(i)$ must be a state "similar" to $\psi(i)$, plus perhaps quantum corrections representing the quantum spread of the wave packet.

We have tested this hypothesis numerically, under a drastic approximation: replacing the Gaussian dependence on the spins with a state concentrated on $j_{nm} = j_0$. That is, we have tested the hypothesis in the $\tau \to \infty$ limit. Explicitly, we considered the boundary state

$$\Psi(j_{nm}, i_n) \propto \prod_{n=1}^{10} \delta_{j_n, j_0} \prod_{m=1}^{5} \psi(i_m)\,. \tag{313}$$

Though the property we wanted to test should be true for the correct boundary state in which the approximation of freezing the spins is not taken, one can study the evolution and see if a positive result is obtained. If this is the case, we are strongly encouraged to believe that the same property holds in the general case.

The hypothesis we want to test is thus the following. We want to compare the evolved state

$$\phi(i) = \sum_{i_1 \ldots i_4} W(i_1, ..., i_4, i) \prod_{n=1}^{4} \psi(i_n) \tag{314}$$

with the coherent tetrahedron state (310), where

$$W(i_n) \equiv W(j_{nm}, i_n)|_{j_{nm}=j_0}. \tag{315}$$

If the function $\phi(i)$ turns out to be sufficiently close to the coherent tetrahedron state $\psi(i)$, we can say that, under the hypotheses given, the flipped vertex amplitude appears to evolve four coherent tetrahedra into one coherent tetrahedron, consistently with the flat solution of the classical Einstein equations. In the first paper (17) we have compared the two functions $\psi(i)$ (coherent tetrahedron) and $\phi(i)$ (evolved state) for the cases $j_0 = 2$ and $j_0 = 4$. The numerical results are shown in the figures below. The overall relative amplitude of $\psi(i)$ and $\phi(i)$ is freely adjusted by fixing the normalization constant N and therefore is not significant. The quantity i_{mean} is the mean value of i. It gives the position of the wave packet. The quantity $\sigma/2$ is the corresponding variance. It gives the (half) width of the wave packet. In Fig. 9 and Fig. 11 we compare the modulus square of the wave function (for the two values of j_0). In Fig. 10 and Fig. 12 we compare the modulus square of the discrete Fourier transform of the wave function: n stands for the n^{th} multiple of the fundamental frequency $2\pi/j_0$.
Case $j_0 = 2$:

The agreement between the evolved state and the coherent tetrahedron state is quite good. Besides the overall shape of the state, notice the concordance of the mean values and the widths of the wave packet. Considering the small value of j_0, which is far from the large scale limit, and the $\tau \to \infty$ limit we have taken, we find this quite surprising.

The same pattern repeats in the $j_0 = 4$ case:

9.2 *Summary of semiclassical properties of fusion coefficients*

In section 8 the fusion coefficients were studied and an analytic asymptotic formula was given; thanks to this formula, we found the asymptotical action of the fusion coefficients on a semi-classical intertwiner. We resume briefly some properties, focusing on the case $\gamma = 0$.

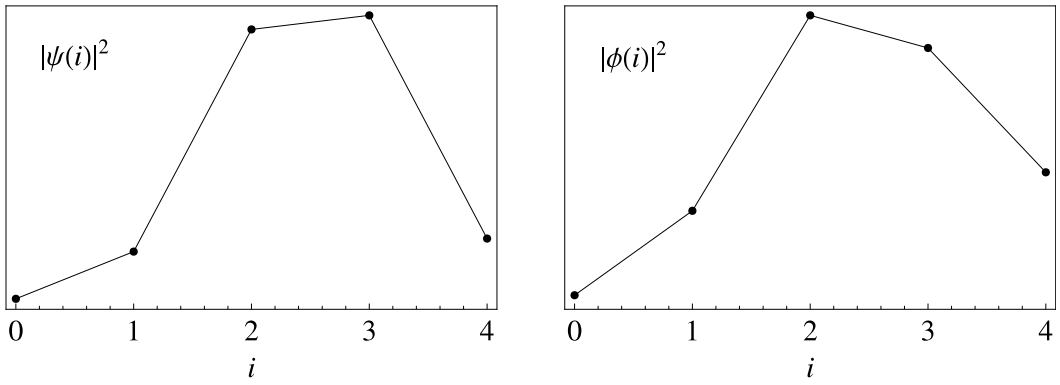

Figure 9: $j_0 = 2$. Modulus square of the amplitude. Left: coherent tetrahedron ($i_{\text{mean}} \pm \sigma/2 = 2.54 \pm 0.39$). Right: Evolved state ($i_{\text{mean}} \pm \sigma/2 = 2.54 \pm 0.46$). CPU time with a 1.8 Ghz processor: few seconds (old code), $\sim 10^{-1}$ s (new code)

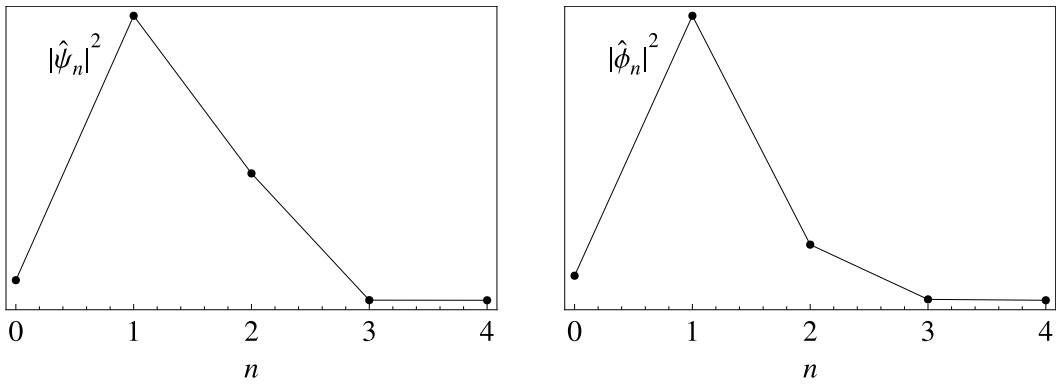

Figure 10: $j_0 = 2$. Modulus square of the (discrete) Fourier transform of the amplitude. Left: coherent tetrahedron ($n_{\text{mean}} \pm \sigma/2 = 1.25 \pm 0.27$). Right: Evolved state ($n_{\text{mean}} \pm \sigma/2 = 1.15 \pm 0.31$).

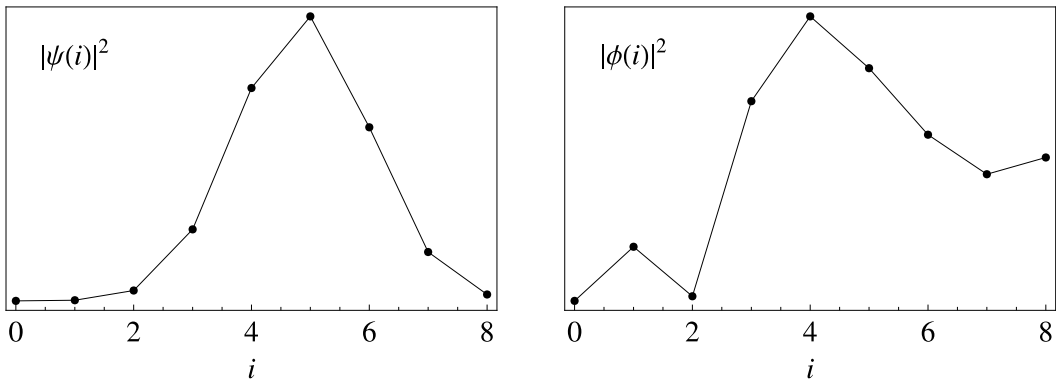

Figure 11: $j_0 = 4$. Modulus square of the amplitude. Left: coherent tetrahedron ($i_{\text{mean}} \pm \sigma/2 = 4.88 \pm 0.56$). Right: Evolved state ($i_{\text{mean}} \pm \sigma/2 = 4.85 \pm 0.96$).CPU time with a 1.8 Ghz processor: 6 h (old code), few seconds (new code)

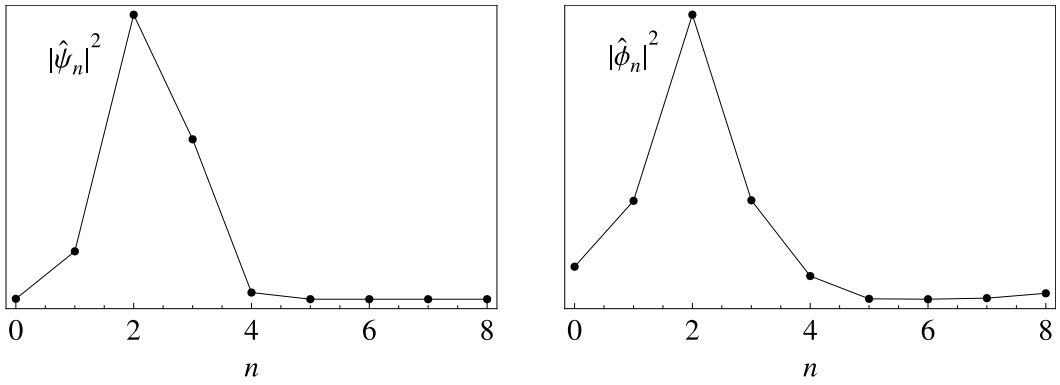

Figure 12: $j_0 = 4$. Modulus square of the (discrete) Fourier transform of the amplitude. Left: coherent tetrahedron ($n_{\text{mean}} \pm \sigma/2 = 2.25 \pm 0.32$). Right: Evolved state ($n_{\text{mean}} \pm \sigma/2 = 2.08 \pm 0.59$).

The action of $f^i_{i_L,i_R}$ (viewed as a map between intertwiner spaces) on a semiclassical intertwiner is given by

$$g(i_L, i_R) \equiv \sum_i f^i_{i_L,i_R} \psi(i). \tag{316}$$

We showed that, for large j_0's

$$g(i_L, i_R) \simeq C \exp\Big(-\tfrac{3}{2j_0}(i_L - \tfrac{i_0}{2})^2 - \tfrac{3}{2j_0}(i_R - \tfrac{i_0}{2})^2 + \mathrm{i}\tfrac{\pi}{2}(i_L + i_R)\Big), \tag{317}$$

where C is an irrelevant normalization factor not depending on i_L and i_R at leading order in $1/j_0$ powers. Hence, asymptotically, the function g factorizes into left and right parts; we indicate them, with abuse of notation, $g(i_L)$ and $g(i_R)$. The values of $g(i_L, i_R)$ are the components of an $SO(4) \simeq SU(2) \times SU(2)$ intertwiner in the basis $|i_L,\, i_R\rangle$, which we call $SO(4)$ semiclassical intertwiner. Also the converse holds: the asymptotical action of the fusion coefficients on an $SO(4)$ semiclassical intertwiner is an $SO(3)$ semiclassical intertwiner, i.e.

$$\sum_{i_L,i_R} f^i_{i_L,i_R}\, g(i_L, i_R) \simeq \psi(i). \tag{318}$$

9.3 *The semi-analytic approach*

The property (317) gives a new picture of the dynamics in the semiclassical regime. The EPR vertex is given by

$$W(i_1 \dots i_5) \equiv \sum_{\{i_{nL}\}\{i_{nR}\}} 15j_N\big(i_{1L}, \dots, i_{5L}\big) 15j_N\big(i_{1R}, \dots, i_{5R}\big) \prod_{n=1}^{5} f^{i_n}_{i_{nL},i_{nR}}\,. \tag{319}$$

The factor $f^{i_1}_{i_{1L},i_{1R}} \dots f^{i_4}_{i_{4L},i_{4R}}$ of (319) is contracted in (314) with four initial packets (making the sum over $i_1 \dots i_4$). By (317), for large j_0's this contraction gives four $SO(4)$ semiclassical

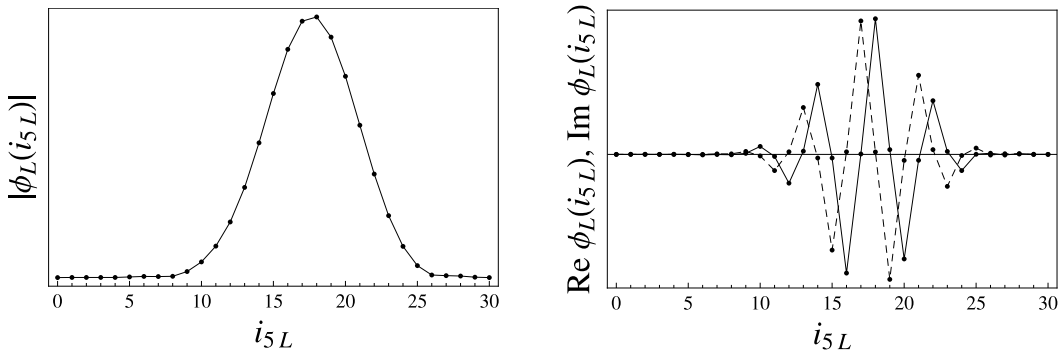

Figure 13: On the left: modulus of the evolved state for the 4-to-1 propagation performed by one $15j$ ($j_0 = 30$). On the right: its real and imaginary (dashed) part. CPU time with a 1.8 Ghz processor: few seconds

intertwiners, so the evolved state (314) becomes

$$\phi(i_5) \simeq \sum_{i_{5L},i_{5R}} \left[\sum_{i_{1L}\dots i_{4L}} 15j_N\big(i_{1L},\dots,i_{5L}\big) g(i_{1L})\dots g(i_{4L}) \right] \times \\ \times \left[\sum_{i_{1R}\dots i_{4R}} 15j_N\big(i_{1R},\dots,i_{5R}\big) g(i_{1R})\dots g(i_{4R}) \right] f^{i}_{i_{5L},i_{5R}}. \tag{320}$$

We can see in the last expression the action of two $15j$'s separately on the left and right part (the expressions in square brackets). Those actions are interpreted as independent 4-to-1-evolutions in the left and right sectors, namely the evolution of the left an right part of four SO(4) semiclassical intertwiners, where the dynamical vertex is the $15j$-symbol. By numerical investigations (Fig. 13), it turns out that the final state of the right (left) partial evolution is the right (left) part of an SO(4) semiclassical intertwiner, with the phase flipped as compared to the incoming packets. For example, for the left part:

$$\phi_L(i_{5L}) \equiv \sum_{i_{1L}\dots i_{4L}} 15j_N\big(i_{1L}\dots i_{5L}\big)\, g(i_{1L})\dots g_L(i_{4L}) \simeq \overline{g(i_{L5})}. \tag{321}$$

Then (320) becomes

$$\phi(i_5) \simeq \sum_{i_{5L},i_{5R}} \overline{g(i_{5L})}\,\overline{g(i_{5R})}\, f^{i_5}_{i_{5L},i_{5R}}. \tag{322}$$

The last expression is the contraction between the fusion coefficients and an $SO(4)$ semiclassical intertwiner. By (318), this gives an $SO(3)$ semiclassical intertwiner:

$$\phi(i_5) \simeq \overline{\psi(i_5)}. \tag{323}$$

While in (17) we expected only a conservation of mean values, and possibly a spread of wave packets, the precedent argument shows that the gaussian shape is conserved, together with its

mean value and width, while the phase is flipped. The 3-to-2-evolution is defined similarly to the 4-to-1 case, as the contraction between the flipped vertex and three initial semiclassical intertwiners. Numerical results about this type of evolution are discussed in section 9.5.

9.4 *Physical expectation values*

Now we want to present the precedent results from another perspective, as results about expectation values of observables. By construction, the boundary state (313) is peaked *kinematically* on a semiclassical geometry. This should be also true in a *dynamical* sense, as it is peaked on a solution of Einstein equations. So consider the physical expectation value of an intertwiner on this boundary state:

$$\langle i_1 \rangle \equiv \frac{\sum_{j_{nm} i_n} W(j_{nm}, i_n)\, i_1\, \Psi(j_{nm}, i_n)}{\sum_{j_{nm} i_n} W(j_{nm}, i_n) \Psi(j_{nm}, i_n)}. \tag{324}$$

We expect this quantity to be equal to i_0 for large j_0's, if the dynamics has the correct semiclassical limit. Analogously, we can consider the expectation value of two intertwiners:

$$\langle i_1\, i_2 \rangle \equiv \frac{\sum_{j_{nm} i_n} W(j_{nm}, i_n)\, i_1\, i_2\, \Psi(j_{nm}, i_n)}{\sum_{j_{nm} i_n} W(j_{nm}, i_n) \Psi(j_{nm}, i_n)}; \tag{325}$$

the last expression should be asymptotically equal to i_0^2. The results about wavepacket propagation give full information about the previous physical expectation values. In fact, (324) can be viewed as the contraction between the evolved state and a semiclassical boundary intertwiner with one insertion, so

$$\langle i_1 \rangle = \frac{\sum_{i_1} \phi(i_1)\, i_1\, \psi(i_1)}{\sum_{i_1} \phi(i_1) \psi(i_1)} \simeq \frac{\sum_{i_1} \overline{\psi(i_1)}\, i_1\, \psi(i_1)}{\sum_{i_1} \overline{\psi(i_1)} \psi(i_1)} = i_0, \tag{326}$$

where we used (323); what we have found is that dynamical and kinematical mean (asymptotically) coincide. We stress that, not only the peakiness of the evolved state is required in order to have the right expectation value, but also the phase of the evolved state must cancel exactly the phase of the initial intertwiner. The same properties (peakiness and right phase) hold for the 3-to-2-propagation (see numerical results in the next section), and the expectation value of two intertwiners turns out to be the correct one, i.e. i_0^2.

9.5 *Improved numerical analysis*

We wrote an improved numerical algorithm performing the 4-to-1 and 3-to-2 evolutions, and calculating the physical expectation values (324)(325); the algorithm computes very big sums serially with a method similar to the one in (106)(107). The results are shown in the figures. In Fig. 14 the result of the 4-to-1 evolution for $j_0 = 30$ is reported. From the plot on the left (the modulus) we can see that the evolved state is a Gaussian peaked on i_0 with the same width of the "incoming" Gaussians. On the right the real and imaginary parts are plotted, and it is clearly visible that the frequency of oscillation is $-\pi/2$, which is exactly the phase opposite to the one of initial packets.

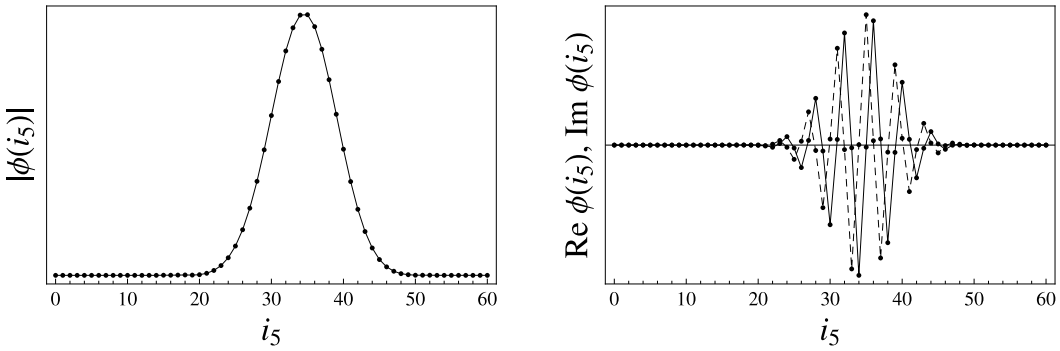

Figure 14: On the left: modulus of the evolved state for the 4-to-1 propagation performed by the flipped vertex ($j_0 = 30$). On the right: its real and imaginary (dashed) part.CPU time with a 1.8 Ghz processor: ~ 10 minutes

In Fig. 18 are shown the results of the 3-to-2 propagation (moduli), from $j_0 = 10$ to $j_0 = 32$ for even j_0's. Compared with the 4-to-1 case, here the Gaussian shape seems not to be conserved, but the state is nevertheless peaked on i_0 and presents a $-\pi/2$ phase in both variables; actually a convergence to an elliptic Gaussian is taking place (we explored up to $j_0 = 56$). Non-Gaussianity has to be imputed to quantum effects. Small deviations from Gaussianity are present also in the 4-to-1-evolution, though less pronounced. Both in the 4-to-1 and 3-to-2 evolution, non-Gaussianity gives rise to deviations of physical expectation values from the classical behavior, well visible in the plots in Fig. 15.
The physical expectation values (Fig. 15) are in complete agreement with the expected ones. The small deviations from the semiclassical values gradually disappear as j_0 increases.

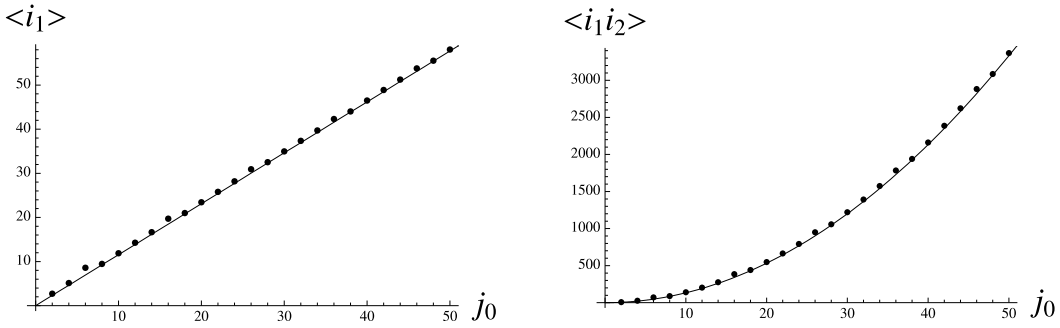

Figure 15: On the left: physical expectation value of i_1. On the right: physical expectation value of $i_1 i_2$. The solid line is the expected behavior.

9.6 *Correlation function*

Here we present some very preliminary results about the graviton propagator in the EPR spinfoam model, in the rough approximation of fixed spins. In other words, we consider the 2-point function over the boundary state (313). With our approximation, the spin-spin and

spin-intertwiner correlation functions vanish, but some components of the graviton propagator are proportional to the intertwiner-intertwiner correlation function and we will study these ones. The 2-point function, or propagator, over the boundary of a 4-simplex is defined by:

$$G^{abcd}_{mn} = \frac{\sum_{j_{pq} i_p} W(j_{pq}, i_p)(E^{(a)}_m \cdot E^{(b)}_m - n^{(a)}_m \cdot n^{(b)}_m)(E^{(c)}_n \cdot E^{(d)}_n - n^{(c)}_n \cdot n^{(d)}_n)\Psi(j_{pq}, i_p)}{\sum_{j_{pq} i_p} W(j_{pq}, i_p)\Psi(j_{pq}, i_p)} \tag{327}$$

where m, n and a, b, c, d run over $\{1, \dots, 5\}$, E^a_m is the electric field (densitized triad) operator at the node m, projected along the normal $n^{(a)}_m$ in m to the face shared by the tetrahedra m and a. In the diagonal-diagonal components ($a = b$, $c = d$) the electric fields act as area operators, so that the 2-point function is essentially an expectation value of two spin insertions "$\delta j \delta j$", which in our case of fixed spins vanishes. In the diagonal-nondiagonal components ($a = b$, $c \neq d$) the first couple of electric fields gives a spin insertion "δj", while the second couple acts nontrivially (in fact the nondiagonal action is the one that "reads" the intertwiner quantum numbers at nodes) but also those components vanish because of the presence of the spin insertion. The only surviving components are the nondiagonal-nondiagonal; they are quite complicated but some of them are simpler, and we will consider only them. Consider in the boundary state a node m labeled by the virtual spin i_m in a certain pairing, and concentrate only on those (a, b) which are coupled to i_m. As an example, if we take the node $m = 1$ and the surrounding spins are labeled as in Fig. 16, then we consider only $a, b \in \{2, 3\}$ or $\{4, 5\}$

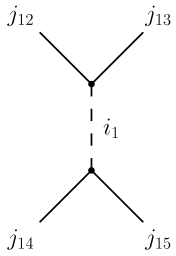

Figure 16: node

($a \neq b$). Then consider another node n labeled by i_n and indices $c \neq d$ coupled to i_n. For those components the action of graviton operators is diagonal and gives insertions of the kind "$(\frac{2}{\sqrt{3}}\delta i - \delta j - \delta j)(\frac{2}{\sqrt{3}}\delta i - \delta j - \delta j)$", so

$$G^{abcd}_{mn} \propto \frac{\sum_{\{j\},\{i\}} W(\{j\},\{i\})\, \delta i_m \delta i_n \Psi(\{j\},\{i\})}{j_0^2 \sum_{\{j\},\{i\}} W(\{j\},\{i\})\Psi(\{j\},\{i\})} \equiv \frac{\langle \delta i_m \delta i_n \rangle}{j_0^2}. \tag{328}$$

If the propagator has the Newtonian scaling in the semiclassical regime, it should scale asymptotically as the inverse of j_0; equivalently, the quantity $\langle \delta i_m \delta i_n \rangle$ should scale linearly with j_0. The plot of $\langle \delta i_m \delta i_n \rangle$ from $j_0 = 2$ to $j_0 = 50$ (with step 2) is shown in Fig. 17. The scaling is clearly not the Newtonian one, and this could be due to our choice of boundary state, which freezes the spins, or maybe to some pathology of the model. The auspicious results about the evolution of wave packets and the physical expectation values seem to exclude the latter possibility.

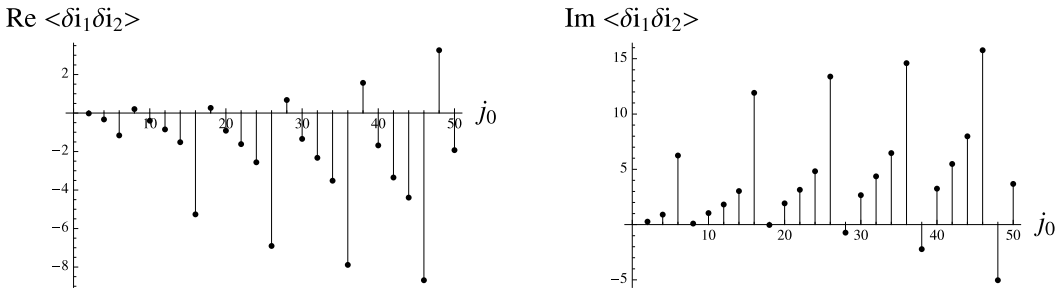

Figure 17: On the left: real part of the intertwiner correlation function, divided by j_0^2. On the right: its imaginary part.

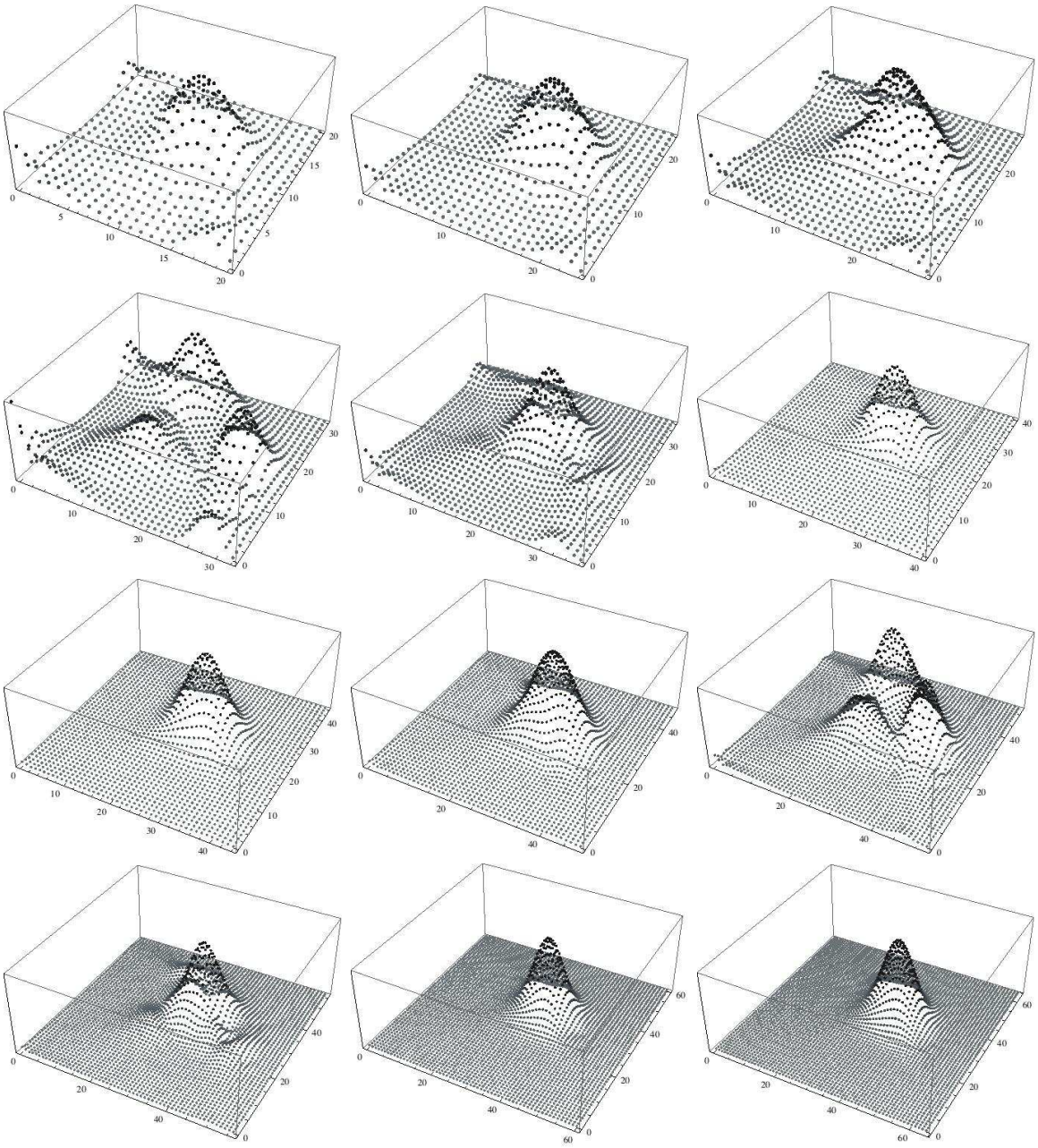

Figure 18: Modulus of the evolved state for the 3-to-2 intertwiner propagation, from $j_0 = 10$ to $j_0 = 32$ with step 2.

10 Outlooks and conclusions

This thesis goes along the last years of the research in the semiclassical limit of Loop Quantum Gravity. The original results presented are:

- We demonstrate (20) that the radial gauge can be consistently imposed together with the Lorenz gauge in Maxwell theory, and with the harmonic traceless gauge in linearized General Relativity. This result has relevance for the comparison of LQG graviton propagator with the one of the perturbative Quantum Gravity.

- We have shown a simple analytic formula for the LQG fusion coefficients, as defined in the EPRL spinfoam model (25). We have given a large spin asymptotic formula for these coefficients making a perturbative asymptotic expansion around a background configuration dictated by the kind of boundary state considered. The picture coming out from our analysis is promising: the fusion coefficients not only give nontrivial dynamics to intertwiners at the quantum level, but they seem to behave very well at semiclassical level, in fact they map semiclassical $SO(3)$ tetrahedra into semiclassical $SO(4)$ tetrahedra. This is to us a highly non-trivial property which, in turn, makes the semiclassical analysis of dynamics less obscure. A first application of the asymptotic formula can be found in (26). Our analysis is a step needed for the study of the full asymptotic expansion of the EPRL vertex, which is part of our work in progress.

- We studied the propagation of semiclassical intertwiners over a 4-simplex, using the EPR spinfoam model. This approach, introduced in (17) and developed in (26), is a way to study the semiclassical limit of spinfoam models for quantum gravity. This study turned out to be viable both analytically and numerically, and gave encouraging answers. In particular, certain coherent states turned out to evolve in accordance with classical General Relativity. Then we read the results as physical expectation values of observables. In the end, we showed a numerical calculation of the intertwiner correlation function, but the scaling law w.r.t. distance is not the one giving rise to Newton law in the semiclassical regime. This has to be expected, as the approximation of freezing the spins could also prevent intertwiner fluctuations (remember that a classical 4-simplex is fully determined by the ten edge lengths, so if those lengths are given then the dihedral angles between triangles are automatically determined). Though positive, we regard our results as partial and tentative: one should get rid of the "fixed spin" approximation and see if the wavepacket propagation is still correct and then compute the 2-point function in the semiclassical limit and see if the scaling with distance is the Newtonian one. Further numerical (107) and analytical investigations have already started and we expect in the next future to be able to give more precise answers.

Acknowledgments

I would like to thank my supervisor prof. Carlo Rovelli for being always present and helpful. I thank my internal supervisor prof. Orlando Ragnisco and the department of physics of "Università degli Studi Roma Tre" for having permitted this thesis in cotutoring with "Université de la Méditerranée" in Marseille. Finally I thank my husband and collaborator Claudio Perini for all the work together and all the "Equipe de gravité quantique" at CPT: Emanuele Alesci, Eugenio Bianchi, Jonathan Engle, Antonino Marciano', Mauricio Mondragon, Roberto Pereira, Alejandro Perez, Daniele Pranzetti, Danilo Rezende, Alejandro Satz, Simone Speziale, Artem Starodubtsev, Francesca Vidotto, and outside the CPT: Maïté Dupuis, Etera Livine, Simone Mercuri, Daniele Oriti.

Appendix

A Properties of $9j$-symbols

The $9j$-symbol with two columns with third entry given by the sum of the first two can be written as

$$\left\{\begin{array}{ccc} a & f & c \\ b & g & d \\ a+b & h & c+d \end{array}\right\} = (-1)^{f-g+a+b-(c+d)} \begin{pmatrix} f & g & h \\ a-c & b-d & -(a+b-(c+d)) \end{pmatrix} \times \tag{329}$$

$$\times \sqrt{\frac{(2a)!(2b)!(2c)!(2d)!(a+b+c+d-h)!(a+b+c+d+h+1)!}{(2a+2b+1)!(2c+2d+1)!(a+c-f)!(a+c+f+1)!(b+d-g)!(b+d+g+1)!}} .$$

An analogous formula for the $9j$-symbol with two columns with third entry given by the difference of the first two can be obtained from the formula above noting that

$$\left\{\begin{array}{ccc} a & f & c \\ b & g & d \\ b-a & h & d-c \end{array}\right\} = \left\{\begin{array}{ccc} b-a & h & d-c \\ a & f & c \\ b & g & d \end{array}\right\} , \tag{330}$$

so we are in the previous case.
The $3j$-symbol with vanishing magnetic numbers has the simple expression

$$\begin{pmatrix} a & b & c \\ 0 & 0 & 0 \end{pmatrix} = (-1)^{a-b}\pi^{1/4} \frac{2^{\frac{a+b-c-1}{2}}}{(\frac{c-a-b-1}{2})!\sqrt{(a+b-c)!}} \sqrt{\frac{(\frac{c+a-b-1}{2})!(\frac{c-a+b-1}{2})!(\frac{a+b+c}{2})!}{(\frac{c+a-b}{2})!(\frac{c-a+b}{2})!(\frac{a+b+c+1}{2})!}} . \tag{331}$$

These formula can be derived from (105; 108).

B Regge asymptotic formula for $3j$-symbols

The asymptotic formula of $3j$-symbols for large spins a, b, c and admitted magnetic numbers, i.e. $m_a + m_b + m_c = 0$, given by G. Ponzano and T. Regge in (72) is

$$\begin{pmatrix} a & b & c \\ m_a & m_b & m_c \end{pmatrix} \sim \frac{(-1)^{a+b-c+1}}{\sqrt{2\pi A}} \cos\left((a+\frac{1}{2})\theta_a + (b+\frac{1}{2})\theta_b + (c+\frac{1}{2})\theta_c + m_a\phi_a - m_b\phi_b + \frac{\pi}{4}\right) \tag{332}$$

with

$$\theta_a = \frac{\arccos\Big(2(a+\frac{1}{2})^2 m_c + m_a\big((c+\frac{1}{2})^2 + (a+\frac{1}{2})^2 - (b+\frac{1}{2})^2\big)\Big)}{\sqrt{\big((a+\frac{1}{2})^2 - m_a^2\big)\Big(4(c+\frac{1}{2})^2(a+\frac{1}{2})^2 - \big((c+\frac{1}{2})^2 + (a+\frac{1}{2})^2 - (b+\frac{1}{2})^2\big)^2\Big)}} \tag{333}$$

$$\phi_a = \arccos\left(\frac{1}{2}\frac{(a+\frac{1}{2})^2 - (b+\frac{1}{2})^2 - (c+\frac{1}{2})^2 - 2m_b m_c}{\sqrt{\big((b+\frac{1}{2})^2 - m_b^2\big)\big((c+\frac{1}{2})^2 - m_c^2\big)}}\right) \tag{334}$$

$$A = \sqrt{-\frac{1}{16}\det\begin{pmatrix} 0 & (a+\frac{1}{2})^2 - m_a^2 & (b+\frac{1}{2})^2 - m_b^2 & 1 \\ (a+\frac{1}{2})^2 - m_a^2 & 0 & (c+\frac{1}{2})^2 - m_c^2 & 1 \\ (b+\frac{1}{2})^2 - m_b^2 & (c+\frac{1}{2})^2 - m_c^2 & 0 & 1 \\ 1 & 1 & 1 & 0 \end{pmatrix}} \tag{335}$$

and $\theta_b, \theta_c, \phi_b$ are obtained by cyclic permutations of (a, b, c).

References

[1] C. Rovelli, "The century of the incomplete revolution: Searching for general relativistic quantum field theory," *J. Math. Phys.* **41** (2000) 3776–3800, arXiv:hep-th/9910131.

[2] J. Alfaro and G. Palma, "Loop quantum gravity and ultra high energy cosmic rays," *Physical Review D* **67** (2003) 083003, arXiv:hep-th/0208193.

[3] R. Aloisio, P. Blasi, A. Galante, and A. F. Grillo, "Planck scale kinematics and the Pierre Auger Observatory," *Lect. Notes Phys.* **669** (2005) 1–30.

[4] G. Amelino-Camelia, "Introduction to quantum-gravity phenomenology," *Lect. Notes Phys.* **669** (2005) 59–100, arXiv:gr-qc/0412136.

[5] G. Amelino-Camelia, J. R. Ellis, N. E. Mavromatos, D. V. Nanopoulos, and S. Sarkar, "Potential Sensitivity of Gamma-Ray Burster Observations to Wave Dispersion in Vacuo," *Nature* **393** (1998) 763–765, arXiv:astro-ph/9712103.

[6] G. Amelino-Camelia and T. Piran, "Planck-scale deformation of Lorentz symmetry as a solution to the UHECR and the TeV-gamma paradoxes," *Phys. Rev.* **D64** (2001) 036005, arXiv:astro-ph/0008107.

[7] C. Rovelli, *Quantum Gravity*. Cambridge University Press, 2004.

[8] C. Rovelli and L. Smolin, "Discreteness of area and volume in quantum gravity," *Nucl. Phys.* **B442** (1995) 593–622, arXiv:gr-qc/9411005.

[9] M. Bojowald and H. A. Morales-Tecotl, "Cosmological applications of loop quantum gravity," *Lect. Notes Phys.* **646** (2004) 421–462, arXiv:gr-qc/0306008.

[10] C. Rovelli, "Black hole entropy from loop quantum gravity," *Phys. Rev. Lett.* **77** (1996) 3288–3291.

[11] A. Ashtekar, J. Baez, A. Corichi, and K. Krasnov, "Quantum geometry and black hole entropy," *Phys. Rev. Lett.* **80** (1998) 904–907, arXiv:gr-qc/9710007.

[12] A. Ashtekar, J. C. Baez, and K. Krasnov, "Quantum geometry of isolated horizons and black hole entropy," *Adv. Theor. Math. Phys.* **4** (2000) 1–94, arXiv:gr-qc/0005126.

[13] K. A. Meissner, "Black hole entropy in loop quantum gravity," *Class. Quant. Grav.* **21** (2004) 5245–5252, arXiv:gr-qc/0407052.

[14] M. Bojowald, "Absence of a singularity in loop quantum cosmology," *Phys. Rev. Lett.* **86** (2001) 5227–5230.

[15] J. Engle, R. Pereira, and C. Rovelli, "Loop-quantum-gravity vertex amplitude," *Phys. Rev. Lett.* **99** (2001) 161301.

[16] K. Noui and A. Perez, "Three dimensional loop quantum gravity: Physical scalar product and spin foam models," *Class. Quantum Grav* **22** (2005) 1739–1761.

[17] E. Magliaro, C. Perini, and C. Rovelli, "Numerical indications on the semiclassical limit of the flipped vertex," *Class. Quant. Grav.* **25** (2008) 095009, arXiv:0710.5034 [gr-qc].

[18] R. Oeckl, "A general boundary formulation for quantum mechanics and quantum gravity," *Phys. Lett.* **B575** (2003) 318–324, arXiv:hep-th/0306025.

[19] E. Bianchi, L. Modesto, C. Rovelli, and S. Speziale, "Graviton propagator in loop quantum gravity," *Class. Quant. Grav.* **23** (2006) 6989–7028, arXiv:gr-qc/0604044.

[20] E. Magliaro, C. Perini, and C. Rovelli, "Compatibility of radial, lorenz, and harmonic gauges," *Phys. Rev.* **D76** (2007) 084031.

[21] E. Alesci and C. Rovelli, "The complete LQG propagator: I. Difficulties with the Barrett-Crane vertex," *Phys. Rev.* **D76** (2007) 104012, arXiv:0708.0883 [gr-qc].

[22] J. Engle, E. Livine, R. Pereira, and C. Rovelli, "LQG vertex with finite Immirzi parameter," *Nucl. Phys.* **B799** (2008) 136–149, arXiv:0711.0146 [gr-qc].

[23] E. R. Livine and S. Speziale, "A new spinfoam vertex for quantum gravity," *Phys. Rev.* **D76** (2007) 084028, arXiv:0705.0674 [gr-qc].

[24] L. Freidel and K. Krasnov, "A New Spin Foam Model for 4d Gravity," *Class. Quant. Grav.* **25** (2008) 125018, arXiv:0708.1595 [gr-qc].

[25] E. Alesci, E. Bianchi, E. Magliaro, and C. Perini, "Asymptotics of lqg fusion coefficients," (2008) , arXiv:0809.3718.

[26] E. Alesci, E. Bianchi, E. Magliaro, and C. Perini, "Intertwiner dynamics in the flipped vertex," arXiv:0808.1971.

[27] P. Bergmann, "Conservation laws in general relativity as the generators of coordinate transformations," *Phys. Rev.* **112** (1958) 287.

[28] P. Bergmann, "Observables in general relativity," *Rev.Mod. Phys.* **33** (1961) 510–514.

[29] P. Bergmann and A. Komar, "The phase space formulation of general relativity and approaches towards quantization," *Gen. Rel.Grav.* **1** (1981) 227–254.

[30] A. Komar, "General relativistic observables via hamilton jacobi functionals," *Phys. Rev.* **D4** (1971) 923–927.

[31] P. A. M. Dirac, "The theory of gravitation in hamiltonian form," *Phys. Rev.* **114** (1959) 924.

[32] R. M. Wald, *General Relativity*. University of Chicago Press, 1984.

[33] R. L. Arnowitt, S. Deser, and C. W. Misner, "The dynamics of general relativity," arXiv:gr-qc/0405109.

[34] A. Perez, "Introduction to loop quantum gravity and spin foams," *gr-qc/0409061* (2004) .

[35] S. Holst, "Barbero's Hamiltonian derived from a generalized Hilbert- Palatini action," *Phys. Rev.* **D53** (1996) 5966–5969, arXiv:gr-qc/9511026.

[36] A. Ashtekar, *Lectures on Non-perturbative Canonical Gravity*. World Scientific, 1991.

[37] J. F. Barbero, "From euclidean to lorentzian general relativity: The real way," *Phys. Rev.* **D54** (1996) 1492–1499.

[38] J. F. Barbero, "Real ashtekar variables for lorentzian signature space times," *Phys. Rev.* **D51** (1995) 5507–5510.

[39] J. F. Barbero, "A real polynomial formulation of general relativity in terms of connections," *Phys. Rev.* **D49** (1994) 6935–6938.

[40] G. Immirzi, "Real and complex connections for canonical gravity," *Class. Quant. Grav.* **14** (1997) L177–L181.

[41] A. Ashtekar and J. Lewandowski, "Projective techniques and functional integration," *J. Math. Phys.* **36** (1995) 2170.

[42] C. Rovelli and L. Smolin, "Spin networks and quantum gravity," *Phys. Rev.* **D52** (1995) 5742–5759.

[43] J. Baez, "Spin network states in gauge theory.," *Adv.Math.* **117** (1996) 253–272.

[44] N. Grott and c. Rovelli, "Moduli spaces structure of knots with intersections," *J. Math. Phys* **37** (1996) 3014.

[45] W. Fairbain and C. Rovelli, "Separable hilbert space in loop quantum gravity," *J. Math. Phys* **45** (2004) 2802.

[46] N. Grott and C. Rovelli, "Moduli spaces structure of knots with intersections," *J. Math. Phys* **37** (1996) 3014.

[47] W. Fairbain and C. Rovelli, "Separable hilbert space in loop quantum gravity," *J. Math. Phys* **45** (2004) 2802.

[48] A. Ashtekar and J. Lewandowski, "Quantum theory of gravity i: Area operators," *Class.Quant. Grav.* **14** (1997) A55–A81.

[49] A. Ashtekar and J. Lewandowski, "Quantum theory of gravity ii: Volume operators," arXiv:gr-qc/9711031.

[50] R. Loll, "Simplifying the spectral analysis of the volume operator," *Nucl.Phys. B* **B500** (1997) 405–420.

[51] R. Loll, "Spectrum of the volume operator in quantum gravity," *Nucl.Phys. B* **B460** (1996) 143–154.

[52] R. Loll, "The volume operator in discretized quantum gravity," *Phys. Rev. Lett.* **75** (1995) 3048–3051.

[53] T. Thiemann, "Closed formula for the matrix elements of the volume operator in canonical quantum gravity," *Nucl.Phys. B* **39** (1998) 3347–3371.

[54] T. Thiemann, "Quantum spin dynamics (qsd)," *Class.Quant.Grav.* **15** (1998) 839–873.

[55] T. Thiemann, "Anomaly-free formulation of non-perturbative, four-dimensional lorentzian quantum gravity.," *Phys. Lett. B* **380** (1998) 257.

[56] L. Smolin, "The classical limit and the form of the hamiltonian constraint in nonperturbative quantum general relativity," `arXiv:gr-qc/9609034`.

[57] T. Thiemann, "Gauge field theory coherent states (gcs) : I. general properties," *Class.Quant.Grav.* **18** (2001) 2025.

[58] T. Thiemann, "Quantum spin dynamics viii. the master constraint," *Class.Quant.Grav.* **23** (2006) 2249–2266.

[59] A. Ashtekar and J. Lewandowski, "Background independent quantum gravity: A status report," *Class. Quant. Grav.* **21** (2004) R53, `arXiv:gr-qc/0404018`.

[60] J. C. Baez, "Spin foam models," *Class.Quant.Grav.* **15** (1998) 1827–1858.

[61] A. Perez, "Spin foam models for quantum gravity," *Class. Quant. Grav.* **20** (2003) R43, `arXiv:gr-qc/0301113`.

[62] J. Halliwell and J. B. Hartle, "Wave functions constructed from an invariant sum over histories satisfy constraints," *Phys. Rev.* **D43** (1991) 1170–1194.

[63] C. Rovelli and M. Reisenberger, "Spacetime states and covariant quantum theory," *Phys.Rev. D* **65** (2002) 125016.

[64] R. Livine, Etera, A. Perez, and C. Rovelli, "2d manifold-independent spinfoam theory," *Class. Quant. Grav.* **20** (2003) 4425–4445.

[65] C. Rovelli, "The projector on physical states in loop quantum gravity," *Phys.Rev. D* **59** (1999) 104015.

[66] M. Reisenberger and C. Rovelli, ""sum over surfaces" form of loop quantum gravity," *Phys.Rev. D* **56** (1997) 3490–3508.

[67] M. Reisenberger and C. Rovelli, "Spacetime as a feynman diagram: the connection formulation," `arXiv:gr-qc/0002083`.

[68] c. Petronio and R. De Pietri, "Feynman diagrams of generalized matrix models and the associated manifolds in dimension 4," *J. Math. Phys.* **41** (2000) 6671–6688.

[69] A. Mikovic, "Quantum field theory of spin networks," *Class.Quant.Grav.* **18** (2001) 2827–2850.

[70] D. Oriti, "The group field theory approach to quantum gravity," `arXiv:gr-qc/0607032`.

[71] T. Regge, "General relativity without coordinates," *Nuovo Cim.* (1961) .

[72] G. Ponzano and T. Regge, "Semiclassical limit of racah coeffecients,". Spectroscopic and Group Theoretical Methods in Physics, edited by F.Block (North Holland, Amsterdam, 1968).

[73] J. W. Barrett and L. Crane, "Relativistic spin networks and quantum gravity," *J.Math.Phys.* **39** (1998) 3296–3302.

[74] J. W. Barrett and L. Crane, "A lorentzian signature model for quantum general relativity," *Class.Quant.Grav.* **17** (2000) 3101–3118.

[75] J. W. Barrett and R. M. Williams, "The asymptotics of an amplitude for the 4-simplex," *Adv. Theor. Math. Phys.* **3** (1999) 209–215, `arXiv:gr-qc/9809032`.

[76] L. Crane and D. N. Yetter, "On the Classical Limit of the Balanced State Sum," `arXiv:gr-qc/9712087`.

[77] J. C. Baez, J. D. Christensen, and G. Egan, "Asymptotics of 10j symbols," *Class. Quant. Grav.* **19** (2002) 6489, `arXiv:gr-qc/0208010`.

[78] L. Freidel and D. Louapre, "Asymptotics of 6j and 10j symbols," *Class. Quant. Grav.* **20** (2003) 1267–1294, `arXiv:hep-th/0209134`.

[79] J. W. Barrett and C. M. Steele, "Asymptotics of relativistic spin networks," *Class. Quant. Grav.* **20** (2003) 1341–1362, `arXiv:gr-qc/0209023`.

[80] L. Modesto and C. Rovelli, "Particle scattering in loop quantum gravity," *Phys. Rev. Lett.* **95** (2005) 191301.

[81] F. Conrady and C. Rovelli, "Generalized Schroedinger equation in Euclidean field theory," *Int. J. Mod. Phys.* **A19** (2004) 4037–4068, `arXiv:hep-th/0310246`.

[82] L. Doplicher, "Generalized Tomonaga-Schwinger equation from the Hadamard formula," *Phys. Rev.* **D70** (2004) 064037, `arXiv:gr-qc/0405006`.

[83] F. Conrady, L. Doplicher, R. Oeckl, C. Rovelli, and M. Testa, "Minkowski vacuum in background independent quantum gravity," *Phys. Rev.* **D69** (2004) 064019, `arXiv:gr-qc/0307118`.

[84] C. Rovelli, "Graviton propagator from background-independent quantum gravity," *Phys. Rev. Lett.* **97** (2006) 151301, arXiv:gr-qc/0508124.

[85] S. Speziale, "Towards the graviton from spinfoams: The 3d toy model," *JHEP* **05** (2006) 039, arXiv:gr-qc/0512102.

[86] E. R. Livine, S. Speziale, and J. L. Willis, "Towards the graviton from spinfoams: Higher order corrections in the 3d toy model," *Phys. Rev.* **D75** (2007) 024038, arXiv:gr-qc/0605123.

[87] D. Colosi *et al.*, "Background independence in a nutshell: The dynamics of a tetrahedron," *Class. Quant. Grav.* **22** (2005) 2971–2990, arXiv:gr-qc/0408079.

[88] C. Ashtekar, Abhay abd Rovelli and L. Smolin, "Weaving a classical metric with quantum threads," *Phys. Rev. Lett* **69** (1992) 237.

[89] E. Bianchi and L. Modesto, "The perturbative Regge-calculus regime of Loop Quantum Gravity," *Nucl. Phys.* **B796** (2008) 581–621, arXiv:0709.2051 [gr-qc].

[90] V. A. Fock, "Proper time in classical and quantum mechanics," *Sov. Phys.* **12** (1937) 044.

[91] J. Schwinger, "'on gauge invariance and vacuum polarization," *Phys. Rev.* **82** (1952) 684.

[92] P. Menotti, G. Modanese, and D. Seminara, "The radial gauge propagators in quantum gravity," *Ann. Phys.* **224** (1993) 110, arXiv:hep-th/9209028.

[93] G. Modanese, "The propagator in the radial gauge," *J. Math. Phys.* **33** (1992) 1523.

[94] S. Leupold and H. Weigert, "Radial propagators and Wilson loops," *Phys. Rev.* **D54** (1996) 7695–7709, arXiv:hep-th/9604015.

[95] S. Leupold, "Feynman rules in radial gauge," arXiv:hep-th/9609222.

[96] E. R. Livine and S. Speziale, "Group integral techniques for the spinfoam graviton propagator," *JHEP* **11** (2006) 092, arXiv:gr-qc/0608131.

[97] C. Rovelli and S. Speziale, "A semiclassical tetrahedron," *Class. Quant. Grav.* **23** (2006) 5861–5870, arXiv:gr-qc/0606074.

[98] E. Alesci and C. Rovelli, "The complete LQG propagator: II. Asymptotic behavior of the vertex," *Phys. Rev.* **D77** (2008) 044024, arXiv:0711.1284 [gr-qc].

[99] J. Engle, R. Pereira, and C. Rovelli, "Flipped spinfoam vertex and loop gravity," *Nucl. Phys.* **B798** (2008) 251–290, arXiv:0708.1236 [gr-qc].

[100] E. R. Livine, "Towards a covariant loop quantum gravity," arXiv:gr-qc/0608135.

[101] E. R. Livine, "Projected spin networks for lorentz connection: Linking spin foams and loop gravity," *Class. Quant. Grav.* **19** (2002) 5525–5542.

[102] S. Alexandrov, "Spin foam model from canonical quantization," *Phys. Rev. D* **77** (2008) 024009, arXiv:0705.3892.

[103] E. Bianchi and A. Satz, "Semiclassical regime of Regge calculus and spin foams," arXiv:0808.1107 [gr-qc].

[104] F. Conrady and L. Freidel, "On the semiclassical limit of 4d spin foam models," arXiv:0809.2280 [gr-qc].

[105] A. Yutsin, I. Levinson, and V. Vanagas, *Mathematical Apparatus of the Theory of Angular Momentum*. Israel Program for Scientific Translation, Jerusalem, Israel, 1962.

[106] J. D. Christensen and G. Egan, "An efficient algorithm for the riemannian 10j symbols," *Class. Quant. Grav.* **19** (2002) 1185, arXiv:gr-qc/0110045.

[107] I. Khavkine, "Evaluation of new spin foam vertex amplitudes," arXiv:0809.3190 [gr-qc].

[108] D. Varshalovich, A. N. Moskalev, and V. K. Khersonskii, "Quantum theory of angular momentum,". (World Scientific Pub., 1988).